2021

Neural mechanisms promoting G-alpha-i2 protein dependent salt sensitive hypertension in the Sprague-Dawley rat

BOSTON UNIVERSITY

SARGENT COLLEGE OF HEALTH AND REHABILITATION SCIENCES

Dissertation

NEURAL MECHANISMS PROMOTING G-alpha-i2 PROTEIN DEPENDENT SALT SENSITIVE HYPERTENSION IN THE SPRAGUE-DAWLEY RAT

by

JESSE DANIEL MOREIRA

B.A., Salem State University, 2017
M.S., Boston University, 2018

Submitted in partial fulfillment of the

requirements for the degree of

Doctor of Philosophy

2021

Approved by

First Reader

Richard D. Wainford, Ph.D.
Associate Professor of Pharmacology & Experimental Therapeutics
Associate Professor of Medicine
Boston University, School of Medicine

Associate Professor of Health Sciences
Boston University, Sargent College of Health and Rehabilitation Sciences

Second Reader

Tara L. Moore, Ph.D.
Associate Professor of Anatomy & Neurobiology
Associate Professor of Neurology
Boston University, School of Medicine

DEDICATION

I am dedicating this work to my wonderful partner Brian. You have made every inch I've pushed possible. Also, to the many, many rats that were used for the advancement of science – thank you.

ACKNOWLEDGMENTS

Brian, thank you for providing me with perspective, optimism, hope, laughter, and anything else I've ever needed. You're an endless source of love and support and I am grateful to have had you by my side for this journey, and be by each other's sides for journeys to come.

Mom, Dad, and Hailey, thank you for your encouragement and for always pushing me to be my best. You are the best family I could ever hope to have and I am me because of you.

Abbey, Nikkie, Josh, Chelsea, Lance, and Drew, thank you for being those friends who I could have a work-life balance with. Supportive when I needed it, but also told me to put down the journal article when I needed that, too. I couldn't fathom doing this without such a wonderful group of people to enjoy life with.

Dr. Susan Kandarian, thank you for being my first major scientific mentor. You encouraged me to be who I was openly in my professional life and to grow as both a scientist and a person, and taught me the two sides of me did not have to be mutually exclusive. You pushed me as much as I needed to pursue a PhD, and this experience changed my life. Thank you for your mentorship and friendship.

Dr. Richard Wainford, thank you for welcoming me into your lab and providing me the opportunity to grow into the scientist I am today. Your mentorship has helped me grow

and learn beyond what I hoped for, and I'm grateful for you. I never could have imagined I'd have published so soon, given so many talks, and even won the awards I did. Your drive to succeed is infectious, and I'm glad to have had your passion to emulate.

Dr. Basilis Zikopoulos, thank you for being the first one to introduce me to neuroscience. Thank you for entertaining my thousand-and-one questions at office hours, and for supporting my scientific endeavors. Your advice and mentorship were always insightful, critical, and immensely helpful.

Dr. Tara Moore, thank you for your kindness. You are always a smiling face to see, and your source of support has made BU a warmer place for me. Many of us often forget the humanistic nature of going through graduate school; you do not. Thank you for your critical insight into science, and for always being a positive influence on me.

Dr. Kathleen Morgan, thank you for your sharp intellect and critical examination of my work, since the beginning of my journey at BU. My experiences with you in your class and throughout my research journey have honed my perception and critical thinking. It has been a pleasure to know and learn from you.

Dr. Yumei Feng Earley, thank you for agreeing to serve as my external examiner. Your intellectual contribution to one of the most significant moments of my PhD as an expert in the field means a lot to me.

Dr. Dustin Allen, thank you for teaching me to teach. Your ability to engage your students is awe-inspiring. Your mastery of the classroom is one of the things that helped me find my passion to be an educator, and I'm so grateful to have learned from you.

Dr. Melissa Farb and Dr. Jessica Fetterman, thank you for being such inspiring humans. You both radiate such a wonderful passion for science and life, and have taught me things about being a scientist and a person. I appreciate all the coffees and lunches, and look forward to a science journey together.

Mandy Pinheiro, thank you for being my PhD buddy! We started together, and while I may be finishing now, I'll always be down for our end of semester celebrations and wine nights. You help drive me to ask better questions. You help me see the light in every situation. You're a wonderful person with a bright future.

Danka Charland, thank you for being an inspiration. Your tenacity and passion for learning has been helpful in keeping me motivated, and you truly are the pillar holding our program up.

The Faculty and Staff of the Department of Health Sciences, thank you for your encouragement and your support. You have all played a role in making this possible and I'm grateful for the environment you have all created.

Jack Ganey, Julia Hacker, Sheshank Mageshwar, Kate Pinson, and Rachel Steiner, thank you for being the OG cohort. I'm so happy to have started my BU journey with you. Our paths took us to different places, but our friendship will endure. You're all terrific scientists and smart, kind, funny people. BU Pub anyone?

Kayla Nist, Eric Abkin, and Katie Tafelski, thank you for being those goofy work friends. I appreciate you for all your hard work helping me get across the finish line both in and out of lab. You've made this experience great. Oh, also, has anyone seen the ratlas?

Dr. Sema Quadir, Dr. Veronica Go-Stevens, Dr. Chelsey LeBlang, and Kate Batterman, Thank you all so much for your friendship and your significant scientific contributions to my learning. You have all been wonderful pals and mentors to me, and I could not have grown nearly as much without you.

Alissa Frame and Franco Puleo, thank you for showing me the ropes. It took me an extra minute to get the hang of things here, but once I figured out that science is better with a healthy dose of sarcasm and tomfoolery, I settled in nicely. I appreciate your mentorship, friendship, and sass. Oh, and four words for you both.

Dr. Parul Chaudhary, Dr. Kiyoung Kim, and Dr. Mohammed Ferdaus, thank you for your insight into my work, your collaborative efforts, and your support in the lab. You were fantastic postdocs to work with, and wonderful people, too.

Jennifer Yoo, Jinyan Zhou, and Razie Amraei, thank you for both your friendship and your scientific contributions to these studies. You will all be excellent and I look forward to seeing how far you all go.

NEURAL MECHANISMS PROMOTING G-alpha-i2 PROTEIN DEPENDENT SALT-SENSITIVE HYPERTENSION IN THE SPRAGUE-DAWLEY RAT

JESSE DANIEL MOREIRA

Boston University, Sargent College of Health and Rehabilitation Sciences, 2021

Major Professor: Richard D. Wainford, Ph.D., Associate Professor of Pharmacology & Experimental Therapeutics, Associate Professor of Medicine, Boston University, School of Medicine; Associate Professor of Health Sciences, Boston University, Sargent College of Health and Rehabilitation Sciences

ABSTRACT

Hypertension (HTN) is a critical public health issue estimated to contribute to 10% of deaths worldwide. Additionally, the salt sensitivity of blood pressure, an exaggerated pressor response to elevated dietary sodium intake, is estimated to be present in approximately 50% of the hypertensive population and 25% of the normotensive population. This is a critical problem as the average American consumes roughly three times the daily sodium intake recommended by the American Heart Association.

Our laboratory has previously identified a critical role of Hypothalamic Paraventricular Nucleus (PVN) $G\alpha i_2$ proteins in the maintenance of salt resistance and normotension in the rat. Salt resistant rats such as the Sprague-Dawley (SD) rat site-specifically upregulate these proteins in response to elevated dietary sodium intake to facilitate sympathoinhibition, natriuresis, and normotension. In contrast, in the Dahl Salt Sensitive (DSS) rat, and in salt resistant rats in which this protein is experimentally downregulated, our laboratory has identified the development of renal nerve-dependent sympathoexcitation and salt-sensitive hypertension (ssHTN). However, the neural

mechanisms whereby PVN Gαi$_2$ proteins facilitate salt resistance are unclear. In addition, there is a robust literature in other rat models of HTN suggesting that both neuroinflammation in the PVN as well as an imbalance between PVN inhibitory GABAergic and excitatory glutamatergic signaling contribute to elevations in sympathetic outflow to promote HTN.

In this study, SD rats infused chronically with either targeted Gαi$_2$ oligodeoxynucleotides (ODNs) or control scrambled (SCR) ODNs and challenged with either normal (0.6% NaCl) or high-salt (4% NaCl) diets were used to demonstrate that 1) PVN microglial activation and associated pro-inflammatory cytokine production contribute to the development of Gαi$_2$ protein dependent ssHTN, 2) sex-dependent PVN microglial-mediated neuroinflammation precedes and likely drives the development of sympathoexcitation following high dietary sodium administration in male but not female Gαi$_2$ protein dependent ssHTN, and 3) PVN GABAergic and glutamatergic signaling is disrupted and imbalanced, favoring excitation over inhibition, following elevated dietary sodium intake in Gαi$_2$ protein dependent ssHTN. Together, these findings shed light on the pathological neural processes that occur in the absence of PVN Gαi$_2$ protein upregulation and reveal potential mechanistic targets in the management of ssHTN.

TABLE OF CONTENTS

LIST OF TABLES

LIST OF FIGURES

LIST OF ABBREVIATIONS

AC	Adenylate Cyclase
AHA	American Heart Association
AIC	Anti-Inflammatory Cytokine
ANOVA	Analysis of Variance
AP	Area Postrema
cAMP	cyclic Adenosine Monophosphate
CNS	Central Nervous System
CVLM	Caudal Ventrolateral Medulla
DBP	Diastolic Blood Pressure
DSR	Dahl Salt Resistant
DSS	Dahl Salt Sensitive
ELISA	Enzyme-Linked Immunosorbent Assay
$G\alpha i_2$	Guanine Nucleotide–Binding Protein Alpha Inhibiting Activity Polypeptide 2
GABA	Gamma-Amino Butyric Acid
GDP	Guanine Dinucleotide Phosphate
GPCR	G-protein Coupled Receptor
GTP	Guanine Trinucleotide Phosphate
HR	Heart Rate
HS	High Salt (4% Sodium Chloride)
HTN	Hypertension

ICV	Intracerebroventricular
IL	Interleukin
IML	Intermediolateral Cell Column
IP	Intraperitoneal
IV	Intravenous
MAP	Mean Arterial Pressure
MINO	Minocycline
mRNA	messenger ribonucleic acid
NaCl	Sodium Chloride
NE	Norepinephrine
NS	Normal Salt (0.6% Sodium Chloride)
NTS	Nucleus Tractus Solitarii
ODN	Oligodeoxynucleotide
OVLT	Organum Vasculosum Lamina Terminalis
PBS	Phosphate-Buffered Saline
PFA	Paraformaldehyde
PIC	Pro-Inflammatory Cytokine
PRA	Plasma Renin Activity
PVN	Paraventricular Nucleus
RAAS	Renin-Angiotensin Aldosterone System
RVLM	Rostral Ventrolateral Medulla
SBP	Systolic Blood Pressure

SC	Subcutaneous
SCR	Scrambled Control
SD	Sprague-Dawley
SD	Standard Deviation
SFO	Subfornical Organ
SNP	Single Nucleotide Polymorphism
SPRINT	Systolic Blood Pressure Intervention Trial
ssHTN	Salt-sensitive Hypertension
TNF	Tumor Necrosis Factor
UAGT	Urinary Angiotensinogen
WHO	World Health Organization

CHAPTER ONE: Introduction

Hypertension

Overview and Epidemiology

Hypertension (HTN), or high blood pressure, is a critical public health issue, estimated to be the leading global cause of death, contributing to 10.4 million deaths worldwide per year (Unger et al., 2020). HTN is also the leading cause of chronic kidney disease, stroke, and myocardial infarction (Lloyd-Jones et al., 2010; Dariush Mozaffarian et al., 2016). Normal blood pressure is defined as a systolic blood pressure (SBP) of less than 120 mmHg and diastolic blood pressure (DBP) of less than 80 mmHg. While stage 1 HTN was previously defined as SBP $\geq$ 140 mmHg and DBP $\geq$ 90 mmHg, the 2017 American College of Cardiology (ACC)/ American Heart Association (AHA) Blood Pressure Guidelines redefined Stage 1 HTN as SBP of $\geq$ 130 mmHg or a DBP of $\geq$ 80 mmHg, increasing the estimated prevalence of HTN to approximately 1 in 2 adults in the United States (Whelton et al., 2018).

Essential Hypertension

HTN can be categorized according to etiology. HTN resulting from an identifiable secondary cause, such as Cushing's Syndrome or renal artery stenosis, is known as secondary HTN, and account for approximately 5-10% of all cases of HTN (Unger et al., 2020). In contrast, HTN without an identifiable cause is considered primary, or essential HTN, and constitutes the rest of the cases of diagnosed HTN. Current medical management of HTN includes the use of what are called first-line antihypertensives, and include thiazide

diuretics, angiotensin II type 1 receptor antagonists, angiotensin-converting enzyme inhibitors, and calcium channel blockers (Wright, Musini, & Gill, 2018). There is a well-established body of literature demonstrating the benefit of reducing blood pressure in reducing HTN-related mortality and morbidity (Hardy et al., 2015; Rashid, Leonardi-Bee, & Bath, 2003). Moreover, the knowledge that reducing blood pressure reduces mortality has been highlighted by the very successful Systolic Blood Pressure Intervention Trial (SPRINT), which found a reduction of systolic blood pressure to <120 mmHg reduced cardiovascular-related and all-cause mortality at one year compared to standard treatment to a systolic blood pressure of <120 mmHg (Group et al., 2015). Effective blood pressure control in essential HTN is difficult to achieve, however, due to the variable and largely unidentified mechanisms contributing to the elevated blood pressure.

Human and animal studies of essential HTN have demonstrated that impairments may exist in one or several of the physiological body systems that contribute to the maintenance of blood pressure, including the renal, nervous, and endocrine systems (Oparil, Zaman, & Calhoun, 2003). There currently exist antihypertensive medications that target all of these systems, but which are prescribed without selectivity for the mechanisms specific to a hypertensive individual. Moreover, progress in generating novel antihypertensive medications has been stagnant in the 21st century (Shah & Stafford, 2017). Thus, there is a need to investigate the mechanisms contributing to essential HTN to identify novel therapeutic targets, as well as reduce HTN-related morbidity and mortality in the human population.

Salt-Sensitivity of Blood Pressure

Decades of research has highlighted an important role of dietary sodium intake in the pathogenesis of HTN (Frohlich & Varagic, 2004; Guyton, Coleman, Young, Lohmeier, & DeClue, 1980; Williams & Hollenberg, 1989). It is well documented that individuals who consume low dietary salt intakes have, generally, normal blood pressures while those who consumption exceed recommended amounts of sodium have a higher incidence of HTN (Guyton et al., 1980).

While those individuals who are salt-resistant possess mechanisms that facilitate sympathoinhibitory, natriuretic, and normotensive responses to an elevated dietary sodium intake (Brooks, Haywood, & Johnson, 2005; Lohmeier, Hildebrandt, & Hood, 1999; Osborn, Collister, & Guzman, 2008), those who display the phenotype of the salt-sensitivity of blood pressure, an exaggerated pressor response to elevated dietary sodium intake, display sympathoexcitation and a rise in blood pressure that is maintained for the duration of the elevation of salt intake (Brooks et al., 2005; Fujita & Fujita, 2013; Stocker, Monahan, & Browning, 2013). Moreover, the salt-sensitivity of blood pressure phenotype appears to be present in ≈ 50% of hypertensive and ≈ 25% of normotensive individuals (Franco & Oparil, 2006), and thus, this phenotype may account for a significant proportion of individuals with essential HTN. The salt sensitivity of blood pressure is particularly relevant in the US population given that the average American is consuming approximately 3.5 g of sodium per day, which is about three times the daily recommended sodium intake of 1.5 g per day by the AHA and 2 g per day recommended by the World Health Organization (WHO) (Appel et al., 2011; D. Mozaffarian et al., 2014; Whelton et al.,

2012). It is likely that, given the role of sympathoexcitation in salt-sensitive hypertension (ssHTN), there are impairments occurring in the autonomic nervous system regulation of fluid and electrolyte homeostasis.

Overview of Blood Pressure Regulation

Blood pressure is primarily determined by multiplying cardiac output and total peripheral resistance. Cardiac output is measured as heart rate (HR) multiplied by stroke volume, and reflects blood pumped by the heart per minute. Total peripheral resistance, the overall resistance to blood flow across the arteriolar vascular beds of the body, is principally determined by arteriolar radius and blood viscosity. The various factors that influence blood pressure are modulated through short-term (acute) and long-term (chronic) mechanisms to maintain a steady blood pressure and to accommodate challenges to fluid, electrolyte, and hemodynamic homeostasis.

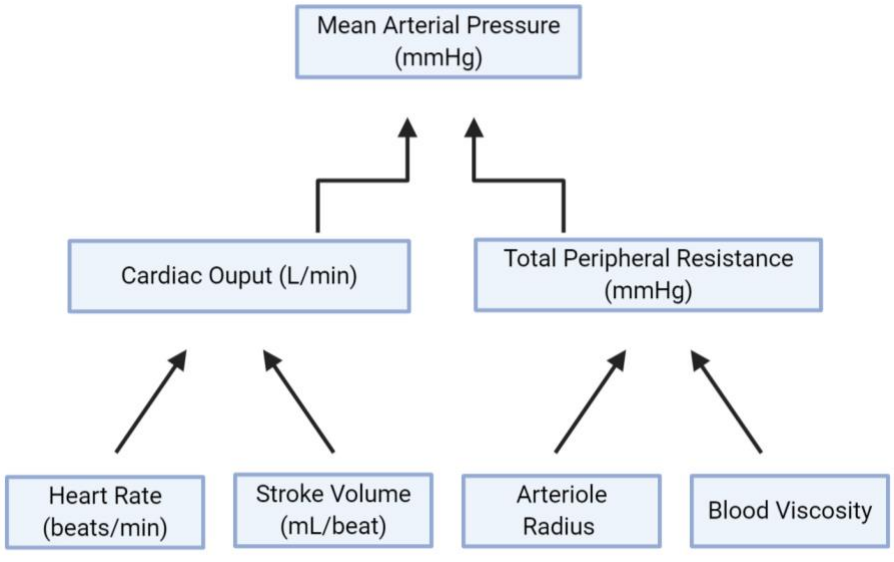

Figure 1.1: The primary determinants of Mean Arterial Pressure (MAP).

A schematic diagram demonstrating the breakdown of physiological factors impacting mean arterial pressure. Figure generated with BioRender software.

Short Term Regulation of Blood Pressure

Blood pressure maintenance is critical to organ blood flow and oxygen delivery. Acute challenges to blood pressure, such as shifting from a prone to standing position or rapid activity (e.g., running), are counteracted with physiological mechanisms intended to maintain normal blood pressure. In order to facilitate this phenomenon, the body must be able to detect blood pressure. The most commonly discussed and well-studied acute blood pressure regulatory mechanism is the carotid arterial baroreflex, intended to provide moment-to-moment feedback about carotid arterial blood pressure to the brain to maintain normal blood pressure (Cowley, Liard, & Guyton, 1973). The carotid baroreceptors, which are sensitive to stretch, identify a blood pressure set point and when pressure, sensed as carotid arterial stretch, changes, they respond accordingly via signaling up afferent glossopharyngeal fibers to the brainstem to modulate sympathetic and parasympathetic tone to the heart (Andani & Khan, 2020; Hart & Charkoudian, 2011).

Under normal circumstances, the carotid arterial baroreflex, which integrates with the brain stem cardiovascular control centers, will facilitate increased parasympathetic tone and inhibit sympathetic tone to lower blood pressure in response to elevations in blood pressure and resultant increases in carotid arterial stretch (Hart & Charkoudian, 2011). In HTN, however, it has been demonstrated that resetting of the carotid arterial baroreflex and associated decreases in baroreflex sensitivity allow higher mean arterial pressures to persist without reflex inhibition of sympathetic tone (Carmichael, Carmichael, Kuwabara, Cunningham, & Wainford, 2016; Lanfranchi et al., 1998; Yamamoto, Eubank, Franzke, & Mifflin, 2013).

Long-Term Regulation of Blood Pressure

While the carotid arterial baroreflex plays an important role in preventing blood pressure from temporarily deviating from a given set point moment-to-moment, neurohumoral mechanisms are largely important in determining and maintaining the set point for blood pressure itself. As previously mentioned, the principal factors that influence mean arterial pressure are cardiac output and total peripheral resistance.

Sympathetic nervous system activity is a particularly important long-term regulator of blood pressure due to its ability to influence both of the aforementioned factors. This will be described further in **Integrative Role of the Autonomic Nervous System in Fluid and Electrolyte Homeostasis (below),** but in brief the sympathetic nervous system release of catecholamines can stimulate the heart and elevate HR (positive chronotropy) and stroke volume (positive inotropy), the vessels to directly induce vasoconstriction and thus influence resistance, and the kidneys to directly influence sodium resorption and renin secretion, which drives renin-angiotensin-aldosterone axis activity. The renin-angiotensin-aldosterone system (RAAS) then acts further through its main effector angiotensin-II, which promotes further vasoconstriction, renal sodium resorption directly, and indirectly (via aldosterone), and vasopressin secretion from the posterior pituitary. Notably, both the sympathetic nervous system and the renin-angiotensin-aldosterone axis heavily influence fluid and electrolyte homeostasis by modulating sodium resorption at the kidney. This in itself highlights the role of electrolyte balance in promoting normotension, and implicates dysregulation of electrolyte homeostasis in HTN.

Integrative Role of the Autonomic Nervous System in Fluid and Electrolyte Homeostasis

Amongst the many mechanisms which are modulated to maintain electrolyte homeostasis in salt-resistance, the sympathetic division of the autonomic nervous system stands out in the HTN literature. While the heightened sympathetic outflow seen in HTN acts to increase blood pressure via vasoconstriction of arterioles, it also plays an important role in influencing sodium resorption in the kidney via action at adrenergic receptors (Frame, Puleo, et al., 2019; Mu et al., 2011; Tanoue et al., 2002). Overall hyperactivity of the sympathetic nervous system can heavily influence blood pressure by increasing sodium retention and disturbing fluid and electrolyte balance as a result.

Overview of the Sympathetic Nervous System

The sympathetic nervous system is structured such that each sympathetic nerve is the result of a multi-neuronal arc in which a preganglionic neuron and a postganglionic neuron come together to innervate a given structure (Figure 1.2). Preganglionic neurons have a cell body located in the intermediolateral cell column (IML) of the spinal cord between the thoracic and upper lumbar regions. These preganglionic neurons then project their axons to a ganglion, usually the paravertebral sympathetic ganglion trunk, where a synapse forms onto the cell body of a postganglionic neuron. The postganglionic neuron then projects to and innervates the target tissue (Figure 1.2).

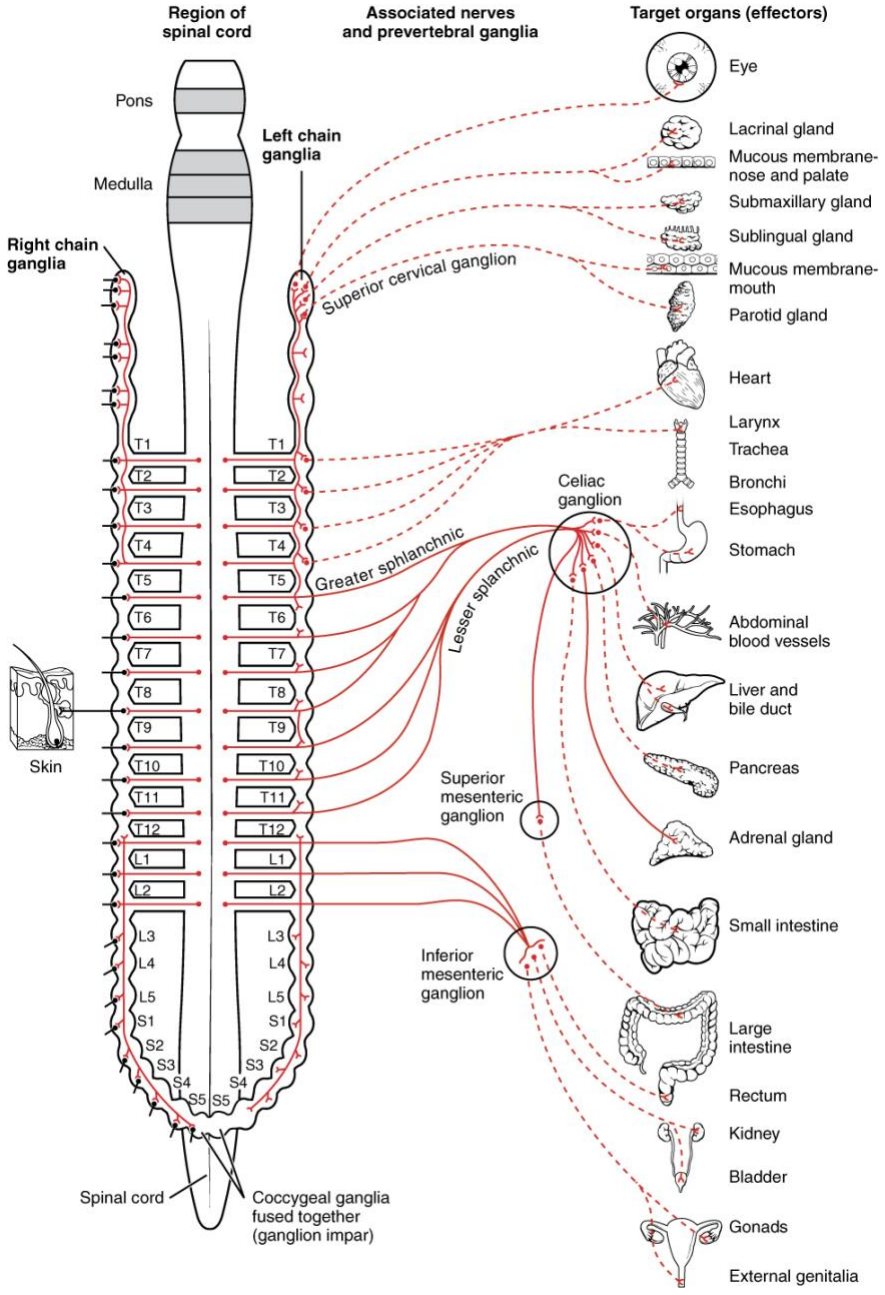

Figure 1.2 Overview of the anatomy of the sympathetic nervous system.

The sympathetic nervous system is comprised of preganglionic neurons residing in the lateral horn of grey matter between the upper thoracic and upper lumbar regions of the spinal cord, which project outward to the paravertebral sympathetic ganglion trunk or a lesser ganglion on either side of the spinal cord and synapse onto a postganglionic neuron, which then projects to the target tissue that it innervates. Reproduced from *Anatomy & Physiology* (College, 2020), download for free at http://cnx.org/content/col11496/latest. (Creative Commons Image Open Access).

The sympathetic nervous system uses the neurotransmitter norepinephrine (NE) to signal at the target site via postganglionic axonal fibers, and stimulation of the adrenal medulla by preganglionic fibers additionally releases epinephrine directly into the circulating blood. NE and epinephrine are catecholamine neurotransmitters. NE has an equal affinity for beta and alpha adrenergic receptors, but a high selectivity for alpha-adrenergic receptors, and then a lower selectivity for beta-adrenergic receptors, whereas epinephrine has no selectivity for a given adrenergic receptor, but a higher affinity for beta-2 adrenergic receptors. NE actions at alpha-adrenergic receptors are site-specific, but include vasoconstriction in the arterioles (Brodde, 1990) and sodium resorption in the kidney (DiBona, 1985; Elhawary & Pang, 1994). Epinephrine acts to heavily influence the heart, and exerts strong chronotropic and inotropic effects (Bristow et al., 1990).

The critical role of the sympathetic nervous system in fluid and electrolyte homeostasis and the resultant maintenance of normal blood pressure is highlighted by the many studies demonstrating that HTN is associated with enhanced central nervous system sympathetic outflow and dysregulation of sodium balance (Foss, Fink, & Osborn, 2013; Stocker, Madden, & Sved, 2010; Stocker et al., 2013).

The Role of Cardiovascular Control Centers in Blood Pressure Regulation

Although preganglionic sympathetic neurons are located in the IML of the spinal cord, the top-down control of the sympathetic nervous system is facilitated by neural control centers in the brain. For example, the brain stem, which facilitates the short-term control of blood pressure via descending pre-sympathetic projection neurons to the IML, is the control center integrating and controlling the carotid arterial baroreflex. In this

example, ascending information about acutely increased blood pressure sensed as increased arterial stretch synapses in the brain stem at the Nucleus Tractus Solitarii (NTS). The NTS then sends an excitatory projection to the Caudal Ventrolateral Medulla (CVLM), which when activated will inhibit the Rostral Ventrolateral Medulla (RVLM). Inhibition of the RVLM decreases cardiovascular sympathetic outflow, which is normally driven by activity of the RVLM. This reflex thus facilitates a decrease in blood pressure via a reduction in cardiac output (Machado, 2001).

While brain stem centers reflexively contribute to the regulation of blood pressure via the input of sensory afferent nerves, they are also in communication with and influenced by higher brain centers such as the Paraventricular Nucleus (PVN) of the hypothalamus and the circumventricular organs, including the Subfornical Organ (SFO), Organum Vasculosum Lamina Terminalis (OVLT), and the Area Postrema (AP). Each of these regions performs a function in exerting top-down control of neural-cardiovascular autonomic integration. For example, the PVN is understood to be involved in the regulation of cardiovascular function via integration of peripheral sensory nerves, particularly the renal nerves (Caverson & Ciriello, 1988; Simon & Ciriello, 1989), and has been shown to influence both cardiac and renal function (Carmichael et al., 2020; Coote, 1995; Kannan, Hayashida, & Yamashita, 1989). The AP is well-connected to the NTS and in studies of cardiovascular function, AP lesions are demonstrated to alter neuronal activation markers in the NTS and other neural control regions (Kato et al., 2004). Like the AP, the SFO influences cardiovascular function. The SFO is understood to sense changes in central sodium in the cerebrospinal fluid through chemoreceptors, and influence autonomic

function via top-down control of the PVN and the brain stem nuclei to restore electrolyte homeostasis and maintain normal blood pressure (Hiyama & Noda, 2016; Hiyama, Watanabe, Okado, & Noda, 2004).

Central Mechanisms in Blood Pressure Regulation

Since the 20th century, significant advancements in research techniques in neuroscience and physiology have helped researchers begin to identify the previously largely unknown mechanisms whereby the central nervous system influences blood pressure. Over the past several decades, as mentioned in the previous section, multiple brain sites have been identified as playing a role in both the normal regulation of blood pressure and in contributing to the dysfunction seen in HTN.

A significant amount of research has been done to understand central neural dysfunction in HTN, and many researchers have identified critical central targets of peripheral hormones such as angiotensin-II which contribute to hypertension (Marques-Lopes et al., 2017; P. Shi et al., 2010), as well as the existence of centrally-derived angiotensinergic pathways in the brain and the existence of the central pro-renin receptor, which can both contribute to the excessive sympathetic activity seen in HTN (Mohsin et al., 2020; Souza et al., 2019; Xue, Zhang, & Johnson, 2020). Moreover, researchers have provided us with an understanding of the dynamic, bidirectional interactions between multiple brain regions such as the PVN and the SFO to coordinate homeostatic responses to fluid and electrolyte perturbations such as excessive salt intake in both salt-sensitive and salt-resistant animals (Dampney, Michelini, Li, & Pan, 2018; Stocker et al., 2013).

The Paraventricular Nucleus as an Integrative Cardiovascular Control Center

Of the many critical cardiovascular regulatory centers mentioned above, the PVN is an exceptionally important cardiovascular control center in the brain which exerts direct, top-down control over the sympathetic nervous system to regulate fluid and electrolyte homeostasis, cardiac function, and overall blood pressure, predominantly through its impact on renal sodium handling. Anatomically, the PVN is divided into a parvocellular preautonomic region, and a magnocellular neuroendocrine region (Swanson & Kuypers, 1980; Swanson & Sawchenko, 1980).

Afferent signals arriving at the PVN come from a variety of central and peripheral locales. For example, the SFO projects to the PVN to influence PVN control of sympathetic outflow in response to centrally sensed sodium (Ferguson, Latchford, & Samson, 2008). Moreover, the afferent renal sensory nerves have been demonstrated to influence PVN neuronal activation and under normal conditions facilitate a sympathoinhibitory reflex to perturbations in fluid and electrolyte homeostasis via both mechanosensitive and chemosensitive mechanisms to maintain normotension (Frame, Carmichael, Kuwabara, Cunningham, & Wainford, 2019; Ye et al., 2020).

Tracer studies have shown that the PVN has two predominant subdivisions, with corresponding efferent projections. The magnocellular division of the PVN possess projections to the pituitary gland, reflecting its role in neuroendocrine control (Swanson & Kuypers, 1980), while the parvocellular divisions of the PVN project to various regions relevant in cardiovascular control, including the RVLM to influence cardiac sympathetic activity (Koba et al., 2018), and the thoracic spinal cord to influence global sympathetic

outflow via the IML (Swanson & Kuypers, 1980). The renal sympathetic efferent nerves have fibers directly originating in the inferior mesenteric ganglion (Figure 1.3), but which stem from centrally originating PVN neurons via a multisynaptic pathway beginning in the PVN and are a significant effector of PVN sympathetic control of blood pressure (Wang et al., 2013; J. H. Yang, Choi, & Gwon, 2013), influencing sodium handling via renal adrenergic receptors (DiBona, 1985; Elhawary & Pang, 1994).

Multiple studies reflect the importance of PVN neuronal activity in modulating blood pressure, and further provide evidence that aberrant PVN function is important in the pathogenesis of HTN (Carmichael et al., 2020; Fujita & Fujita, 2016; Gabor & Leenen, 2009; Jiang et al., 2018; Ribeiro, Panizza Hdo, Santos, Ferreira-Neto, & Antunes, 2015).

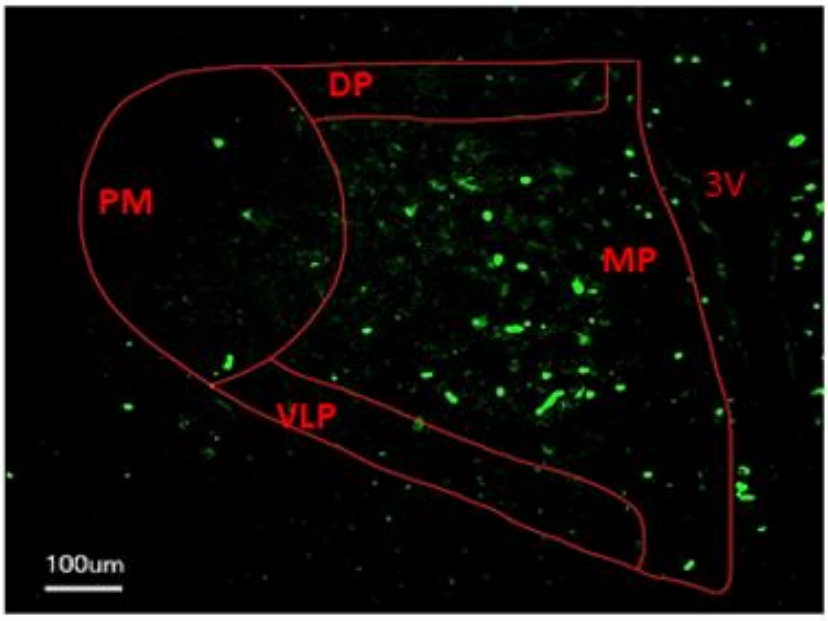

Figure 1.3 Anatomical subcategories of Paraventricular Nucleus subnuclei.

The principal subdivisions of the PVN contain neurons projecting to various regions. First, parvocellular subdivisions (MP, VLP, DP) contain neurons projecting to the median eminence

and spinal sympathetic centers. Second, magnocellular subdivisions (PM) contain neurons projecting to the pituitary to control hormonal release.

Basic Structure and Function of GPCRs

G-protein coupled receptors (GPCRs), seven-pass transmembrane proteins coupled to intracellular signal transduction proteins, represent a large class of membrane receptor proteins in the Central Nervous System (CNS) responsible for neurotransmission, and serve several other physiological roles in the body (Rosenbaum, Rasmussen, & Kobilka, 2009). Intracellularly, these receptors are bound to a G-protein α-subunit, and a heterodimerized βγ-subunit (Flock et al., 2017). At resting states, and without ligand binding, the α-subunit is bound to guanine-dinucleotide phosphate (GDP). Upon ligand binding, the α-subunit switches out its bound GDP for guanine trinucleotide phosphate (GTP) and becomes active, dissociating away from the receptor complex to act in a manner specific to its subtype. Additionally, upon ligand binding, the βγ-subunit dissociates to perform various context-dependent functions.

With respect to the subtypes of G-protein α-subunits, there are four classically recognized categories. Gα(s) subunits are stimulatory to the enzyme adenylate cyclase (AC) and increase concentrations of the intracellular secondary messenger cyclic adenosine monophosphate (cAMP). Gα(i/o) and Gα(z) subunits are inhibitory and inhibit AC to reduce cAMP levels. Lastly, Gα(q) proteins work to activate phospholipase C, which results in intracellular calcium signaling as a secondary messenger (Flock et al., 2017).

Gαi2 Proteins and Blood Pressure

While some of the central mechanisms involved in the regulation of blood pressure, as discussed above, have been identified, certain central pathways remain incompletely understood. Our laboratory has identified a novel role of PVN-specific GPCR-coupled Guanine Nucleotide–Binding Protein Alpha Inhibiting Activity Polypeptide 2 (Gαi2) proteins in mediating PVN responses to both acute and chronic perturbations to fluid and electrolyte homeostasis and in the maintenance of salt-resistance and normotension under these conditions.

Gαi2 Proteins and Acute Blood Pressure Regulation

First, utilizing either control scrambled (SCR) or targeted Gαi2 antisense oligodeoxynucleotide (ODN) intracerebroventricular (ICV) administrations, which have been well-demonstrated to result in target-specific protein downregulation following oligodeoxynucleotide DNA- complementary mRNA hybridization (Hadjimarkou, Silva, Rossi, Pasternak, & Bodnar, 2002; Silva et al., 2000; Wainford & Kapusta, 2012), our laboratory has assessed the physiological role of PVN Gαi2 proteins in mediating responses to acute stimuli. In SCR ODN pretreated rats, ICV administration of the α2-adrenergic receptor agonist guanabenz evoked decreases in MAP and HR, as well as inducing diuresis and natriuresis. In contrast, Gαi2 ODN pretreated rats did not display the natriuretic or the hypotensive response, suggesting specificity of the Gαi2 protein in mediating central α2-adrenergic receptor-dependent hypotensive and natriuretic pathways (Wainford & Kapusta, 2012).

In further studies, acute physiological challenges were provided using a similar paradigm pretreating salt-resistant rats with either SCR or Gαi$_2$ ODNs. For example, following a 5% body weight isotonic volume expansion, SCR pretreated rats displayed a robust sympathoinhibitory response seen as a decrease in measured renal sympathetic nerve activity, which facilitated natriuresis. Pretreatment with Gαi$_2$ ODNs significantly attenuated this response, and demonstrated the role of PVN Gαi$_2$ proteins in mediating sympathoinhibitory responses to acute vole expansions (Kapusta, Pascale, & Wainford, 2012). Additionally, in a study conducted using a 3M sodium chloride bolus infusion, pretreatment with Gαi$_2$ ODNs significantly impaired neuronal activation assessed via immunohistochemistry, natriuresis, suppression of plasma NE, and time to restore MAP to baseline (Carmichael et al., 2016). These studies together, among other acute paradigms our laboratory has performed, suggest a critical role of PVN Gαi$_2$ proteins in responding to acute perturbations to both fluid and electrolyte homeostasis and in the acute regulation of blood pressure.

Gαi$_2$ Proteins and Chronic Blood Pressure Regulation

Our laboratory additionally demonstrated the role of PVN Gαi$_2$ proteins in mediating sympathoinhibitory and normotensive responses to chronic challenges, such as an elevated high dietary sodium intake. Over several studies, we have identified that in SCR ODN infused salt-resistant rats, a chronic high-salt diet evokes site-specific upregulation of PVN Gαi$_2$ proteins (Kapusta et al., 2012), decreases in plasma NE content indicative of sympathoinhibition (Kapusta, Pascale, Kuwabara, & Wainford, 2013; Kapusta et al., 2012), and normotension. In contrast, Gαi$_2$ ODN infused rats fed a high salt

diet displayed elevations in plasma NE, indicative of sympathoexcitation, (Kapusta et al., 2013; Kapusta et al., 2012) as well as sodium retention and elevated MAP, suggestive of the development of ssHTN (Kapusta et al., 2013).

A recent report from our laboratory further supports the role of $G\alpha i_2$ proteins in mediating normotensive responses to elevations in dietary sodium intake, and extends our findings to suggest site-specificity of the role of $G\alpha i_2$ proteins in salt-resistance by utilizing a PVN-specific infusion of $G\alpha i_2$ ODNs to site-specifically induce knockdown. Even with the $G\alpha i_2$ protein knockdown occurring solely in the PVN, $G\alpha i_2$ ODN infused rats displayed significant elevations in plasma and renal NE, indicative of global and renal sympathoexcitation, and elevations in sodium retention and MAP suggesting the development of ssHTN to an equivalent magnitude as seen in whole-CNS $G\alpha i_2$ protein knockdowns achieved via ICV ODN infusion (Carmichael et al., 2020).

Altogether, studies from our laboratory have demonstrated a critical role of PVN $G\alpha i_2$ proteins in the neural signaling networks designed to respond to disturbed fluid and electrolyte balance. The presence of these proteins is necessary for proper sympathoinhibitory and natriuretic responses to acute volume loading, as well as to chronic elevations in dietary sodium intake. Additionally, the absence of these proteins results in a failure to properly facilitate these salt-resistant mechanisms and instead facilitates the development of ssHTN.

The Role of Excitation-Inhibition Coupling in Hypertension

The central nervous system plays a clear, significant role in maintaining normal blood pressure as well as fluid and electrolyte homeostasis via facilitating alterations to

autonomic outflow in response to stimuli. In HTN, it has been demonstrated that appropriate changes to maintain normal blood pressure and fluid and electrolyte balance are not made (Carmichael et al., 2020; Ferreira-Junior et al., 2019; Korpal, Han, Schwenke, & Brown, 2017; Li & Pan, 2010; Stern et al., 2012; Wainford, 2014). In many of these studies, it has been shown that the failure to make these homeostatic changes likely represent alterations to firing in, and possibly alterations in the phenotypic composition of, neuronal populations in cardiovascular control centers. However, the literature is not entirely clear on the origin and homogeneity of these changes across different models of HTN.

Basics of Neurotransmission

Neurons are classified in many ways, but predominantly according to the function role of the neurotransmitter they release. Neurons expressing gamma-amino-butyric acid (GABA), for example, are classified as the predominant inhibitory neuronal population in the CNS, as the release of GABA from their synaptic terminals exerts a suppressive effect on the firing of the receptive neuron(s) via a local hyperpolarizing effect (Ngo & Vo, 2019). Glutamate, in contrast, is the predominant excitatory neurotransmitter in the CNS, which when released at the synapse produces a local depolarizing effect on the receptive neuron, increasing the chance of a firing event occurring in that receptive neuron (Palmada & Centelles, 1998; Tapiero, Mathe, Couvreur, & Tew, 2002). Additional neurotransmitters in the brain are known as neuromodulatory, and through their respective receptors can influence the receptiveness of given neurons to GABA and glutamatergic neurotransmission.

With respect to signaling in the PVN, many studies have highlighted the role of both GABAergic and glutamatergic neurons, amongst many neuromodulatory neuronal phenotypes such as adrenergic neurons, in the physiological regulation of blood pressure, with a particular focus on the normotensive role GABAergic neurons appear to play, along with the influence of noradrenergic signaling on sympathoinhibition (Ferreira-Junior et al., 2019; Korpal et al., 2017; Nishihara, Takesue, & Hirooka, 2017; Patel, 1991; Takenaka et al., 1996; Wainford & Kapusta, 2012).

GABAergic Signaling and Blood Pressure Regulation

GABA, as the principal inhibitory neurotransmitter in the nervous system, stands to play a significant role in dampening neuronal firing events that if unchecked would be pathological. As such, it is not entirely surprising to find that there is a well-studied reduction in GABAergic input to the PVN in many models of HTN and that many therapeutic interventions appear to normalize blood pressure via restoration of GABAergic input (Ferreira-Junior et al., 2019; Li & Pan, 2006; Nishihara et al., 2017). What remains unclear, and controversial across different studies, is the role of the GABA(A) receptor, a ligand-gated ion channel functioning to quickly hyperpolarize the postsynaptic cell via influx of chloride anions, versus the GABA(B) receptor, a metabotropic G-protein coupled receptor which serves to reduce intracellular cAMP concentrations as well as active inwardly rectifying potassium channels, amongst other functions to result in a slow hyperpolarization (Jembrek & Vlainic, 2015; Kuriyama, Hirouchi, & Nakayasu, 1993; Nakayasu, Kimura, & Kuriyama, 1995). GABA(B) receptors, in particular, are of interest as previous studies have identified them as coupled to Gαi-subunit proteins, and they have

been shown to localize to both presynaptic terminals to inhibit neurotransmitter release, as well as postsynaptic membranes to hyperpolarize neurons (Cheng, Wang, Schmid, & Han, 2014; Jembrek & Vlainic, 2015).

Glutamatergic Signaling and Blood Pressure Regulation

Like GABA, glutamate signaling, as the principal excitatory neurotransmitter in the brain, represents another important component of blood pressure regulation as a certain degree of excitatory tone drives sympathetic outflow necessary to maintain appropriate global vascular tone, as well as fluid and electrolyte balance at the kidney. A fine balance exists, however, and enhancement of glutamatergic tone, either intrinsically or through a reduction in GABAergic regulation of glutamatergic tone, can result in excessive sympathetic activity and elevated blood pressure (Gabor & Leenen, 2012b; Li & Pan, 2017) and is a documented feature of HTN.

The Role of Neuroinflammation in Hypertension

In many models of hypertension, it is becoming increasingly clear that in addition to changes in neuronal function in cardiovascular control centers, there are disturbances to neural immune cells that in turn contribute to the development of salt-sensitive HTN. The brain possesses, amongst many cell types, two cell types which have been demonstrated to contribute in various ways to the development of multiple forms of HTN. Microglia, the resident innate-immune cells of the brain, may become activated or reactive by a whole host of pathological stimuli and in turn drive inflammatory processes linked with the development of HTN (Biancardi, Stranahan, Krause, de Kloet, & Stern, 2016; Gilman, Mitchell, Daws, & Toney, 2019; Sharma et al., 2018; P. Shi et al., 2010). Additionally,

astrocytes, neural stem cell-derived glia which play a role in tissue homeostasis, neurotransmitter reuptake, vascular integrity, and more (Pekny, Wilhelmsson, & Pekna, 2014; Verkhratsky & Nedergaard, 2018) have been demonstrated to respond to insults by producing cytokines and chemokines and generating their own processes which drive neural activity in HTN (Stern et al., 2016).

Microglia, Astrocytes, and Neuroinflammation

Microglia, the innate immune cells of the brain, are key mediators of neuroinflammation. Microglia constantly survey the surrounding tissue in their respective domains to help maintain normal tissue function, clear debris and pathogens, and support neural function (Miron & Priller, 2020). When microglia encounter pathogens, or are otherwise stimulated via pro-inflammatory signal cascades, their morphology changes and they become reactive or activated. These activated microglia then behave as classic macrophage-like cells and engulf targets, produce and release pro-inflammatory cytokines (PIC) and reactive oxygen species, and produce an overall inflammatory microenvironment to resolve the issue (Rodriguez-Gomez et al., 2020). As such, microglia are key drivers of neuroinflammation.

In certain diseases, including HTN, it has been well documented that microglia may remain persistently active and propagate an inappropriate and chronic inflammatory response, ultimately making conditions worse through changing neuronal function or resorption of synapses (Biancardi et al., 2016; Galic, Riazi, & Pittman, 2012; Gerber et al., 2018; Kaur, Sharma, & Deshmukh, 2019; X. Z. Shen et al., 2015). The production of PICs

has been demonstrated to alter neuronal firing and other intrinsic properties (Galic et al., 2012), and active microglia may even engulf and phagocytize synapses (Roy et al., 2020).

Astrocytes are critical regulators of central nervous system homeostasis. Astrocytes maintain extracellular pH, reuptake excess neurotransmitters such as glutamate, and contribute end-foot processes to the blood brain barrier to protect the nervous system from toxins and pathogens (Verkhratsky & Nedergaard, 2018). In addition, astrocytes may become reactive in response to noxious stimuli (Pekny et al., 2014) and contribute to neuroinflammatory responses in multiple diseases, including HTN (Stern et al., 2016), via production of PICs as well as chemokines which recruit other immune cells such as microglia and macrophages to respond.

Impacts of Cytokines on Neural Control Centers

Mechanistically, neuroinflammation has been linked to changes in neuronal activity via the production of certain PICs which can impact neuronal firing (Chen et al., 2017; Clarkson, Kahoud, McCarthy, & Howe, 2017). Following injury or insult, activated microglia release local inflammatory mediators such as interleukins (IL) or tumor necrosis factor (TNF) which bind to receptors on neurons and intrinsically change firing properties. The significance of this in the context of neurogenic hypertension is that locally released cytokines may increase intrinsic firing rates of spinally projecting PVN neurons, or neurons in other cardiovascular control centers, to enhance sympathetic tone. Supporting this, several studies have confirmed through a multitude of interventions that significant neuroinflammation is present in hypertensive animals compared to normotensive controls (Du et al., 2017; Jiang et al., 2018; Segiet, Smykiewicz, Kwiatkowski, & Zera, 2019; P.

Shi et al., 2010), and that suppression of local inflammation or inflammatory signaling pathways in cardiovascular control centers dampens sympathetic outflow and the magnitude of HTN (Qi et al., 2019; P. Shi et al., 2010). These studies together implicate neuroinflammation not just as a minor component of HTN, but as a significant determinant of hypertensive magnitude and thus represent a mechanistic target to be further studied as well as considered for therapeutic intervention.

Sex-Specificity and Hypertension

In both human populations and in animal studies, research has identified an effect of sex on both the development, maintenance and magnitude of HTN. In human premenopausal females, who still produce estrogens and other sex steroid hormones, there is a resistance to HTN, as well as other cardiovascular diseases (Ashraf & Vongpatanasin, 2006; Dubey, Oparil, Imthurn, & Jackson, 2002). Many studies have attempted to identify the mechanisms whereby estrogens exert their cardioprotective effects, and some have been delineated while others remain unknown.

With respect to the mechanisms influencing blood pressure, estrogens in females have been demonstrated to protect against excessive vasoconstriction (J. G. Kim et al., 2018; Riedel et al., 2019), renal and cardiac oxidative injury (Ozdemir Kumral et al., 2016), coronary artery remodeling (Matrai et al., 2016), overactivation of the RAAS pathway (da Silva et al., 2019), and pro-inflammatory neuroimmune cell activity (Singh, Song, Dutta, Gonzalez, & Malik, 2020). Additionally, the literature has shown not only an antihypertensive effect of estrogens in animal studies, but also a prohypertensive effect of testosterone, the male sex steroid hormone (Mishra, More, Gopalakrishnan, & Kumar,

2019; Pingili et al., 2015), reinforcing the findings of human trials demonstrating that males are more susceptible to HTN than premenopausal women, and providing potential mechanisms.

Sex and Inflammation

With respect to inflammation as a recently renewed topic of interest in studies of the mechanisms mediating HTN, there has also been the identification of a sex-dependency to inflammation as estrogens have been shown to exert a strong anti-inflammatory effect on immune cells. Studies in models of HTN, as well as in other diseases, have shown that estrogens act both in the CNS on microglia and astrocytes (Lee, Choi, Ju, & Yune, 2018; Singh et al., 2020) as well as on peripheral immune cells (Ni et al., 2019). While these studies aren't as numerous as other studies in HTN, they are beginning to provide mechanistic insight into the ways in which estrogens protect against newly identified inflammatory pathways that cause damage to, and induce changes in, nearby cells in the brain and in the peripheral organs such as the kidney to worsen HTN.

Sex and the PVN

The PVN, as discussed in the section **Integrative Role of the Autonomic Nervous System in Fluid and Electrolyte Homeostasis (above),** is a critical regulator of blood pressure via its output influencing both neuroendocrine and autonomic function. Research over the past several years, aimed at identifying mechanisms involved in observed sex differences in HTN, has sought to understand if there are anatomic differences in the PVN that may account for the heightened sympathetic tone seen in male but not female models

of HTN. Interestingly, several studies identified a lack of sex differences in the PVN with respect to neuronal distribution and receptor distribution, but were able to determine that the PVN is a specific site for high expression of sex steroid hormone receptors, particularly the Estrogen Receptor-β (Kanaya, Higo, & Ozawa, 2019; Stern & Zhang, 2003), which some functional studies suggest may play a role in dampening excessive excitation (Gingerich & Krukoff, 2006; Jonklaas & Buggy, 1984). These studies just highlight potential mechanisms, however, and the full influence of estrogens on the PVN remains unknown.

Hypothesis and Specific Aims

Hypothesis

PVN $G\alpha i_2$ proteins gate anti-inflammatory and neuronal inhibitory pathways, facilitating sympathoinhibitory and normotensive responses to elevated dietary sodium intake in salt-resistant Sprague-Dawley (SD) rats.

Specific Aims

Specific Aim 1*:* To establish that PVN-specific $G\alpha i_2$ proteins protect against the activation of sex- and sodium-dependent neuroinflammatory pathways in salt-resistant male SD rats. In brief, rats will be instrumented with an intracerebroventricular (ICV) cannula to infuse control or targeted oligodeoxynucleotides (ODN), placed on a normal (NS) or high (HS) salt diet, and several parameters will be assessed over a time course including sodium balance and blood pressure. At the end of these studies, animals will be euthanized and tissue harvested for analysis of brain immune cells and cytokines via

immunohistochemistry, plasma and urine hormones via ELISA, and protein expression via western blot.

Specific Aim 2*:* To establish that PVN-specific $G\alpha i_2$ proteins facilitate inhibitory neurotransmission and sympathoinhibitory responses to high sodium in male SD rats. In brief, rats will be instrumented with either an ICV or PVN cannula to infuse control or targeted ODNs and then placed on NS or HS diet. Rats will then be instrumented for the measurement of blood pressure and responses to PVN microinjections of various receptor antagonists. Finally, tissue will be harvested from euthanized rats for analysis of neuronal phenotypic markers in the brain by in situ hybridization.

CHAPTER TWO: General Methods

This chapter contains detailed descriptions of the surgical procedures, in-vivo studies, and molecular and analytical techniques used in Chapters 3–5. Chapters 3–5 each contain a brief, chapter-specific methods section which provide a context-specific overview referring to the methods detailed below.

Animals

Male and female Sprague-Dawley (SD) rats weighing 275–299 g and 200–225 g (approximately 3 months of age), respectively, were purchased from Envigo (Indianapolis, IN, USA). All animals were pair-housed prior to surgical intervention and single-housed post-intervention. Animals were housed at all times in a temperature-controlled (20-26°C) and humidity-controlled (30–70%) facility under a 12-hour light-dark cycle. Tap water and standard rodent diet (Teklad, Envigo, Indianapolis, IN, USA) or experimental high sodium diet (Teklad, Envigo, Indianapolis, IN, USA) (detailed in Table 2.1 below) *ad libitum*. All animals were randomly assigned to experimental groups and all study personnel were blind to group assignment. All animal protocols were approved by the Boston University Institutional Animal Care and Use Committee in accordance with the National Institutes of Health *Guide for the Care and Use of Laboratory Animals* (8th edition).

Parameter	Standard (Normal Salt or NS) Diet	Experimental (High Salt or HS) Diet
total NaCl content	0.6% (174 mEq Na+/kg)	4% (678 mEq Na+ /kg)
Total K^+ content	0.6%	0.8%
Total Fiber	5%	3%
Total Protein	18%	19%
Crude Fat	5%	5%

Table 2.1 Components of Teklad Standard Normal Salt and Experimental High Salt Diets.

Surgical Procedures

Intracerebroventricular Cannula and Subcutaneous Osmotic Minipump Implantation

Animals were first anesthetized with intraperitoneal (IP) Ketamine/Xylazine (Ketamine 30 mg/kg IP + Xylazine 3 mg/kg IP). An incision was then made on the ventral neck, rostral to the scapulae, and a pocket was made in the subscapular region. A subcutaneous (SC) osmotic minipump with an infusion rate of 6 µL/day and a max fill volume of approximately 200 µL (Model 2004, Alzet, Cupertino, CA, USA) was placed into the SC pocket. Then, the animal was placed in a stereotaxic headholder (Stoelting Co., Wood Dale, IL, USA) and implanted with a stainless steel cannula (P1 Technologies, Roanoke, VA, USA) into the right lateral cerebral ventricle utilizing coordinates from Paxinos and Watson *The Rat Brain* atlas (AP -0.3 mm from bregma, ML +1.3 mm from bregma, DV -4.5 mm from the skull surface) (Kapusta & Kenigs, 1999; Paxinos & Watson, 2007). This cannula was connected via silastic tubing to the SC minipump, such that an infusion of either control scrambled (SCR) or targeted $G\alpha i_2$ oligodeoxynucleotides (ODNs) would infuse at a rate of 25 µg/ 6 µL/ day. The cannula was cemented in place and the wound on the back of the neck was sutured closed.

A National Center for Biotechnology Information Basic Local Alignment Search Tool was used to determine i.) that the SCR ODNs possessing the sequence (5′-GGGCGAAGTAGGTCTTGG-3′) would not target any known brain mRNA in the rat brain (*Rattus norvegicus*) and ii.) that the targeted $G\alpha i_2$ ODNs possessing the sequence (5′-CTTGTCGATCATCTTAGA-3′) were sequence-specific to the mRNA for the rat $G\alpha i_2$ sequence, and would not result in unwanted knockdown of off-target mRNA. Moreover,

these sequences have been highly validated in prior studies from our lab and others (Carmichael et al., 2016; Carmichael et al., 2020; Rossi, Standifer, & Pasternak, 1995; Standifer, Rossi, & Pasternak, 1996; Wainford, Carmichael, Pascale, & Kuwabara, 2015; Wainford & Kapusta, 2012).

PVN Cannula and Subcutaneous Osmotic Minipump Implantation

In a subset of studies outlines in Chapter 5, animals received an infusion of either control SCR ODNs or targeted $G\alpha i_2$ ODNs, with the same sequences and validations as mentioned in the section *Intracerebroventricular Cannula and Subcutaneous Osmotic Minipump Implantation*, directly into the PVN to assess the impact of site-specific downregulation on cardiovascular function compared to whole CNS downregulation as occurs during ICV infusion, as previously described (Carmichael et al., 2020). Animals were anesthetized with intraperitoneal (IP) Ketamine/Xylazine (Ketamine 30 mg/kg IP + Xylazine 3 mg/kg IP). An incision was then made on the ventral neck, rostral to the scapulae, and a pocket was made in the subscapular region. Two osmotic minipumps, each with an infusion rate of 3.6 μL/day and a max fill volume of approximately 150 μL (Model 2006; Alzet, Cupertino, CA, USA) were inserted into the SC pocket. The animal was then placed in a stereotax and stereotaxically implanted with a bilateral stainless steel cannula (P1 Technologies, Roanoke, VA, USA) into the PVN utilizing coordinates from Paxinos and Watson *The Rat Brain* atlas (AP -1.8 mm from bregma, ML ±0.5 mm from bregma, DV -8.0 mm from the skull surface) (Paxinos & Watson, 2007). Cannulation site was confirmed at the end of the study when microinjections of L-glutamate (15 nmol/side) were made into the PVN to elicit a pressor response. Animals lacking the pressor response were

considered mis-cannulations (Carmichael et al., 2020). The PVN cannulas were connected one per side via silastic tubing to the respective SC minipump, such that an infusion of either control SCR or targeted $G\alpha i_2$ ODNs would infuse at a rate of 300 ng/ side / day. The cannula was cemented in place and the wound on the back of the neck was sutured closed.

Chronic Radiotelemeter Implantation and MAP Measurement

In Chapter 3, we describe the radiotelemeter implantation that was performed and used to assess the chronic changes in MAP occurring in male SD rats following either targeted $G\alpha i_2$ or control SCR ODN ICV infusion. Five days before ICV cannula implantation, animals were anesthetized with IP Ketamine/Xylazine (Ketamine 30 mg/kg IP + Xylazine 3 mg/kg IP) and the femoral triangle was shaved and an incision was made. A radiotelemetry device (PA-C40; Data Sciences International, New Brighton, MN, USA) was implanted via a cannula into the abdominal aorta via the left femoral artery and the telemeter was stored in a SC pocket. The wound was closed and sutured and the animals received buprenorphine for 48 h after radiotelemetry probe implantation (0.05 mg kg^{-1} s.c.). Radiotelemetry data were collected via scheduled sampling for 10 s every 10 min in all groups of rats, stored and analyzed using Dataquest A.R.T. v.4.2 software (Data Sciences International, St. Paul, MN, USA).

Acute Femoral Artery and Vein Cannulation and MAP Measurement

In Chapters 4-5, we describe the MAP that was assessed via an acute cannulation protocol at the end of dietary sodium intake and ODN infusion studies. Animals were anesthetized with Sodium Brevital IP (Sodium Brevital 20 mg/kg IP + 10 mg/kg

Intravenous (IV) as needed). The left femoral triangle was shaved and then dissected to isolate the femoral vein. The left femoral vein was cannulated using a PE50 catheter for the infusion of IV anesthetics and IV isotonic saline, and the left femoral artery cannulated in the same manner for the measurement of MAP. Rats were placed in a plexiglass rat holder and an isotonic infusion of saline (20 μL/min IV) was given over a 2-hour recovery period allowing rats to return to full consciousness and stable renal and cardiovascular function. MAP and heart rate (HR) were recorded continuously via the femoral artery cannula using computer driven BIOPAC data acquisition software (MP150 and AcqKnowledge 3.8.2; BIOPAC Systems In., Goleta, CA, USA) connected to an external pressure transducer (P23XL; Viggo Spectramed Inc., Oxnard, CA, USA).

Transcardial Perfusion

In certain studies for histologic examination of tissues, transcardial perfusion was used to procure fixed tissue for immunohistochemical, immunofluorescent, and in-situ hybridization staining techniques. Animals were deeply anesthetized with Ketamine/Xylazine IP (Ketamine 30 mg/kg IP + Xylazine 3 mg/kg IP). The thorax of the animal was then opened on a surgical tray and the animal was perfused through the heart with ice cold 0.1M phosphate-buffered saline (PBS) until the liver and kidneys cleared of blood and then perfused with ice cold 4% paraformaldehyde (PFA) until the tissue was fixed. Tissues were then extracted and post-fixed in 4% PFA for 24-48 hours before being switched to and stored in 30% sucrose in 0.1M PBS at 4°C.

In-vivo Approaches

In-vivo PVN Microinjection Studies

In a subset of animals in Chapter 5, PVN microinjections of GABAergic and glutamatergic agents were used to determine the impact of PVN $G\alpha i_2$ protein downregulation on neuronal circuit function. Following acute femoral artery and vein cannulation and the 2-hour recovery period, a baseline MAP and HR was recorded for 20 minutes, and then animals were microinjected with kynurenate (1.4µg/side, glutamatergic antagonist) or CGP52432 (3nmol/ side, GABA(B) antagonist) to determine basal activity of both glutamatergic (NMDA, AMPA, Kainate) and GABA(B) receptors, and the MAP and HR responses were recorded for 60 minutes following injections.

Metabolic Balance Studies

In subgroups of animals, to assess the impact of central $G\alpha i_2$ protein downregulation on sodium handling, metabolic balance studies were undertaken. Animals in these studies were first moved to and acclimated in metal meshwire bottom metabolic cages for a 48-h period before studies began. Following acclimation, animals were allotted a measured daily amount of food (~100 g) and water, and this was reset each day. Additionally, 24-hour urine was collected each day for sodium excretion measurement. To calculate sodium balance, sodium intake was determined from the known amount of food consumed, and then sodium excreted as measured via urinalysis was subtracted from sodium consumed to obtain a difference for each 24-hour period for 2-3 days of a NS diet to measure baseline, and then for each 24-hour period over 7 days on experimental HS diet.

Experimental Approaches

Harvest of Plasma, Fresh Brain, and Fresh Kidneys

In subgroups of animals in which plasma and fresh frozen brain and kidney tissue were needed, rats were euthanized in accordance with our approved IACUC protocols via conscious decapitation using a standard rodent guillotine. Whole blood was collected in potassium-EDTA tubes and centrifuged at 3000 x g for 10 minutes at 4°C. Plasma was then aliquoted and stored at -80°C until further use. Fresh frozen brains and kidneys were harvested and were snap frozen and stored at -80°C until further use.

Assessment of Plasma and Renal NE Levels, Plasma Renin Activity, and Urinary Angiotensinogen

Frozen plasma and fresh frozen kidney samples were used for the determination of plasma and renal NE levels via enzyme-linked immunosorbent assay (ELISA) per manufacturer's instructions. Plasma and Renal NE content were analyzed via ELISA (IB89552, IB89537 respectively; Immuno-Biological Laboratories, Inc., Minneapolis, MN, USA) as previously described (Carmichael et al., 2020; Wainford et al., 2015). Plasma Renin Activity (PRA) was assessed via PRA ELISA (DB52011; Tecan, Mannerdorf, Switzerland) for the quantitative determination of PRA by the immunoassay of generated angiotensin I, according to the manufacturer's instructions. Urinary angiotensinogen (UAGT) in Chapter 3 was assessed from urine samples obtained from a 4 h urine collection period (09.00–13.00 h) in individual metabolic cages, during which time the animals had free access to food and water. UAGT was determined via ELISA (IB27412, Immuno-

Biological Laboratories, Inc.) according to the manufacturer's instructions.

Cytokine mRNA studies

From a subset of fresh frozen brains, a tissue punching tool was used to take bilateral PVN punches for RNA isolation. Total RNA was isolated using RNeasy kits (Qiagen, Hilden, Germany) according to the manufacturer's instructions, and 200 ng of purified RNA was quantified using a NanoDrop. Reverse transcription was performed using a high-capacity complementary DNA RT kit to obtain coding DNA (Qiagen, Hilden, Germany). The IL-1β, IL-6, TNFα and IL-10 mRNA (cDNA as a proxy for mRNA) levels were analyzed by quantitative real-time PCR using targeted primers in a PRISM 7000 sequence detection system (Applied Biosystems, Bedford, MA, USA) (P. Shi et al., 2010). Data were normalized to 18S ribosomal RNA, and the $2^{-\Delta\Delta\ CT}$ method was used to calculate relative changes in gene expression for determination of relative fold change between groups.

Assessment of PVN Gαi₂ Protein Levels

In certain studies, we elected to assess PVN Gαi₂ protein levels. First, in Chapter 3, we elected to do so in animals receiving co-infusion of minocycline with ODNs to validate that minocycline's function in reducing MAP was not due to interference with the ability of the targeted Gαi₂ ODN to infuse the animal. Second, in Chapter 4, we elected to measure levels in the brains of female SD rats to confirm the efficacy of our targeted ODN as we have not previously done so in females. Fresh frozen brains were taken to a cryostat and sliced to the anterior level of the PVN. Then, a brain punching tool (Stoelting Co.,

Wood Dale, IL, USA) was used to harvest PVN punches from each brain. Tissue lysates were made and protein levels quantified using a BCA assay according to the manufacturer's instructions (Thermo Scientific, Waltham, MA, USA) against standards provided. Lysates were resolved on a 10% SDS–PAGE gel in studies in Chapter 3, and a 7.5% SDS-PAGE gel in studies in Chapter 4, and transferred to nitrocellulose membranes (catalogue no. 456-1033; Bio-Rad, Hercules, CA, USA). $G\alpha i_2$ levels were determined as previously published by our laboratory using commercially available antibodies from Santa Cruz Biotechnologies (Santa Cruz, CA, USA), against $G\alpha i_2$ (see Table 2.2, Santa Cruz Biotechnology catalogue no. sc-13534, 1:200, RRID:AB_627644) (Carmichael et al., 2020; Kapusta et al., 2013; Wainford et al., 2015). Protein levels were normalized to total protein via Coomassie Blue-stained gels. Chemiluminescent immunoreactive bands were detected by a horseradish peroxidase-conjugated secondary antibody; data were imaged and semi-quantified using Bio-Rad Quantity One and ImageJ image analysis software.

Immunohistochemistry of Brain Tissues

For the detection of microglia, astrocytes, and cytokines in brain sections, fixed brain tissues were taken and sliced coronally at 40μm between approximately Bregma -1.6 and Bregma -2.2, the anterior and posterior limits of the PVN respectively, on a cryostat and stored in cryoprotectant solution (30% weight/volume sucrose, 30% ethylene glycol, and 1% polyvinyl-pyrrolidone in 0.1M PBS).

Free-floating slices were then selected for immunohistochemistry as previously described (Carmichael et al., 2016; Carmichael et al., 2020). First slices were washed in 0.1 M PBS at room temperature on an orbital shaker, then endogenous peroxidase activity

was removed with incubation for 30 minutes in 1% hydrogen peroxide at room temperature on an orbital shaker. Slices were then blocked with 3% horse serum and permeabilized in 0.25% Triton-X at room temperature on an orbital shaker. The tissue was incubated in primary antibodies dissolved in PBS diluent (0.25% Triton-X and 3% horse serum in 0.1M PBS, primary antibody specifics detailed in Table 2.2) for 2 hours on an orbital shaker at room temperature and then for 48 hours at 4°C. Slices were washed, and then incubated in secondary antibodies (see specific antibody in Table 2.2) dissolved in PBS diluent at room temperature on an orbital shaker for 2 hours. Slices were then washed and incubated for one hour in a biotin-streptavidin signal enhancer (VectaStain Kit; Vector Laboratories), washed, and exposed to 3-3-diaminobenzidine and nickel sulfate solution for staining. Slices were finally wet mounted in 0.1M PBS onto gelatin-subbed slides (Southern Biotechnology, Birmingham, AL, USA) and cover-slipped with Permount toluene mounting solution (UN1294 toluene solution; Fisher Chemical, Waltham, MA, USA), and stored until imaging.

Immunofluorescence of Brain Tissues

Similarly to immunohistochemistry, immunofluorescence was used for the detection of cytokines in the brain. Slices obtained via the same coronal sectioning process, sliced at 40μm, and stored in cryoprotectant solution (30% weight/volume sucrose, 30% ethylene glycol, and 1% polyvinyl-pyrrolidone in 0.1M PBS) were selected for immunofluorescence. Free-floating slices were then washed in 0.1M PBS on an orbital shaker at room temperature, permeabilized with 0.25% Triton-X and blocked with 3% horse serum at room temperature on an orbital shaker, washed again in 0.1M PBS, and

incubated in primary antibodies (see Table 2.2 for specific antibodies) against cytokines for 2 hours at room temperature on an orbital shaker, and then for 48 hours at 4°C on an orbital shaker. Slices were then washed, and incubated in Alexa-fluor-conjugated secondary antibodies (see Table 2.2 for specific antibodies) diluted in PBS diluent in the dark at room temperature for 2 hours on an orbital shaker. Slices were finally washed and wet-mounted on gelatin-subbed slides in 0.1M PBS, and cover-slipped with Prolong

Target antigen	Vendor or Source	Catalog #	Working concentration
CD 11b/c (mouse anti-rat primary)	BD Biosciences/Fisher Sci	550299	1:60-1:100
Mouse IgG (goat anti-mouse, biotinylated secondary, histochemistry)	Vector Laboratories/Fisher Sci	BA-9200	1:100
IL-6 (mouse anti-rat primary)	Santa Cruz Biotech	Sc-28343	1:100
IL-1β (mouse anti-rat primary)	Santa Cruz Biotech	Sc-32294	1:100
TNFα (mouse anti rat primary)	Santa Cruz Biotech	Sc-133192	1:100
Mouse IgG (goat anti-mouse, alexa-fluor 488 conjugated secondary, immunofluorescence)	Invitrogen/Fisher Sci	A11001	1:200
IL-10 (rabbit polyclonal to synthetic antigen)	Abbiotec	250713	1:100
Rabbit IgG (goat anti-rabbit IgG biotinylated secondary, histochemistry)	Invitrogen	31820	1:100
GFAP (goat anti-rat primary)	Abcam	Ab53554	1:60-1:500
Goat IgG (horse anti-goat, biotinylated, histochemistry)	Vector Laboratories/Fisher Sci	BA-9500	1:1000
$G\alpha i_2$ protein (mouse anti-rat primary)	Santa Cruz Biotech	Sc-13534	1:200
Mouse IgG (goat anti-mouse, HRP conjugated secondary, western blot)	Abcam	Ab6789	1:2000

Table 2.2 Listed Antibodies Used in Immunofluorescent, Immunohistochemical, and Immunoblotting Studies.

Diamond anti-fade mounting media (Fisher- P36961, Fisher Scientific, Waltham, MA, USA) and stored in the dark until imaging.

In-situ Hybridization of Brain Slices

For the co-localization of the *Gnai2* mRNA with *vGlut2* and *Gad1* in the PVN to determine the percent distribution of neuronal phenotypes expressing the $G\alpha i_2$ protein, in-situ hybridization was performed as recently described by our laboratory (Chaudhary & Wainford, 2021). Coronally sliced sections of fixed brains were cut on a cryostat at 20 μm and stored in cryoprotectant until tissue processing. In situ hybridization was performed using the Manual RNAscope Assay Fluorescent multiplex kit (ACD 32850, Hayward, CA, USA). Optimization and specificity were determined using 3-Plex positive (ACD 320891, Hayward, CA, USA) and negative (ACD 320871, Hayward, CA, USA) controls. First, sections were rinsed with 1X PBS and mounted on superfrost plus slides (Fisher 1255015, Fisher Scientific, Waltham, MA, USA). Slides were then washed in RNase free water (Fisher 10-977-015, Fisher Scientific, Waltham, MA, USA) for 5 minutes and dehydrated through serial concentrations of ethanol, air dried, permeabilized using hydrogen peroxide (ACD 322335, Hayward, CA, USA) to block endogenous peroxidase activity and protease III (ACD 322337, Hayward, CA, USA). Slices were then hybridized using specific target probes for 2 hours at 40°C. Readily available C2 probes *Gad1* (ACD 316401-C2, Hayward, CA, USA) and *Slc17a6*(vGLUT2, ACD 317011-C2, Hayward, CA, USA) were used along with a custom-designed targeted C1 *Gnai2* probe (NPR-0001497; ACD 805201) detecting specific Gai_2 target RNA. The custom probe was designed using the National Center for Biotechnology Information Gene ID 81664 for *Rattus norvegicus Gnai2*. For hybridization

channels C1 (1X concentration) and C2 (50X concentration), and for the multiplex probe mixture at 1X concentration, the C2 probes were diluted at 1:50 in the C1 probe.

Following probe hybridization, tissue section slides were rinsed twice with 1X wash buffer (ACD 310091; 50X diluted in RNase free water, Hayward, CA, USA) at room temperature for 2 minutes each time. The signal amplification was performed using an RNA scope set of amplifiers (ACD 320851, Hayward, CA, USA) (Amp 1, 30 minutes at 40°C; Amp 2, 15 minutes at 40°C; Amp 3, 30 minutes at 40°C; and Amp 4A, 15 min at 40°C). Washing steps with 1X wash buffer (2 minutes at room temperature x2) were included between Amplification steps. Slides were then coated with Prolong Diamond anti-fade mounting media (Fisher-P36961) to preserve fluorescent signals.

Microscopy and Image Analysis

All brain section staining protocols were imaged on a Keyence BZ-9000 fluorescence microscope (BZ-9000, BIOREVO, Keyence, Tokyo, Japan) which possesses DAPI (excitation: 360 ± 20 nm; absorption: 460 ± 25 nm), GFP (excitation: 470 ± 20 nm; absorption: 535 ± 25 nm), and Texas Red (excitation: 560 ± 20 nm; absorption: 630 ± 30 nm) filters. The microscope was set to bright field utilizing a standard halogen lamp for immunohistochemistry, and set to fluorescence for immunofluorescence and in-situ hybridization. For immunohistochemistry of microglia stained by Cd 11b/c, astrocytes stained by GFAP, and cytokines IL-1β, IL-10, IL-6, and TNFα, images were captured on brightfield at standard microscope configurations and only exposure was adjusted to obtain similar images in all samples, determined by the brightness in the third ventricle adjacent to the PVN. No changes were made to the contrast or brightness of any images obtained

on brightfield following capture on the microscope.

Analysis of Glia and Cytokines Stained via Immunohistochemistry

For analysis of microglial morphology, randomly sampled images were taken at 40X from the PVN and blinded. The total number of microglia in a randomly drawn 200 μm x 200 μm box on that image was then counted for each animal, as well as the number of microglia in each box that were determined to be reactive, or activated. Activated microglia were determined to be those that were stained more darkly on a subjective scoring of 1-3 with 1 being lightest and 3 being most immunoreactive, as well as those that possessed processes that were overall shorter than the approximate diameter of the soma of that microglia, and which possessed a hypertrophied or amoeboid somal shape. The percent of the sampled microglia that were reactive were then calculated as number active divided by total number. Group averages were then compared for each of these parameters. Additionally, for a less subjective measure of microglial reactivity, 2D Sholl analysis was performed. In brief, 10 microglia from each animal tissue section were randomly selected in a systematic fashion via a grid placed over the image. Each glia was cropped into its own image and then opened in ImageJ/FIJI (ImageJ 1.52p, Java 1.8.0_172; US National Institutes of Health). The center of the soma of each glia was then selected, and the whole glia was highlighted using the "adjust→ threshold" function. The Sholl analysis plugin tool was then run, and it placed concentric rings equidistant from another (1 μm) radiating from the soma and calculated the number of times processes intersected the rings in all directions. These data were then plotted for each glia, averaged for each animal and group, and plotted against one another and the mean peak number of intersections was used for

statistical comparison of each group to determine if significant differences existed in branching complexity, which is considered to increase with increased mean number of ring intersections.

To measure astrocyte activation, images captured at 20X in the PVN were captured and blinded. As astrocytic activation can be more subtle than microglia, and involve only a slight swelling of the soma and upregulation of GFAP, on ImageJ, the PVN was traced out and the percent area stained positively for GFAP was then calculated as pixels stained divided by total pixels in that PVN section. This helps to normalize the percent area of astrocyte staining in accounting for different sized PVN areas. Data were compared as group average percent areas.

Cytokine immunohistochemistry was then analyzed qualitatively for visual differences in cytokine protein expression and taken into context with quantitative PCR data to determine if differences were observable.

Analysis of Cytokines Stained via Immunofluorescence

Immunofluorescence was performed on brain slices in a subset of studies on cytokine expression. Following staining in these studies, images were taken on the GFP setting of the microscope at 20X under similar exposures, and without alterations to the gamma setting. Images were then blinded and shuffled and then opened in ImageJ/FIJI. The PVN was traced out on these images and cytokine percent area was determined by utilizing a threshold tool to identify the total number of pixels in the PVN and the number of pixels positive for fluorescent staining, and then dividing positively stained pixels by total pixels. This normalizes the potential differences in PVN area between samples. Group

averages were then determined for comparison.

Analysis of Neuronal Phenotypic Markers Stained via In-situ Hybridization

For in-situ hybridization studies on brain slices, slides were imaged utilizing the GFP filter for green stains and Texas Red filter for red stains at 10X and 20X. To determine positive RNA puncta staining compared to background, the brightness setting was enhanced linearly to an equal degree with respect to the background in all images to allow small puncta to become visible, while contrast was also enhanced equally and linearly in all images to enable signal detection and discrimination from background. To ensure background was identifiable, negative control probes and positive control probes commercially available from Advanced Cell Technology/BioTechne were employed for image comparison. After image capture, colocalization of *Gad1* and *Gnai2* or *vGlut2* and *Gnai2* was determined using ImageJ/FIJI. On blinded images, a 300 μm x 300 μm box was drawn over the PVN. Cells were then counted using the cell counter plugin available on ImageJ. A cell was determined to be positive for the respective mRNA if it contained >5 punctate dots in that foci. Quantifications of each slice were then used to determine percent of *Gnai2*-expressing neurons that were GABAergic or Glutamatergic, as well as percent of GABAergic neurons containing *Gnai2* and percent of glutamatergic neurons containing *Gnai2*. Data were averaged and these figures used for comparison across groups.

Statistical Analyses

All data in Chapters 3-5 are expressed as mean ± SD. The magnitude of change in cardiovascular (radiotelemetry MAP) and renal excretory studies (urinary sodium balance)

at different time points of chronic dietary sodium intake studies, as well as temporal changes in MAP to microinjections, was compared with the mean group control value by a one-way repeated-measures analysis of variance (ANOVA) with subsequent Dunnett's test. Differences between different ODN infusion groups, as well as different dietary intake groups for a single time point were assessed via a two-way ANOVA, with ODN infusion being one fixed effect and dietary sodium intake the other, with the interaction included. Time (day), if used, was the repeated factor. Post-hoc analyses were performed using Bonferroni's test in comparing differences in variations between groups. Additional statistical analyses between control and experimental animals receiving the same ODN and on same diet were validated using Student's unpaired *t* tests. Statistical analysis was carried out using GraphPad Prism software (v.8, GraphPad Software, CA). Statistical significance was defined as Probability $P<0.05$.

CHAPTER THREE: Inhibition of Microglial Activation in Rats Attenuates Paraventricular Nucleus Inflammation in Gαi$_2$ Protein-Dependent, Salt-Sensitive Hypertension

This section was previously published as: Moreira, J.D., Chaudhary, P., Frame, A.A., Puleo, F., Nist, K.M., Abkin, E.A., Moore, T.L., George, J.C., and Wainford, R.D. "Inhibition of microglial activation in rats attenuates paraventricular nucleus inflammation in Gαi$_2$ protein-dependent, salt-sensitive hypertension." Experimental Physiology 104(12):1892-1910. PMCID: PMC6884700 © 2019 The Authors. Experimental Physiology published by John Wiley & Sons Ltd on behalf of The Physiological Society.

Introduction

Hypertension (HTN) is one of the most significant public health issues in the USA; according to 2017 American Heart Association (AHA) guidelines, it is estimated that one in two people are hypertensive (Reboussin et al., 2018). Furthermore, HTN is the leading cause of chronic kidney disease, stroke and ischaemic heart disease (Lloyd-Jones et al., 2010; Dariush Mozaffarian et al., 2016) and is estimated to contribute to 10.4 million deaths worldwide per year (Unger et al., 2020). Excess dietary sodium intake, which can drive the salt-sensitivity of blood pressure and increase the risk of developing salt-sensitive HTN (ssHTN), is of great public health significance, because the average American is consuming almost three times the daily sodium intake recommended by the American Heart Association (Lloyd-Jones et al., 2010).

Our laboratory has previously shown that in salt-resistant animals, upregulation of the G-protein-coupled receptor αi$_2$ subunit (Gαi$_2$) protein in the paraventricular nucleus (PVN) of the hypothalamus of salt-resistant rats mediates high dietary sodium-evoked sympathoinhibitory responses to facilitate normotension and the maintenance of salt resistance (Kapusta et al., 2013; Wainford et al., 2015). In contrast, hypertensive Dahl salt-

sensitive (DSS) rats fail to upregulate PVN Gαi$_2$ proteins in response to high dietary sodium intake (Wainford et al., 2015). Restoration of the upregulation of Gαi$_2$ proteins in the DSS rat via the use of the 8-congenic rat line attenuated the magnitude of DSS HTN (Wainford et al., 2015). Thus, PVN Gαi$_2$ upregulation in response to high dietary sodium intake is crucial for the maintenance of salt resistance.

Several recent studies have suggested that central inflammatory processes contribute to the development of HTN, and include the upregulation of pro-inflammatory cytokines (PICs) such as tumor necrosis factor-α (TNFα), interleukin (IL)-6 and IL-1β (Jiang et al., 2018; P. Shi et al., 2010; Z. Shi et al., 2011). Furthermore, these processes have been shown to feature downregulation of the anti-inflammatory cytokine IL-10 (Segiet et al., 2019). Inflammatory processes have also been demonstrated to mediate neuronal excitability and even influence the firing rates of neurons, potentially disrupting neural homeostasis (Galic et al., 2012; Z. Shi et al., 2011). Glial cells, including microglia and astrocytes, can become activated in response to a pathological stimulus and have been demonstrated to produce inflammatory cytokines and reactive oxygen species and to disrupt neural homeostasis (Biancardi et al., 2016; Wolf, Boddeke, & Kettenmann, 2017). Therefore, we hypothesized that central inflammatory processes, involving activation of microglia and astrocytes, contribute to the development of Gαi$_2$ protein-dependent, ssHTN. To test this hypothesis, we used a male Sprague–Dawley rat model infused centrally with either a scrambled (SCR) control oligodeoxynucleotide (ODN) or targeted Gαi$_2$ ODN alone or in combination with centrally administered minocycline, during a challenge with either a normal- or high-salt diet. In these animals, we assessed several markers of central

inflammation via mRNA and immunohistochemical approaches.

Methods

Ethical approval

All animal protocols were approved by the Institutional Animal Care and Use Committee under protocol number AN15241, in accordance with the guidelines of the Boston University School of Medicine and the US National Institutes of Health *Guide for the Care and Use of Laboratory Animals*, 8th edition (2011). Please note that all possible steps were taken to minimize pain and suffering, and euthanasia was conducted in accordance with approved protocols. We used decapitation in a small, clearly defined subset of animals, in which we were measuring basal concentrations of plasma norepinephrine, which are suppressed by the administration of sedatives and anaesthetics.

Animals

Male Sprague–Dawley rats weighing 275–300 g were purchased from Envigo (Indianapolis, IN, USA). Rats were pair-housed before surgical intervention and housed separately after survival surgery. Animals were housed in a facility with controlled temperature (range 20–26°C) and humidity (range 30–70%) under a 12 h–12 h light–dark cycle and were allowed tap water and standard irradiated rodent diet as described in Table 2.1 in Chapter 2 or experimental high-sodium as described in Chapter 2 *ad libitum*. Rats were randomly assigned to experimental groups.

Surgical procedures

Chronic blood pressure measurement: A radiotelemetry device (PA-C40; Data

Sciences International, New Brighton, MN, USA) was implanted into the abdominal aorta via the left femoral artery under general anaesthesia (ketamine, Zoetis, Inc., Kalamazoo, MI, USA, 30 mg/kg IP; xylazine, Akorn, Inc., Lake Forest, IL, USA, 3 mg/kg IP). In these studies, animals received buprenorphine (Reckitt Benckiser Pharmaceuticals, Richmond, VA, USA) for 48 h after radiotelemetry probe implantation (0.05 mg/kg SC). In all cases, radiotelemetry probes were implanted 5 days before intracerebroventricular (ICV) osmotic mini pump implantation. Radiotelemetry data were collected, stored and analyzed using Dataquest A.R.T. v.4.2 software (Data Sciences International, St. Paul, MN, USA) (Brouwers, Smolders, Wainford, & Dupont, 2015; Frame, Carmichael, et al., 2019; Wainford et al., 2015).

Intracerebroventricular oligodeoxynucleotide infusion: Chronic downregulation of brain $G\alpha i_2$ proteins was achieved by continuous ICV infusion of a phosphodiesterase ODN probe that selectively and specifically targets $G\alpha i_2$ proteins (5′-CTTGTCGATCATCTTAGA-3′). Control animals received an ICV infusion of a SCR ODN (5′-GGGCGAAGTAGGTCTTGG-3′). In these studies, SCR and $G\alpha i_2$ ODNs were dissolved in isotonic saline and infused ICV at 25 µg/ 6 µl/ day, a technique previously reported by our laboratory selectively to downregulate $G\alpha i_2$ subunit proteins throughout the brain of conscious Sprague–Dawley rats (Carmichael et al., 2020; Kapusta et al., 2013; Wainford et al., 2015). Several publications from our laboratory have confirmed effective (~85%) ODN-mediated downregulation of $G\alpha i_2$ protein expression after chronic ICV ODN infusion as assessed by western blotting(Kapusta et al., 2013; Wainford et al., 2015).

To achieve ICV ODN infusion, animals were anaesthetized (ketamine, 30 mg/kg IP in combination with xylazine, 3 mg/kg IP) and implanted stereotaxically with a stainless-steel cannula into the right lateral cerebral ventricle (Plastics One Inc., Roanoke, VA, USA), which was connected via Silastic tubing to an osmotic minipump (Model 2004; Durect Corporation, Cupertino, CA, USA). A National Center for Biotechnology Information (NCBI) Basic Local Alignment Search Tool (BLAST) search of the *Rattus norvegicus* Reference Sequence (RefSeq) protein database was conducted to confirm: (i) the specificity of the $G\alpha i_2$ ODN for the $G\alpha i_2$ rat protein sequence; and (ii) that the SCR ODN does not match any known rat protein sequence. In addition, our prior studies (Carmichael et al., 2020; Kapusta et al., 2012; Wainford et al., 2015; Wainford, Pascale, & Kuwabara, 2013) and the studies from other laboratories examining the effects of opioid analgesia and opioid-induced feeding (Hadjimarkou et al., 2002; Rossi et al., 1995; Silva et al., 2000; Standifer et al., 1996) have demonstrated the selectivity and specificity of this $G\alpha i_2$ ODN sequence in the downregulation of brain $G\alpha i_2$ proteins in rats.

Intracerebroventricular minocycline and oligodeoxynucleotide co-infusion: Chronic downregulation of brain $G\alpha i_2$ proteins during microglial inhibition was achieved by continuous ICV infusion of an ODN probe that targets $G\alpha i_2$ proteins, as described above, in combination with ICV minocycline infusion. In these studies, SCR and $G\alpha i_2$ ODNs were dissolved in isotonic saline and infused ICV at 25 µg/ 6 µl/ day in combination with minocycline at a rate of 25 µg/ 6 µl/ day (P. Shi et al., 2010).

Experimental approaches

Dietary sodium intake: After ICV osmotic minipump implantation, animals were randomly assigned to a normal-salt (0.6% NaCl) or high-salt (4% NaCl) diet for a period of 7 days. At the end of the 7-day experimental period, animals were either killed by conscious decapitation or received ketamine anaesthesia (ketamine, 30 mg kg^{-1} i.p.) before undergoing cardiac perfusion.

Chronic blood pressure measurement: In certain studies, radiotelemetry was used for the chronic measurement of blood pressure. Data were collected via scheduled sampling for 10 s every 10 min in all groups of rats. Rats were maintained on a normal-salt diet (0.6% NaCl) for a 5-day baseline period and were then randomly assigned (n = 6 per group) to either a normal-salt (0.6% total NaCl) or high-salt (4% total NaCl) diet, and blood pressure was recorded for a further 7 days.

Plasma renin activity, urinary angiotensinogen and norepinephrine assays: Plasma renin activity (PRA), urinary angiotensinogen and plasma norepinephrine (NE) concentrations were determined as previously described (Kapusta et al., 2012; Wainford et al., 2015). In brief, after plasma extraction, from blood samples obtained after conscious decapitation, samples were frozen at −80°C until later analysis. For the PRA assay, samples were analyzed using a plasma renin activity enzyme-linked immunosorbent assay (ELISA) kit (DB52011; Tecan, Mannerdorf, Switzerland) for the quantitative determination of PRA by the immunoassay of generated angiotensin I, according to the manufacturer's instructions. Plasma NE concentrations were quantified using an ELISA kit (IB89552; Immuno-Biological Laboratories, Inc., Minneapolis, MN, USA) according to the

manufacturer's instructions. For the urinary angiotensinogen assay, urine samples were obtained from a 4 h urine collection period (09.00–13.00 h) in individual metabolic cages, during which time the animals had free access to food and water. These samples were analyzed by ELISA (IB27412, Immuno-Biological Laboratories, Inc.) according to the manufacturer's instructions.

Cytokine mRNA studies: On day 7, a subset of animals ($n = 6$ per group) was sacrificed via conscious decapitation and whole blood was collected for analysis. Fresh frozen brains were harvested, and a tissue punching tool was used to take bilateral PVN punches (Kapusta et al., 2013; Kapusta et al., 2012). Total RNA was isolated using RNeasy kits (Qiagen) according to the manufacturer's instructions, and 200 ng of purified RNA was reverse transcribed with a high-capacity complementary DNA reverse transcription kit (Qiagen, Hilden, Germany). The IL-1β, IL-6, TNFα and IL-10 mRNA levels were analyzed by quantitative real-time PCR using specific primers and probes in a PRISM 7000 sequence detection system (Applied Biosystems, Bedford, MA, USA) (P. Shi et al., 2010). Data were normalized to 18S ribosomal RNA, and the $2^{-\Delta\Delta\ CT}$ method was used to calculate relative changes in gene expression (Zuriaga et al., 2017).

Measurement of brain $G\alpha i_2$ protein levels: After completion of experimental protocols, the rats were killed via conscious decapitation, and whole brains were removed from subsets of animals co-infused with both SCR and $G\alpha i_2$ ODN–minocycline, and frozen at −80°C. Paraventricular nucleus samples were extracted from frozen brains cut on a cryostat using a brain punch tool (Stoelting Co., Wood Dale, IL, USA) as previously described (Carmichael et al., 2020; Kapusta et al., 2012; Wainford et al., 2015; Wainford

et al., 2013). Tissue lysates were prepared and protein levels quantified using the BCA assay according to the manufacturer's instructions (Thermo Scientific, Waltham, MA, USA). Lysates were resolved on a 10% SDS–PAGE gel and transferred to nitrocellulose membrane (catalogue no. 456-1033; Bio-Rad, Hercules, CA, USA). $G\alpha i_2$ levels were determined as previously published by our laboratory (Kapusta et al., 2012; Wainford et al., 2015) using commercially available antibodies purchased from Santa Cruz Biotechnologies (Santa Cruz, CA, USA), directed against $G\alpha i_2$ (Santa Cruz Biotechnology catalogue no. sc-13534, 1:200, RRID:AB_627644); protein levels were normalized to total protein via Coomassie Blue-stained gels. Chemiluminescent immunoreactive bands were detected by a horseradish peroxidase-conjugated secondary antibody; data were imaged and semi-quantified using Bio-Rad Quantity One image analysis software.

Immunohistochemistry: Brain tissue from transcardially perfused animals was post-fixed for 24 h in 4% paraformaldehyde and then for 72 h in 30% sucrose before being sliced on a cryostat. Slices 40 µm thick were obtained, and immunohistochemistry was performed in six-well plates as described in Chapter 2. Slices of the PVN were selected based on coordinates from Paxinos & Watson *The Rat Brain* atlas (Paxinos & Watson, 2007), being between bregma −1.6 and −2.16 mm. Slices were taken caudal to the interventricular foramen and rostral to the CA1 region of the hippocampus. Slices were washed in 0.1 m PBS, incubated in 1% hydrogen peroxide to block endogenous peroxidase, blocked with 3% horse serum and primary antibodies against rat OX-42 (BD Biosciences catalogue no. 550299, RRID:AB_393594, 1:60, East Rutherford, NJ, USA) were used to stain for microglia and against rat GFAP (Abcam catalogue no. ab53554,

RRID:AB_880202, 1:60, Cambridge, MA, USA) to stain for astrocytes. Secondary antibodies used were biotinylated IgG (Vector Laboratories catalogue no. BA-9200, RRID:AB_2336171, 1:100, Burlingame, CA, USA). Slices were blocked with avidin (VectaStain Kit; Vector Laboratories), and stained with 3′,3′-diaminobenzidine. After immunohistochemistry, slices were mounted on gelatin-subbed slides (Southern Biotechnology, Birmingham, AL, USA) and dehydrated using deionized water to xylenes, coverslipped with Permount (UN1294 toluene solution; Fisher Chemical, Waltham, MA, USA) and visualized. Furthermore, the same procedure was used, and primary antibodies against rat IL-1β (Santa Cruz Biotechnology catalogue no. sc-32294, RRID:AB_627790, 1:100, Santa Cruz, CA, USA; (Somsanith et al., 2018), rat IL-6 (Santa Cruz Biotechnology catalogue no. sc-28343, RRID:AB_627805, 1:100, Santa Cruz, CA, USA; (Jiang et al., 2018), rat TNFα (Santa Cruz Biotechnology catalogue no. sc-133192, RRID:AB_1567355, 1:100, Santa Cruz, CA, USA; (Jiang et al., 2018) and IL-10 (Abbiotec catalogue no. 250713, RRID:AB_2125107, 1:100, San Diego, CA, USA) were used to identify cytokine protein distribution in the brain tissue. Secondary antibodies used were biotinylated IgG (Vector Laboratories catalogue no. BA-9200, RRID:AB_2336171, 1:100). After immunohistochemistry, slices were mounted on gelatin-subbed slides (Southern Biotechnology, Birmingham, AL, USA) and dehydrated using deionized water to xylenes, coverslipped with Permount and visualized. Control experiments for immunohistochemistry performed include those done without primary antibodies and those done without secondary antibodies (Figure 3.14). All antibodies were previously validated and published.

Microscopy and image analysis: Stained tissues were visualized using a Keyence BZ-9000 fluorescence microscope set to bright field. Paraventricular nucleus-containing slices were visualized and images captured at ×20 and ×40 magnifications.

Morphological analysis of microglia: Level 2 PVN slices were obtained (approximately bregma −1.8 to −2.0 mm) and SFO slices were obtained (approximately bregma −1.8 to −2.0 mm) and microglia in the sections were graded according to immunoreactivity on a scale from one to three, with one representing low reactivity and faint staining, two representing moderate reactivity with moderate staining, and three representing high reactivity with dark staining. In blinded, randomly sampled 200 µm × 200 µm squares at ×40 magnification, PVN and SFO microglia were determined to be 'activated' if they demonstrated characteristic morphological changes that including becoming amoeboid, where their projections were reduced to a size less than the diameter of the microglial soma (4–5 µm) and if the immunoreactivity was a grade 2 or 3 on staining (Bardgett, Holbein, Herrera-Rosales, & Toney, 2014; P. Shi et al., 2010).

Sholl analysis of microglia: Images of level 2 of the PVN at ×40 magnification were obtained as previously described. Images were blinded and shuffled, and each image was opened in Adobe CC Photoshop (Adobe, 20.0.4 20190227.r.76), and images were overlaid with a 5 × 2 grid. Ten microglia were sampled randomly and systematically from individual grid squares and cropped so that the new image contained only the single microglial cell and its processes. In each group, 10 microglia from each of six animals were run, for a total of 60 microglia per group. Each new cropped image was opened in ImageJ/FIJI (ImageJ 1.52p, Java 1.8.0_172; US National Institutes of Health). Each image

was then converted to 8-bit, and the 'measure → threshold' function was used to identify the microglia from the background. The selected microglial cell was then subjected to Sholl analysis via the 'Analysis' function of FIJI, where concentric rings were placed equally distant (1 µm) from one another, radiating outwards from the center of the soma. The number of ring intersections at each ring, for a distance of 25 rings, was saved and analyzed using GraphPad Prism software (v.7; GraphPad Software, La Jolla, CA, USA) and plotted as group means at each given ring with standard deviations. One-way ANOVA was used to compare the overall differences between trend lines within ODN infusion groups.

Analysis of astrocytes: Astrocytes were analyzed using ImageJ software, in which the images were converted to a greyscale and set to 'Image → Type → RGB' and then analysis was performed to quantify the total percentage area of the PVN that the astrocytes composed, i.e. their density in the PVN. Astrocytes stained for GFAP, which is purportedly upregulated in astrogliosis (Pekny et al., 2014), were quantified (in pixels) and divided by the total number of pixels composing the PVN to obtain a percentage of composition, or tissue density.

Cytokine immunohistochemistry: Cytokine immunohistochemistry was analyzed qualitatively for visible differences in stain immunoreactivity in both the PVN and the SFO.

Statistical analysis

Data are expressed as means ± SD. Differences occurring between treatment groups (e.g. SCR *versus* $G\alpha i_2$ ODN) were assessed by a two-way ANOVA, with treatment group being one fixed effect and dietary intake the other, with the interaction included. *Post*

hoc analysis was performed using Bonferroni's test and individual Student's unpaired *t* tests. Statistical analysis was carried out using a software program (GraphPad Prism v.8). Statistical significance was defined as probability $P < 0.05$.

Results

Impact of brain Gαi$_2$ protein downregulation during 7 days of high salt intake on plasma NE: In control SCR ODN-infused male Sprague–Dawley rats, HS diet for 7 days had no impact on MAP and evoked global sympathoinhibition (SCR ODN; plasma NE: NS 65 ± 5 *versus* HS 37 ± 6 nmol l^{-1}, $P < 0.05$; Figure 3.1). In contrast, male Sprague–Dawley rats receiving a targeted Gαi$_2$ ODN infusion, which selectively downregulates brain Gαi$_2$ proteins, developed ssHTN (Gαi$_2$ ODN; MAP day 7 of HS diet: NS 103 ± 1.1 *versus* HS 128 ± 2 mmHg, $P < 0.05$) and dietary sodium-evoked sympathoexcitation, measured as plasma NE (Gαi$_2$ ODN; plasma NE: NS 67 ± 6 *versus* HS 91 ± 8 nmol l^{-1}, $P < 0.05$). Additionally, in these hypertensive rats we observed suppression of plasma renin activity and urinary angiotensinogen to the same levels as those seen in SCR ODN-infused rats (Figure 3.1). In control SCR ODN-infused rats maintained on HS intake for 7 days, minocycline infusion had no impact on MAP, suppression of plasma NE, plasma renin activity or urinary angiotensinogen (Figure 3.1). Significantly, central minocycline co-infusion attenuated the magnitude of HTN in rats on HS diets receiving a Gαi$_2$ ODN infusion (Gαi$_2$ ODN; MAP on day 7 of HS diet: HS 128 ± 2 *versus* HS + MINO 114 ± 1.1 mmHg, $P < 0.05$; Figure 3.1b) and abolished dietary salt-evoked elevations in plasma NE (Gαi$_2$ ODN; plasma NE: HS 91 ± 8 *versus* HS +

MINO 72 ± 6 nmol l^{-1}, $P < 0.05$; Figure 3.1c).

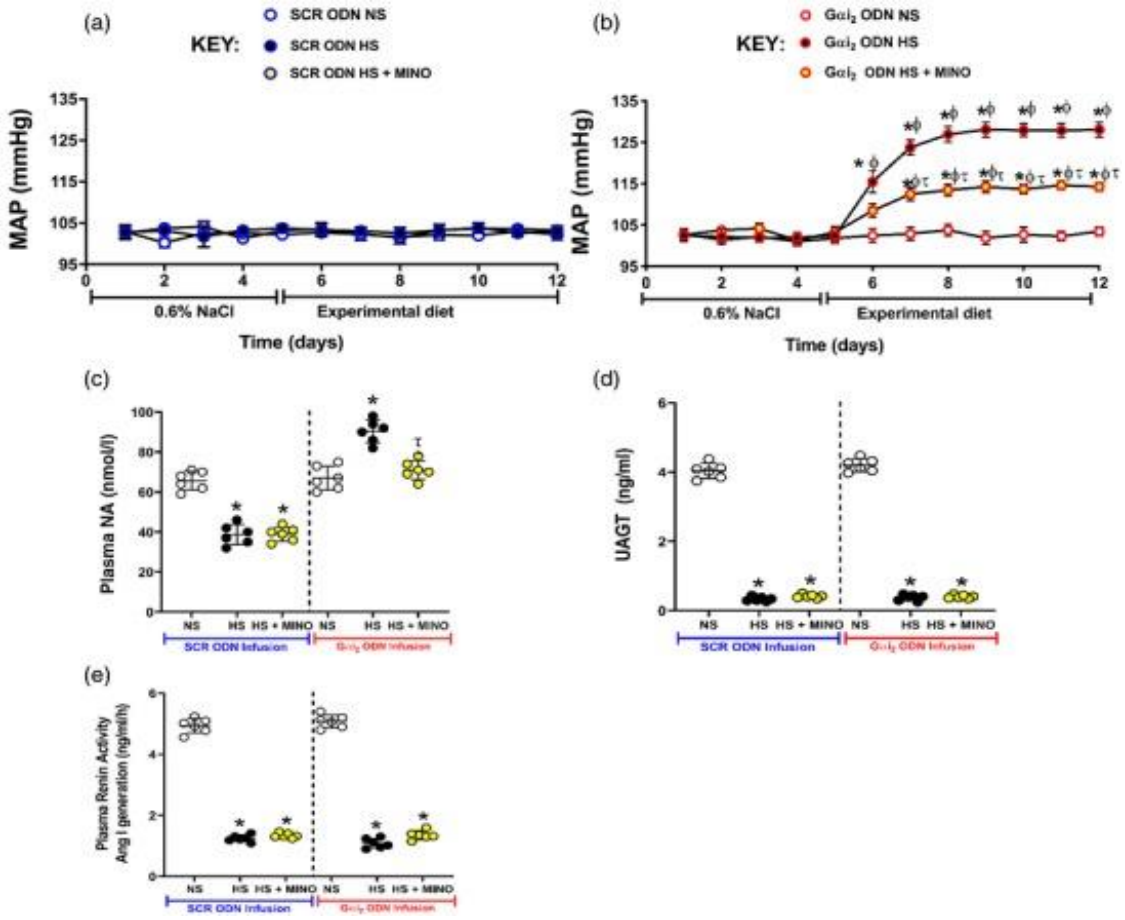

Figure 3.1. Impact of ODN Infusion and MINO co-infusion on MAP, Plasma NE, Plasma Renin Activity, and Plasma UAGT in SD Rats on NS and HS diet.

Impact of control scrambled (SCR) and targeted Gαi2 intracerebroventricular oligodeoxynucleotide (ODN) infusion [25 µg/ 6 µl/ day for 7 days] and minocycline (MINO)–ODN co-infusion [ODN, 25 µg/ 6 µl/ day; MINO: 120 µg/ day for 7 days in high-salt (HS) group only] in male Sprague–Dawley rats receiving 7 days of normal-salt (NS; 0.6% NaCl) or HS (4% NaCl) diets on: (a,b) mean arterial pressure (MAP) as assessed via radiotelemetry over 5 days preceding the experimental diet and the 7 days of the experimental diet; (c) plasma norepinephrine (NE) concentrations; (d) urinary angiotensinogen (UAGT) concentrations; and (e) plasma renin activity. (n = 6 per group, * $P < 0.05$ versus pre-experimental diet NS in respective ODN treatment group; τ $P < 0.05$ versus 7 days of experimental HS in respective ODN treatment group; ϕ $P < 0.05$ versus 7 days of experimental NS diet in the respective ODN treatment group, means ± SD.)

Impact of minocycline on Gαi₂ ODN-mediated downregulation of PVN Gαi₂ proteins: In subsets of animals co-infused with ODN and minocycline, immunoblotting was performed to assess the impact of co-infusion of minocycline and ODNs on targeted Gαi₂ protein downregulation. The Gαi₂ ODN–MINO co-infusion resulted in an average 79% reduction in PVN-specific Gαi₂ protein expression as assessed by immunoblotting, normalized to total protein in Coomassie Blue-stained gels (Figure 3.2; SCR ODN fold change HS + MINO 1.04 ± 0.24 *versus* Gαi₂ HS + MINO 0.209 ± 0.12, $P < 0.0001$). Therefore, minocycline did not appear to have an impact on the ability of the ODN to induce protein knockdown successfully.

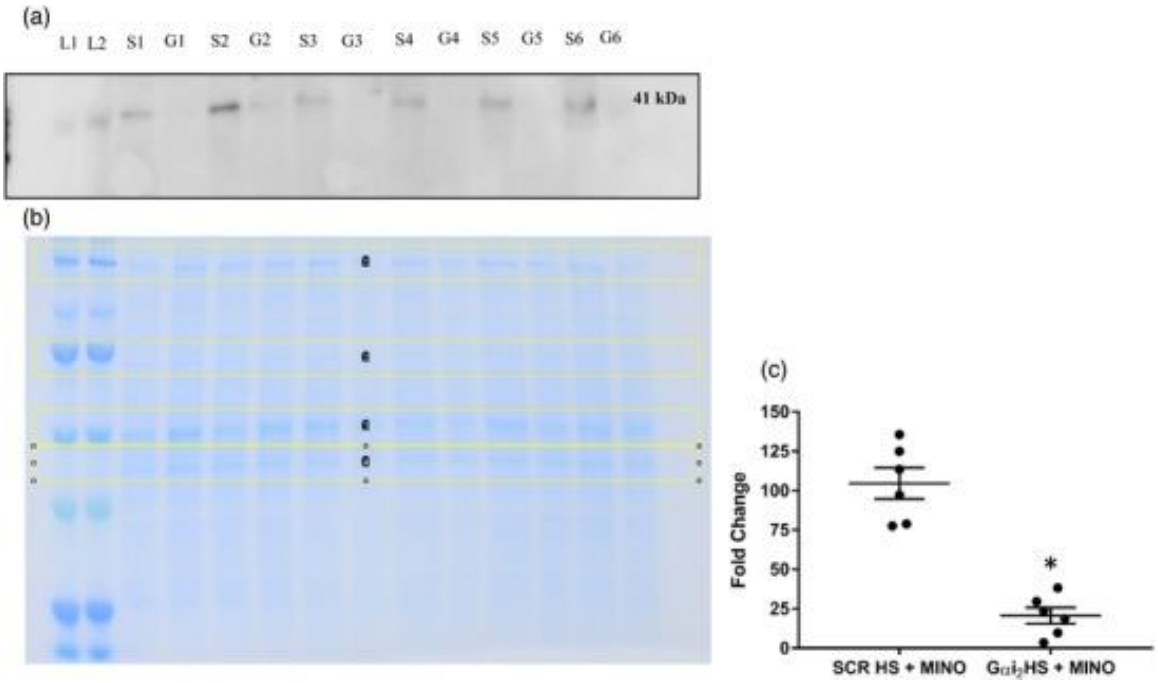

Figure 3.2. Impact of MINO on ODN Infusion in SD Rats.

(a) Representative immunoblot demonstrating impact of Gαi₂ oligodeoxynucleotide (ODN)–minocycline co-infusion [25 µg/ 6 µl/ day + MINO: 120 µg/ day for 7 days] on paraventricular nucleus (PVN) Gαi₂ protein expression. L1 and L2 are ladder, S1–S6 are protein extracts from the PVN of scrambled control (SCR) ODN–minocycline co-infused animals, and G1–G6 are protein extracts from the PVN of Gαi₂ ODN–minocycline co-infused animals. (b) Representative Coomassie Blue-stained gel demonstrating total protein loaded, and bands outlined in yellow for

normalization of bands in (a). (c) Quantification of the fold change in PVN $G\alpha i_2$ protein expression between SCR ODN–minocycline co-infused animals on high salt (HS) diet (4% NaCl) and $G\alpha i_2$ ODN–minocycline co-infused animals on HS diet. (***n*** = 6 per group, * ***P*** < 0.05 ***versus*** SCR ODN treatment group, mean ± SD.)

Impact of brain $G\alpha i_2$ protein downregulation during 7 days of high salt intake on PVN inflammatory cytokine levels: In control SCR ODN-infused male Sprague–Dawley rats, 7 days of HS diet had no impact on the PVN mRNA expression of the pro-inflammatory cytokines IL-1β, IL-6 and TNFα or the anti-inflammatory cytokine IL-10 (Figure 3.3). In contrast, in male Sprague–Dawley rats receiving a targeted $G\alpha i_2$ ODN infusion, which develop ssHTN (Figure 3.1a), dietary sodium evoked a ∼2- to 2.5-fold increase ($P < 0.05$) in the PVN mRNA levels of the pro-inflammatory cytokines IL-1β, IL-6 and TNFα (Figure 3.3a–c). Additionally, in these same rats, we observed suppression of PVN mRNA expression of the anti-inflammatory cytokine IL-10 (Figure 3.3d). In control SCR ODN-infused rats maintained on 7 days of HS intake, minocycline infusion had no impact on the expression of cytokine mRNA levels (Figure 3.3). Significantly, central minocycline co-infusion abolished dietary sodium-evoked increases in pro-inflammatory cytokines and the decrease in anti-inflammatory IL-10 (Figure 3.3a–d) in targeted $G\alpha i_2$ ODN-infused rats.

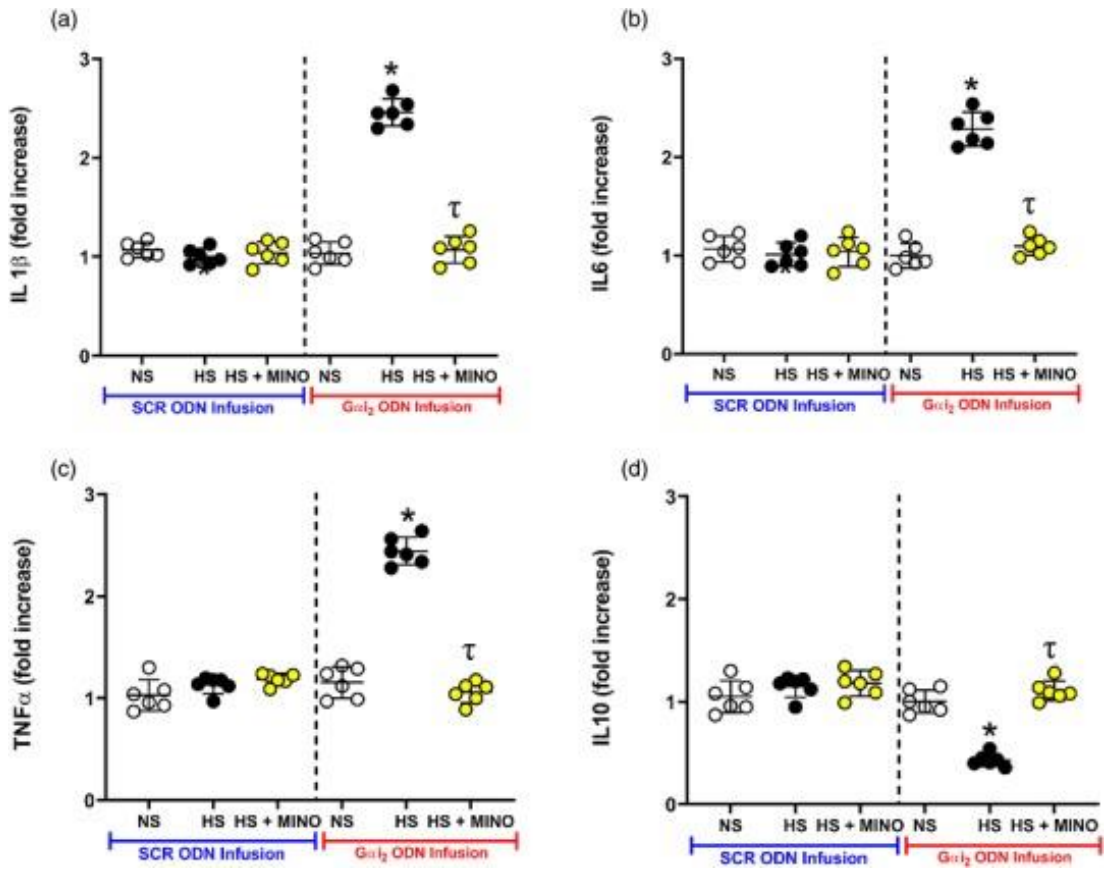

Figure 3.3: Impact of targeted Gαi$_2$ or control scrambled ICV oligodeoxynucleotide infusion and minocycline co-infusion on PVN cytokines.

Impact of targeted Gαi$_2$ or control scrambled (SCR) intracerebroventricular oligodeoxynucleotide (ODN) infusion [25 µg/ 6 µl/ day for 7 days] and minocycline (MINO)–ODN co-infusion [ODN, 25 µg/ 6 µl/ day; MINO, 120 µg/ day for 7 days in HS group only] in male Sprague–Dawley rats receiving 7 days of normal-salt (NS; 0.6% NaCl) or high-salt (HS; 4% NaCl) diets on paraventricular nucleus (PVN) mRNA levels of IL-1β (a), IL-6 (b), TNFα (c) and IL-10 (d) (n = 6 per group, * $P < 0.05$ *versus* control in respective ODN treatment group, $^{\tau}$ $P < 0.05$ *versus* HS in respective ODN treatment group, mean ± SD.)

In control SCR ODN-infused male Sprague–Dawley rats, 7 days of HS diet had no impact on the PVN protein expression of the pro-inflammatory cytokines IL-1β, IL-6 or TNFα as determined via immunohistochemistry (Figures 3.4, 3.5, 3.6). In these same normotensive SCR ODN-infused animals, 7 days of HS intake increased the immunoreactivity of the anti-inflammatory cytokine IL-10 (Figure 3.7). In contrast, in

male Sprague–Dawley rats receiving a targeted Gαi$_2$ ODN infusion, which develop ssHTN (Figure 3.1a), high salt intake evoked increased protein expression of the pro-inflammatory cytokines IL-1β and IL-6 but no change in the expression of TNFα (Figures 3.4, 3.5, 3.6). Furthermore, in contrast to the response seen in controlled SCR ODN-infused rats, the HS diet did not increase IL-10 immunoreactivity in Gαi$_2$ ODN-infused rats (Figure 3.7).

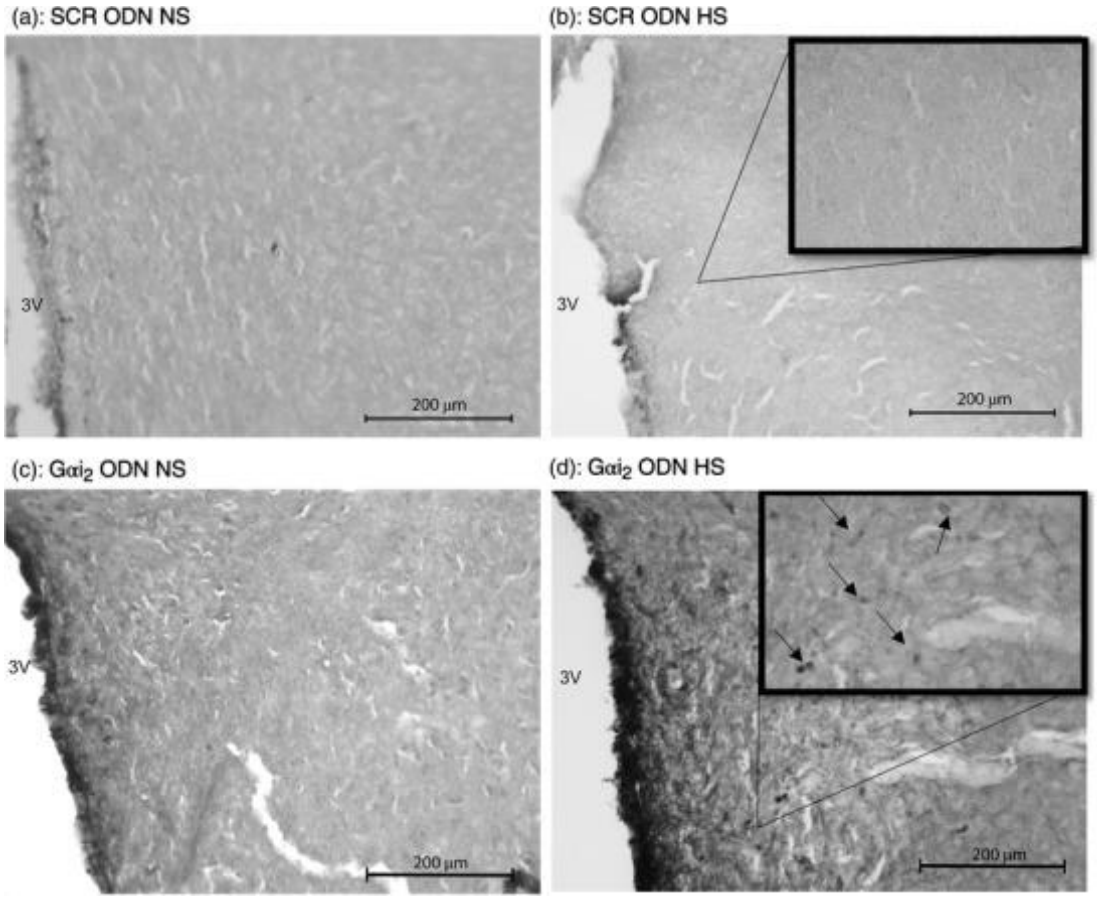

Figure 3.4: Representative photomicrographs of IL-6 immunoreactivity in the PVN of targeted Gαi$_2$ or control scrambled ICV oligodeoxynucleotide-infused SD rats.

Representative photomicrographs of IL-6 immunoreactivity in the paraventricular nucleus (PVN) of targeted Gαi$_2$ or control scrambled (SCR) intracerebroventricular oligodeoxynucleotide (ODN)-infused [25 µg/ 6 µl/ day for 7 days] male Sprague–Dawley rats on 7 days of normal-salt (NS; 0.6% NaCl) or high-salt (HS; 4% NaCl) diet. (a) SCR ODN-infused rat on NS diet. (b) SCR ODN-infused rat on HS diet. (c) Gαi$_2$ ODN-infused rat on NS diet. (d) Gαi$_2$ ODN-infused rat on HS diet. Abbreviation: 3V, third ventricle. (n = 6 per group, scale bars: 200 µm; large images ×20 magnification, inset ×40 magnification, arrows point to IL-6 stain.)

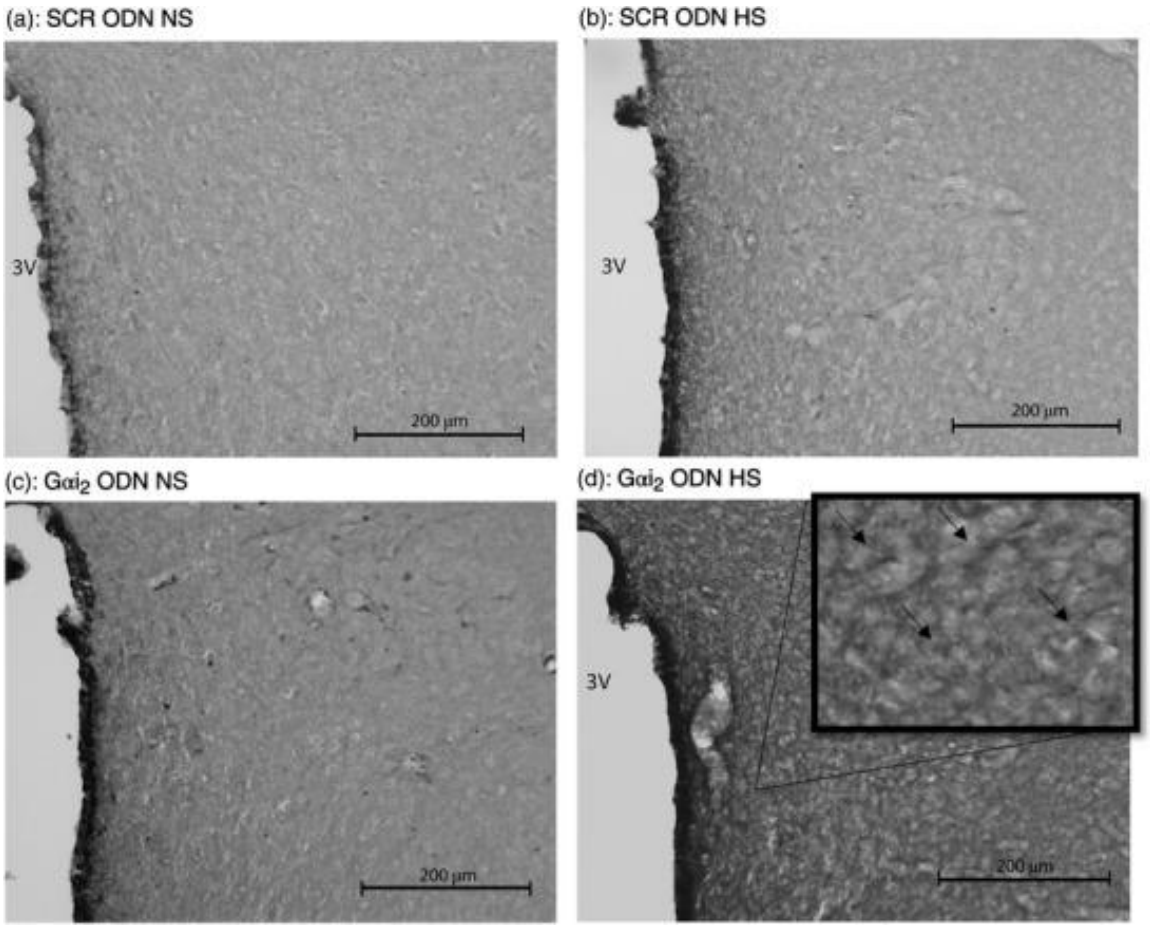

Figure 3.5: Representative photomicrographs of IL-1β immunoreactivity in the PVN of targeted Gαi$_2$ or control scrambled ICV oligodeoxynucleotide-infused SD rats.

Representative photomicrographs of IL-1β immunoreactivity in the paraventricular nucleus (PVN) of targeted Gαi$_2$ or control scrambled (SCR) intracerebroventricular oligodeoxynucleotide (ODN)-infused [25 µg/ 6 µl/ day for 7 days] male Sprague–Dawley rats on 7 days of normal-salt (NS; 0.6% NaCl) or high-salt (HS; 4% NaCl) diet. (a) SCR ODN-infused rat on NS diet. (b) SCR ODN-infused rat on HS diet. (c) Gαi$_2$ ODN-infused rat on NS diet. (d) Gαi$_2$ ODN-infused rat on HS diet. Abbreviation: 3V, third ventricle. (n = 6 per group, scale bars: 200 µm; large images ×20 magnification, inset ×40 magnification; arrows point to IL-1β stain.)

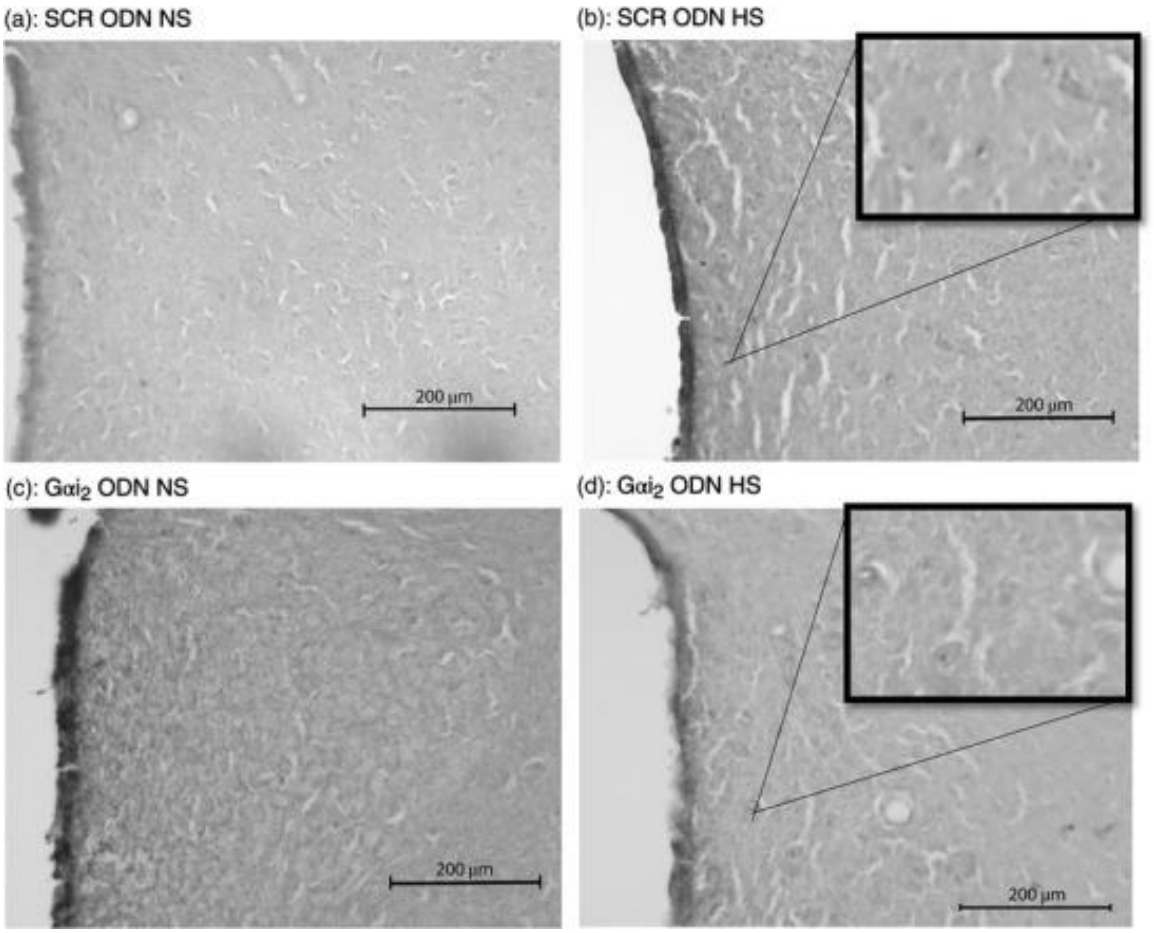

Figure 3.6: Representative photomicrographs of TNFα immunoreactivity in the PVN of targeted Gαi_2 or control scrambled ICV oligodeoxynucleotide-infused SD rats.

Representative photomicrographs of TNFα immunoreactivity in the paraventricular nucleus (PVN) of targeted Gαi_2 or control scrambled (SCR) intracerebroventricular oligodeoxynucleotide (ODN)-infused [25 µg/ 6 µl/ day for 7 days] male Sprague–Dawley rats on 7 days of normal-salt (NS; 0.6% NaCl) or high-salt (HS; 4% NaCl) diet. (a) SCR ODN-infused rat on NS diet. (b) SCR ODN-infused rat on HS diet. (c) Gαi_2 ODN-infused rat on NS diet. (d) Gαi_2 ODN-infused rat on HS diet. Abbreviation: 3V, third ventricle. (*n* = 6 per group, scale bars: 200 µm; ×20 magnification, insets ×40 magnification.)

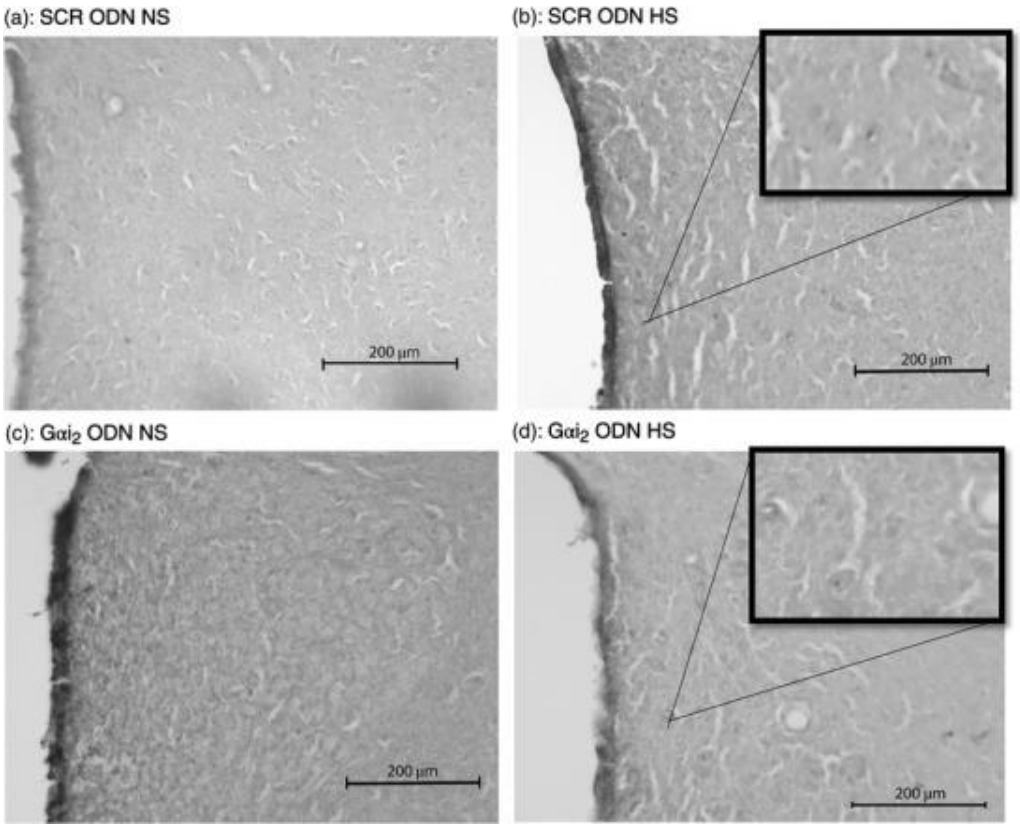

Figure 3.7: Representative photomicrographs of TNFα immunoreactivity in the PVN of targeted Gαi$_2$ or control scrambled ICV oligodeoxynucleotide-infused SD rats.

Representative photomicrographs IL-10 immunoreactivity in the paraventricular nucleus (PVN) of targeted Gαi$_2$ or control scrambled (SCR) intracerebroventricular oligodeoxynucleotide (ODN)-infused [25 µg/ 6 µl/ day for 7 days] male Sprague–Dawley rats on 7 days of normal-salt (NS; 0.6% NaCl) or high-salt (HS; 4% NaCl) diet. (a) SCR ODN-infused rat on NS diet. (b) SCR ODN-infused rat on HS diet. (c) Gαi$_2$ ODN-infused rat on NS diet. (d) Gαi$_2$ ODN-infused rat on HS diet. Abbreviation: 3V, third ventricle. (*n* = 6 per group, scale bars: 200 µm; ×20 magnification, insets ×40 magnification; arrows point to IL-10 stain.)

Impact of brain Gαi2 protein downregulation during 7 days of high salt intake on PVN microglia and astrocytes: Immunohistochemistry for OX-42 (CD11b/c; microglial antigen) in control SCR ODN-infused male Sprague–Dawley rats demonstrated that 7 days of HS diet had no impact on PVN microglial density, assessed as the average number of microglia (Figure 3.8) or as microglial activation (Figure 3.9). In contrast, in hypertensive male Sprague–Dawley rats receiving a targeted Gαi$_2$ ODN infusion, the HS diet increased

PVN microglial recruitment (Gαi2 ODN; number of microglia: NS 22 ± 8 versus HS 35 ± 7, P < 0.05; Figure 3.8) and activation (Gαi2 ODN; activation of microglia: NS 17 ± 6 versus HS 29 ± 2%, P < 0.05; Figure 3.9). Central minocycline co-infusion in control SCR ODN-infused rats maintained on 7 days of HS intake reduced average microglial density without impacting levels of microglial activation (Figures 3.8 and 3.9). Significantly, central minocycline co-infusion abolished the HS diet-evoked increase in microglial infiltration and activation in rats receiving a Gαi2 ODN infusion (Gαi2 ODN; number of microglia: HS 36 ± 7 versus HS + MINO 16 ± 6, P < 0.05; Figure 3.8; activation of microglia: HS 29 ± 2 versus HS + MINO 13 ± 6%, P < 0.05; Figure 3.9).

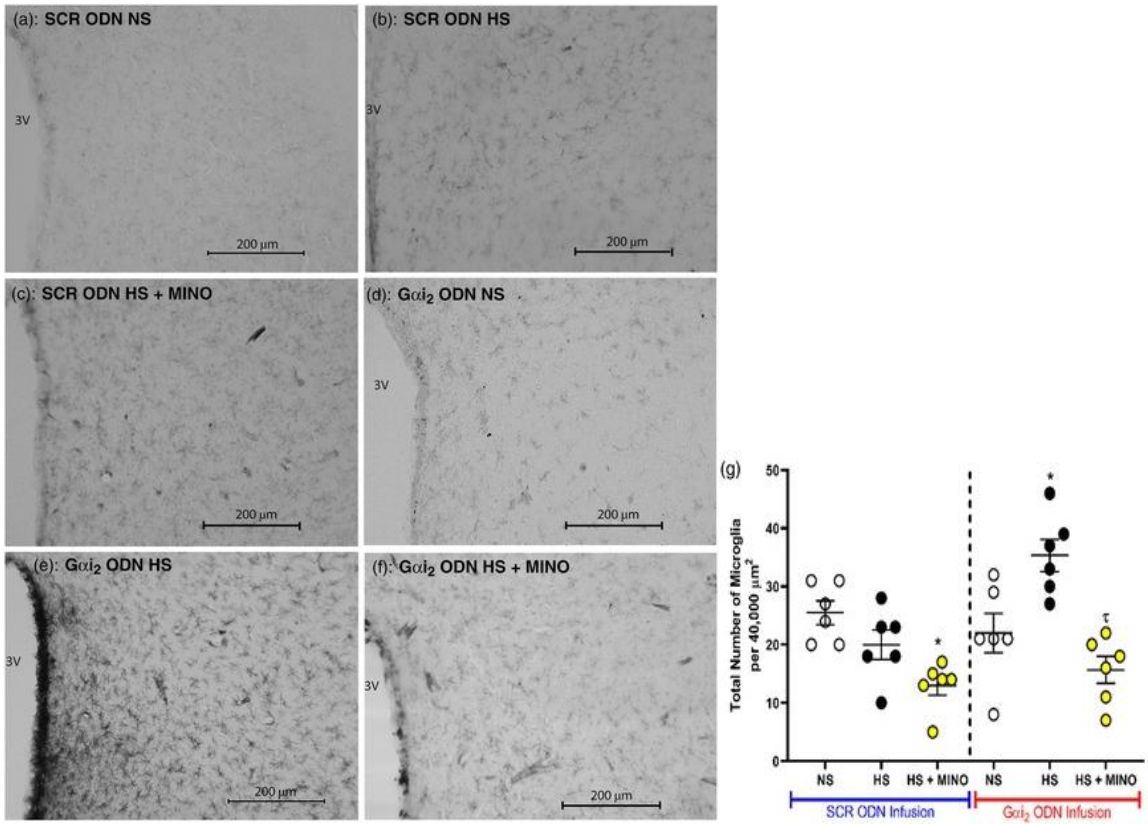

Figure 3.8: Representative photomicrographs (20X) of microglia in the PVN of targeted Gαi2 or control scrambled ICV oligodeoxynucleotide-infused SD rats.

(a–f) Representative photomicrographs of microglia (primary antibody against OX-42) in the paraventricular nucleus (PVN) of targeted $G\alpha i_2$ or control scrambled (SCR) intracerebroventricular oligodeoxynucleotide (ODN)-infused [25 µg/ 6 µl/ day for 7 days] and minocycline (MINO)–ODN co-infused [ODN, 25 µg/ 6 µl/ day; MINO, 120 µg/ day for 7 days in HS only] male Sprague–Dawley rats on 7 days of normal-salt (NS; 0.6% NaCl) or high-salt (HS; 4% NaCl) diet. (a) SCR ODN-infused rat on NS diet. (b) SCR ODN-infused rat on HS diet. (c) SCR ODN-infused rat on HS diet co-infused with minocycline. (d) $G\alpha i_2$ ODN-infused rat on NS diet. (e) $G\alpha i_2$ ODN-infused rat on HS diet. (f) $G\alpha i_2$ ODN-infused rat on HS diet co-infused with MINO (scale bars: 200 µm, ×20 magnification). (g) Average number of PVN microglia in randomly selected 200 µm × 200 µm box in Sprague–Dawley rats during SCR or $G\alpha i_2$ ODN infusion maintained on NS or HS diet and minocycline–ODN co-infusion on HS diet. Abbreviation: 3V, third ventricle. ($n = 6$ per group, * $P < 0.05$ *versus* NS in respective ODN treatment group; $^{\tau}$ $P < 0.05$ *versus* HS in respective ODN treatment group, mean ± SD.)

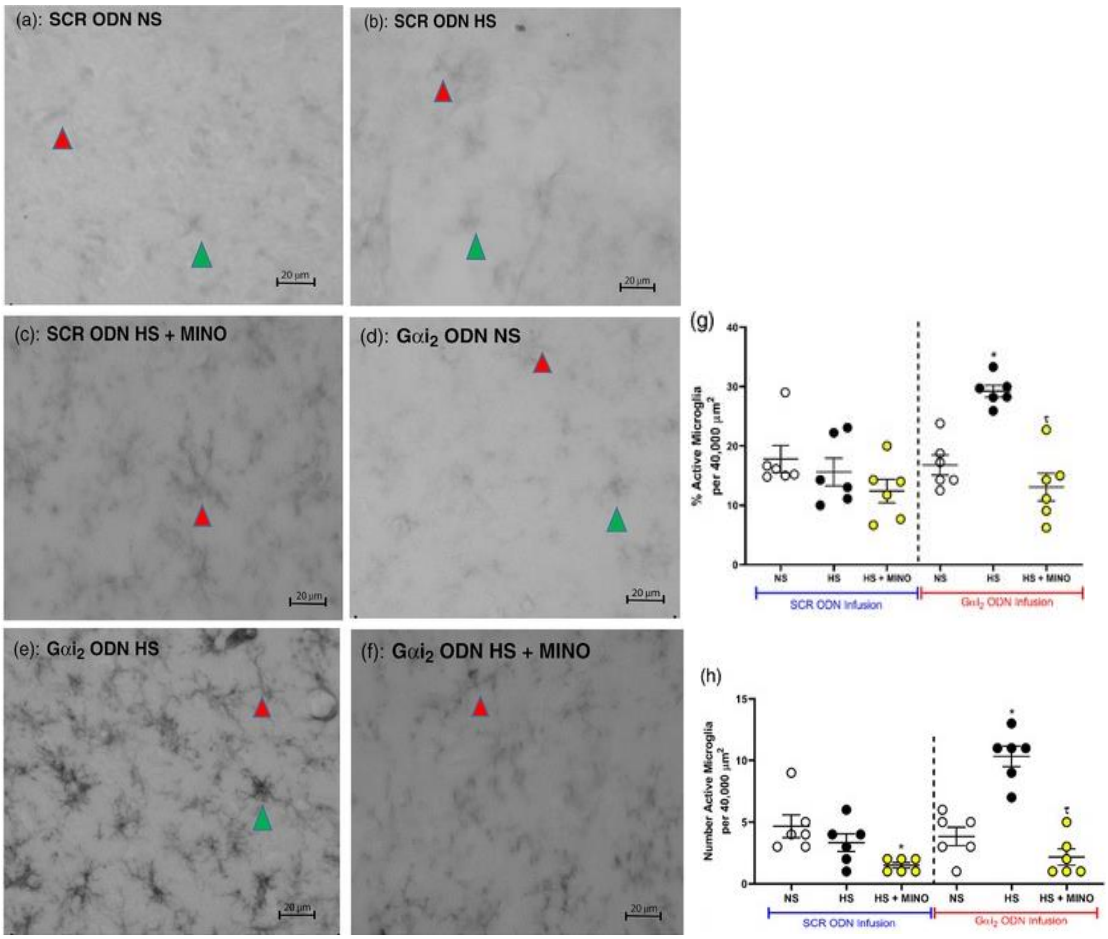

Figure 3.9: Representative photomicrographs (40X) of microglia in the PVN of targeted $G\alpha i_2$ or control scrambled ICV oligodeoxynucleotide-infused SD rats.

Representative photomicrographs of microglia in the paraventricular nucleus (PVN) of targeted $G\alpha i_2$ or control scrambled (SCR) intracerebroventricular oligodeoxynucleotide (ODN)-infused

[25 µg/ 6 µl/ day for 7 days] and minocycline (MINO)–ODN co-infused [ODN, 25 µg/ 6 µl/ day; MINO, 120 µg/ day for 7 days in HS only] male Sprague–Dawley rats on 7 days of normal-salt (NS; 0.6% NaCl) or high-salt (HS; 4% NaCl) diet. (a) SCR ODN-infused rat on NS diet. (b) SCR ODN-infused rat on HS diet. (c) SCR ODN-infused rat on HS diet co-infused with minocycline. (d) $G\alpha i_2$ ODN-infused rat on NS diet. (e) $G\alpha i_2$ ODN-infused rat on HS diet. (f) $G\alpha i_2$ ODN-infused rat on HS diet co-infused with minocycline. (g) Impact of minocycline co-infusion (120 µg day^{-1} for 7 days) on percentage activation of PVN microglia in Sprague–Dawley rats during SCR or $G\alpha i_2$ ODN infusion maintained on HS diet. (h) Impact of minocycline on number of PVN active microglia in Sprague–Dawley rats during SCR or $G\alpha i_2$ ODN infusion maintained on HS diet. (n = 6 per group, scale bars: 20 µm; green arrowheads indicate representative activated microglia; red arrowheads indicates representative inactivated microglia; ×40 magnification; * $P < 0.05$ *versus* NS in respective ODN treatment group; $^{\tau}$ $P < 0.05$ *versus* HS in respective ODN treatment group, mean ± SD.)

Sholl analysis of microglia in control SCR ODN-infused male Sprague–Dawley rats demonstrated that 7 days of HS diet had no impact on PVN microglial branching complexity, because there were no statistically significant differences in the trend lines (Figure 3.10a). In contrast, in hypertensive male Sprague–Dawley rats receiving a targeted $G\alpha i_2$ ODN infusion, the HS diet significantly decreased the branching complexity of microglia, as shown by the decreased number of ring intersections along the entire trend line compared with animals on the NS diet ($P < 0.05$; Figure 3.10b). Central minocycline co-infusion in control SCR ODN-infused rats maintained on 7 days of HS diet significantly increased microglial branching complexity, as shown by a significant elevation in ring intersections distant from the soma ($P < 0.05$; Figure 3.10a). Significantly, central minocycline co-infusion abolished the HS diet-evoked reduction in microglial branching complexity in rats receiving a $G\alpha i_2$ ODN infusion ($P < 0.05$; Figure 3.10b).

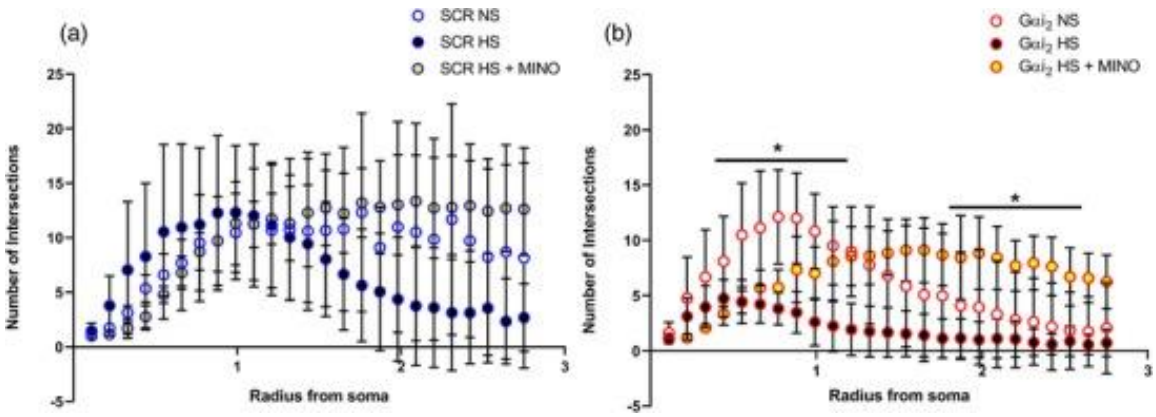

Figure 3.10: Sholl analyses of microglia in the PVN of targeted Gαi$_2$ or control scrambled ICV oligodeoxynucleotide-infused and minocycline co-infused SD rats.

Sholl analyses of microglia in the paraventricular nucleus (PVN) of the hypothalamus of targeted Gαi$_2$ or control scrambled (SCR) intracerebroventricular oligodeoxynucleotide (ODN)-infused [25 µg/ 6 µl/ day for 7 days] and minocycline (MINO)–ODN co-infused [ODN, 25 µg/ 6 µl/ day; MINO, 120 µg/ day for 7 days in HS only] male Sprague–Dawley rats on 7 days of normal-salt (NS; 0.6% NaCl) or high-salt (HS; 4% NaCl) diet. Sholl analysis of microglia, depicting branching intersections as a function of radius from the soma, in: (a) control SCR ODN-infused animals on NS and HS diets and SCR ODN–minocycline co-infused animals on HS diet; and (b) targeted Gαi$_2$ ODN-infused animals on NS and HS diets and Gαi$_2$ ODN–minocycline co-infused animals on HS diet. (* $P < 0.05$ *versus* HS in respective ODN treatment group, mean ± SD.)

Immunohistochemistry for the astrocytic marker GFAP demonstrated that, in both control SCR and targeted Gαi$_2$ ODN-infused rats, the dietary salt intake had no impact on astrocyte density within the PVN (Figure 3.11).

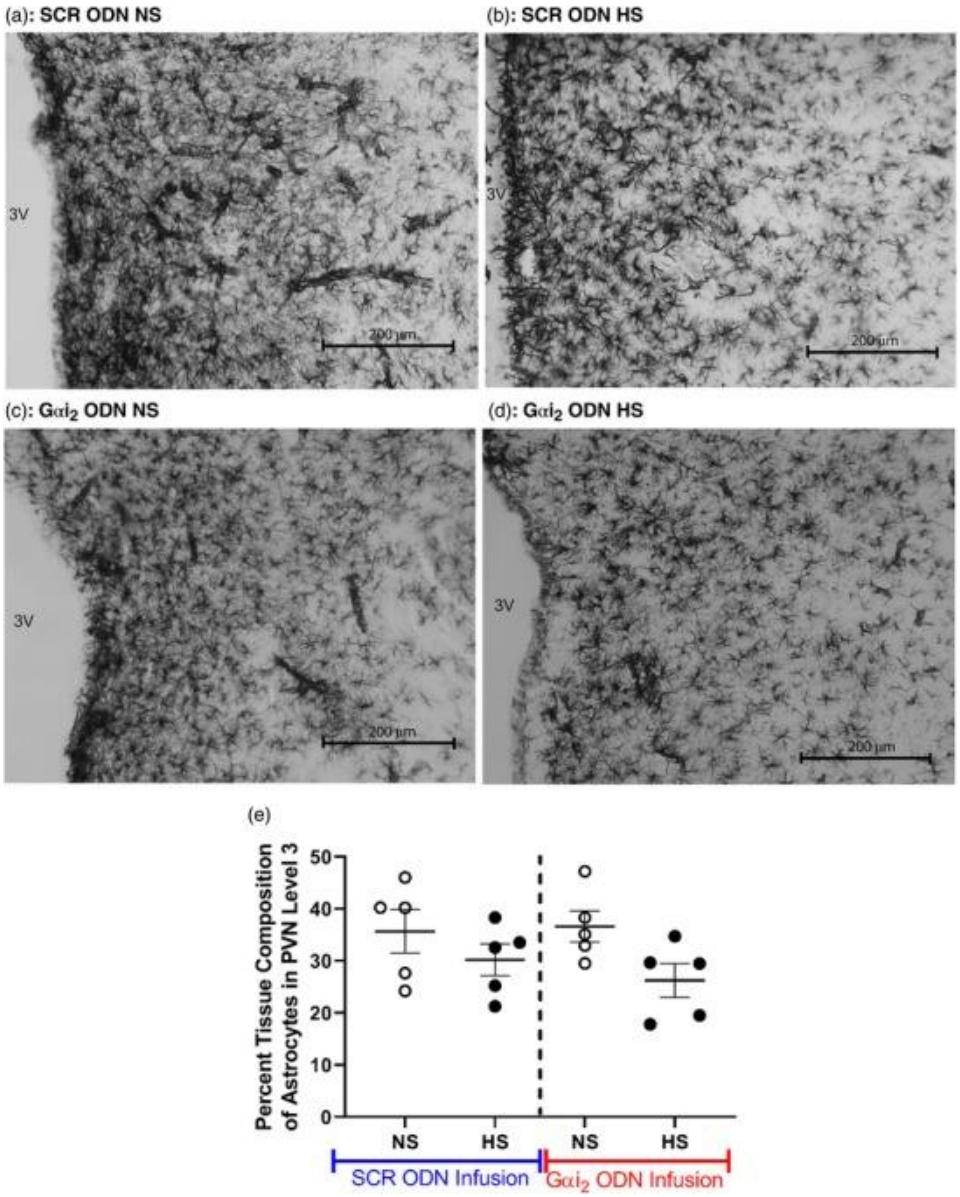

Figure 3.11: Representative photomicrographs of astrocytes in the third level of the PVN of targeted Gαi$_2$ or control scrambled ICV oligodeoxynucleotide-infused SD rats.

(a–d) Representative photomicrographs of astrocytes in the third level of the paraventricular nucleus (PVN) of targeted Gαi$_2$ or control scrambled (SCR) intracerebroventricular oligodeoxynucleotide (ODN)-infused [25 µg/ 6 µl/ day for 7 days] male Sprague–Dawley rats on 7 days of normal-salt (NS; 0.6% NaCl) or high-salt (HS; 4% NaCl) diet. (a) SCR ODN-infused rat on NS diet. (b) SCR ODN-infused rat on HS diet. (c) Gαi$_2$ ODN-infused rat on NS diet. (d) Gαi$_2$ ODN-infused rat on HS diet. (e) Percentage tissue composition of astrocytes in the PVN of Sprague–Dawley rats during SCR or Gαi$_2$ ODN infusion maintained on NS or HS diet. Abbreviation: 3V, third ventricle. (n = 5 per group, scale bar: 200 µm; ×20 magnification; mean ± SD.)

Impact of brain Gαi2 protein downregulation during 7 days of high salt intake on SFO microglia and cytokines: Immunohistochemistry for OX-42 (CD11b/c; microglial antigen) demonstrated that 7 days of HS diet had no impact on SFO microglial density, number of active microglia or percentage of active microglia, regardless of ODN infusion (Figure 3.12). Furthermore, minocycline co-infusion had no statistically significant impact on the aforementioned parameters, regardless of ODN infusion.

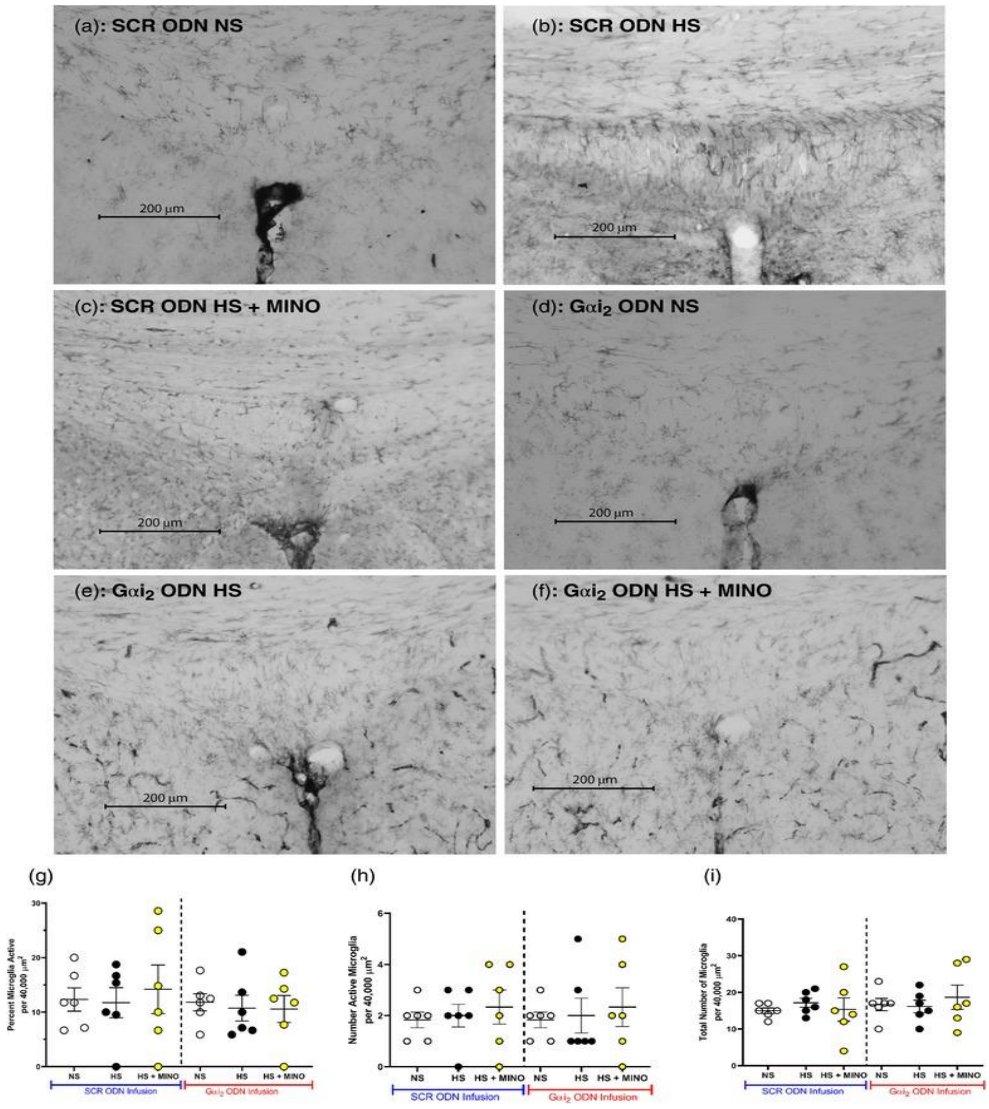

Figure 3.12: Representative photomicrographs (20X) of microglia in the SFO of targeted Gαi2 or control scrambled ICV oligodeoxynucleotide-infused SD rats

(a–f) Representative photomicrographs of microglia (primary antibody against OX-42) in the subfornical organ (SFO) of targeted $G\alpha i_2$ or control scrambled (SCR) intracerebroventricular oligodeoxynucleotide (ODN)-infused [25 µg/ 6 µl/ day for 7 days] and minocycline (MINO)–ODN co-infused [ODN, 25 µg/ 6 µl/ day; MINO, 120 µg/ day for 7 days in HS only] male Sprague–Dawley rats on 7 days of normal-salt (NS; 0.6% NaCl) or high-salt (HS; 4% NaCl) diet. (a) SCR ODN-infused rat on NS diet. (b) SCR ODN-infused rat on HS diet. (c) SCR ODN-infused rat on HS diet co-infused with minocycline. (d) $G\alpha i_2$ ODN-infused rat on NS diet. (e) $G\alpha i_2$ ODN-infused rat on HS diet. (f) $G\alpha i_2$ ODN-infused rat on HS diet co-infused with MINO. (g) Impact of minocycline co-infusion (120 µg day^{-1} for 7 days) on percentage activation of PVN microglia in Sprague–Dawley rats during SCR or $G\alpha i_2$ ODN infusion maintained on HS diet. (h) Impact of minocycline co-infusion (120 µg day^{-1} for 7 days) on number of active PVN microglia in Sprague–Dawley rats during SCR or $G\alpha i_2$ ODN infusion maintained on HS diet. (I) Impact of minocycline co-infusion (120 µg day^{-1} for 7 days) on total number of PVN microglia in Sprague–Dawley rats during SCR or $G\alpha i_2$ ODN infusion maintained on HS diet. (n = 6 per group, scale bar: 200 µm, ×20 magnification, mean ± SD.)

Immunohistochemistry in the subfornical organ suggested that 7 days of HS diet elicited no change in SFO PIC protein levels of IL-6, IL-1β or TNFα, or anti-inflammatory cytokine IL-10 protein levels between SCR ODN-infused and $G\alpha i_2$ ODN-infused rats (Figure 3.13).

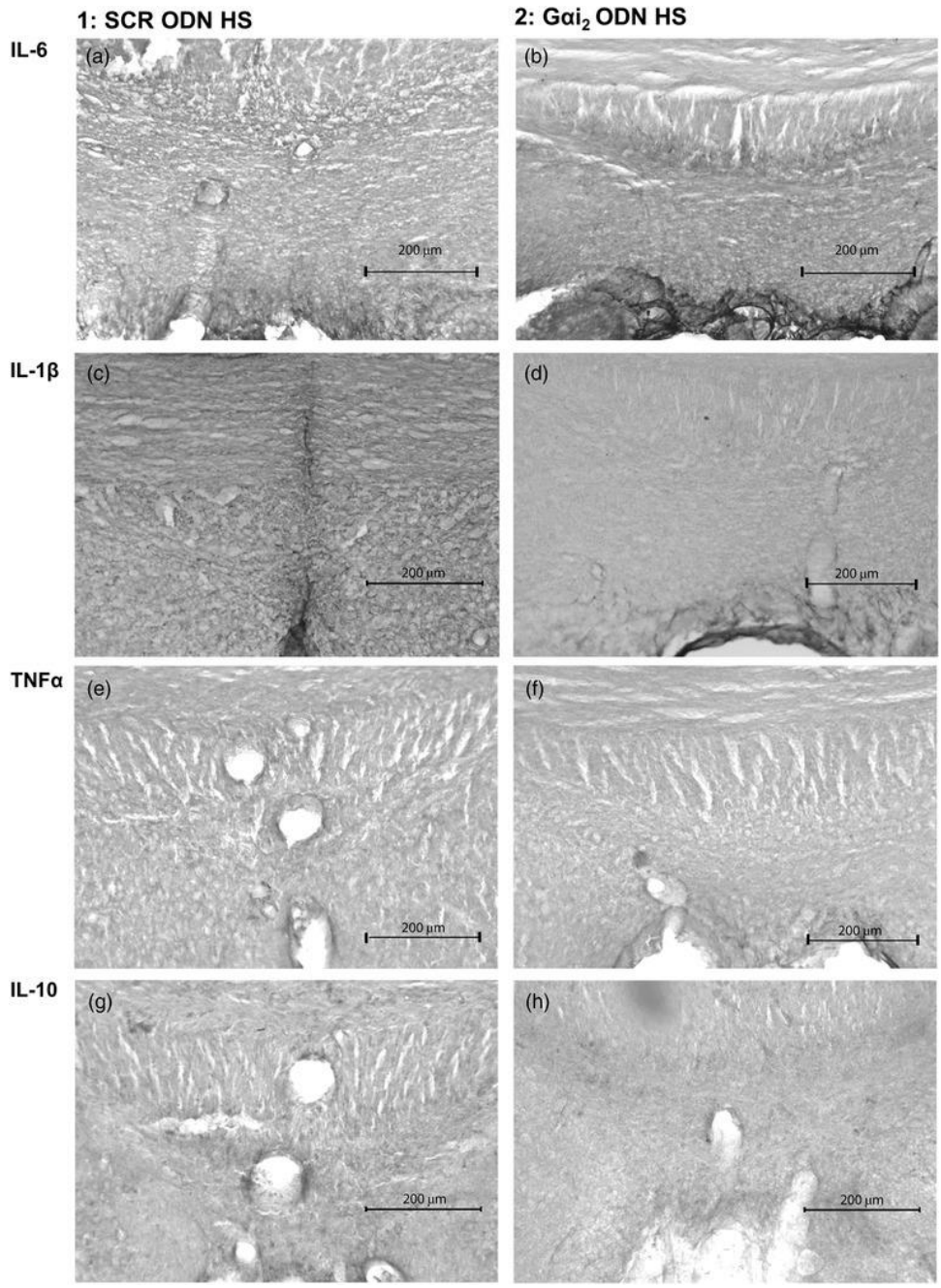

Figure 3.13: Representative photomicrographs of cytokine immunoreactivity in the SFO of targeted Gαi$_2$ or control scrambled ICV oligodeoxynucleotide-infused SD rats.

Representative photomicrographs of cytokine immunoreactivity in the subfornical organ (SFO) of control scrambled (SCR; a,c,e,g) or targeted Gαi$_2$ (b,d,f,h) intracerebroventricular oligodeoxynucleotide (ODN)-infused [25 µg/ 6 µl/ day for 7 days] male Sprague–Dawley rats on 7 days of high-salt (HS; 4% NaCl) diet. (a,b) IL-6 stain. (c,d) IL-1β stain. (e,f) TNFα stain. (g,h) IL-10 stain. (n = 6 per group, scale bar: 200 µm; ×20 magnification.)

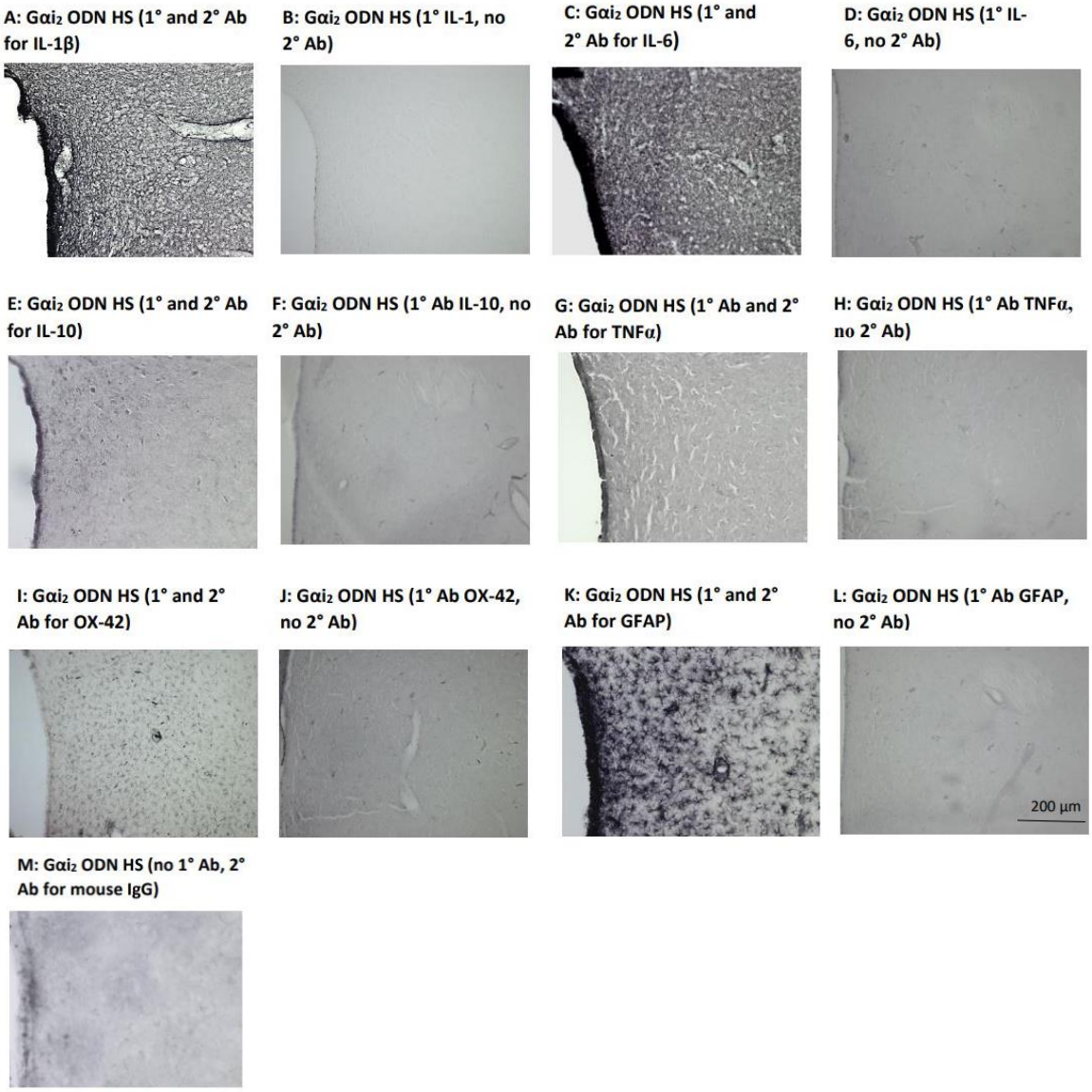

Figure 3.14: Validation of antibodies used in microglial, astrocyte, and cytokine immunohistochemistry.

(A-M) Photomicrographs of immunoreactivity in the paraventricular nucleus (PVN) of the hypothalamus in male Sprague Dawley rats infused with targeted $G\alpha i_2$ intracerebroventricular (ICV) oligodeoxynucleotide (ODN) on high salt (4% NaCl, HS) diet. (A) $G\alpha i_2$ ODN infused rat on HS diet with primary antibody (1° Ab) against rat IL-1β and secondary antibody (2° Ab) against mouse IgG, (B) $G\alpha i_2$ ODN infused rat on HS diet with 1° Ab against IL-1β and no 2° Ab, (C) $G\alpha i_2$ ODN infused rat on HS diet with 1° Ab against rat IL6 and 2° Ab against mouse IgG, (D) $G\alpha i_2$ ODN infused rat on HS diet with 1° Ab against rat IL-6 and no 2° Ab, (E) $G\alpha i_2$ ODN infused rat on HS diet with 1° Ab against rat IL-10 and 2° Ab against mouse IgG, (F) $G\alpha i_2$ ODN infused rat on HS diet with 1° Ab against rat IL-10 and no 2° Ab, (G) $G\alpha i_2$ ODN infused rat on HS diet with 1° Ab against rat TNFα and 2° Ab against mouse IgG, (H) $G\alpha i_2$ ODN infused rat on

HS diet with 1° Ab against rat TNFα and no 2° Ab, (I) $G\alpha i_2$ ODN infused rat on HS diet with 1° Ab against rat OX-42 and 2° Ab against mouse IgG, (J) $G\alpha i_2$ ODN infused rat on HS diet with 1° Ab against rat OX-42 and no 2° Ab, (K) $G\alpha i_2$ ODN infused rat on HS diet with 1° Ab against rat GFAP and 2° Ab against mouse IgG, (L) $G\alpha i_2$ ODN infused rat on HS diet with 1° Ab against rat GFAP and no 2° Ab, and (M) $G\alpha i_2$ ODN infused rat on HS diet with no 1° Ab and 2° Ab against mouse IgG. (Images at 20X, scale bar = 200 μm).

Discussion

The present study was designed to investigate the potential involvement of central inflammation in $G\alpha i_2$ protein-dependent, ssHTN. First, we demonstrated that PVN inflammation, but not SFO inflammation, involving increased PVN PIC levels, PVN microglial activation and infiltration, occurred in $G\alpha i_2$ protein-dependent, ssHTN. Additionally, central administration of minocycline, a known inhibitor of microglia, attenuated PVN microglial activation and infiltration, abolished PVN inflammation, attenuated the elevation in plasma norepinephrine and attenuated the magnitude of HTN in $G\alpha i_2$ ODN-infused rats fed a HS diet. These data together suggest a new mechanism whereby microglial activation and PVN inflammation contribute to the development of $G\alpha i_2$ protein-dependent, ssHTN and suggest a potential role of $G\alpha i_2$ protein signaling in countering PVN inflammatory processes during HS intake in the salt-resistant Sprague–Dawley rat.

In agreement with our previous data generated in male Sprague–Dawley rats (Kapusta et al., 2013), we observed the development of sympathetically mediated ssHTN after the central ODN-mediated downregulation of $G\alpha i_2$ proteins. These data extend our earlier report that $G\alpha i_2$ protein downregulation evokes ssHTN after 21 days of 8% NaCl intake (Kapusta et al., 2013), confirm our data generated in Dahl salt-resistant rats that

Gαi2 protein downregulation evokes HTN by day 7 (Wainford et al., 2015) and establish that the salt sensitivity of blood pressure after central downregulation of Gαi2 protein develops at a lower, more physiologically relevant dietary intake level (4% NaCl). Owing to the incompatible methods of tissue preparation for immunohistochemistry (paraformaldehyde fixation) and western blotting (snap-freezing) of PVN tissue, it was not possible to validate Gαi2 protein knockdown in animals in which microglia and cytokine expression were assessed by immunohistochemistry. However, to determine whether minocycline co-infusion was impacting ODN-mediated Gαi2 protein downregulation, in separate groups of animals co-infused with Gαi2 or SCR ODN and minocycline, we performed immunoblotting of PVN punches. In these animals, minocycline did not impact ODN infusion, and Gαi2 ODN infusion successfully reduced PVN Gαi2 protein expression by 79%. In certain groups of animals in which we were unable to validate knockdown via western blot, blood pressure and plasma NE concentrations were used as a physiological measure of the development of ssHTN (Carmichael et al., 2016; Kapusta et al., 2013; Wainford et al., 2015). Despite experimental limitations preventing the confirmation of Gαi2 protein knockdown, based on our many earlier publications demonstrating the efficacy of our ODN approach to downregulate central Gαi2 proteins acutely and chronically, our confirmatory studies presented in minocycline-infused animals, and the clear differences observed in Gαi2 *versus* SCR ODN-infused animals in several inflammatory markers, we are confident that Gαi2 knockdown was achieved.

Several studies, conducted in different models of HTN, including the spontaneously hypertensive rat and the angiotensin II infusion model in Sprague–Dawley rats, have

reported the presence of neuroinflammation, including increased production of pro-inflammatory cytokines (Bardgett et al., 2014; Biancardi et al., 2016; P. Shi et al., 2010). A recent study conducted in the DSS rat model also reported an upregulation of PVN pro-inflammatory cytokines in response to high dietary sodium intake (Jiang et al., 2018). As such, we elected to investigate the potential role of PVN inflammation in our salt-sensitive $G\alpha i_2$ protein-dependent ssHTN model. On day 7 of high salt intake, we observed increased PVN PIC production of *IL-6*, *IL-1β* and *TNFα* mRNA. Interestingly, immunohistochemistry for these cytokines in the PVN suggested the increased protein expression of IL-6 and IL-1β only. It is possible that TNFα protein levels may be increased only transiently during the development of ssHTN and are not required to maintain established HTN. Alternatively, it is possible that although *TNFα* mRNA is upregulated, the neuroinflammatory response observed after $G\alpha i_2$ protein downregulation is TNFα independent, as reported in angiotensin II-dependent HTN (Bardgett et al., 2014). At present, we are unable to determine the cell types to which pro-inflammatory cytokines are localized. Given the high expression of multiple G-Protein Coupled Receptors, metabotropic receptors containing alpha, beta and gamma subunits which activate upon ligand binding (GPCRs) in neurons and the impact of $G\alpha i_2$ protein downregulation on sympathetic outflow, we speculate that the observed inflammatory processes might be occurring in neurons. To address this issue experimentally, future studies might use the double labelling of cells types in combination with cytokine expression to determine the cell type to which inflammatory cytokines in the PVN are localized. Interleukin-10, an anti-inflammatory cytokine, has previously been shown to be neuroprotective (P. Shi et al.,

2010; Song et al., 2014). Levels of IL-10 were downregulated at both the mRNA and protein levels during $G\alpha i_2$ ODN infusion on the HS diet, suggesting a decrease in neuroprotective signaling in the PVN, consistent with literature suggesting that IL-10 is protective against other forms of HTN (Drews et al., 2019; Segiet et al., 2019). Lastly, minocycline administration, which lowered blood pressure and plasma NE levels in $G\alpha i_2$ ODN-infused rats on a HS diet, restored mRNA levels of PIC and anti-inflammatory cytokines to baseline, suggesting a direct role of neuroinflammation in $G\alpha i_2$ protein-dependent ssHTN. We speculate that there is an imbalance between anti-inflammatory and pro-inflammatory mechanisms occurring within the PVN that contributes to the development of ssHTN, potentially via modulation of sympathetic outflow, a hypothesis supported by the recent data generated in DSS rats (Jiang et al., 2018). Given that in our previous study, we reported that an absence of PVN $G\alpha i_2$ protein upregulation during high salt intake in the DSS rat contributes to sympathoexcitation and HTN (Wainford et al., 2015), we speculate that impaired PVN $G\alpha i_2$ protein signaling might contribute to PVN inflammation in the Dahl rat phenotype.

To attempt to identify the source of the PICs being produced in the PVN in the setting of $G\alpha i_2$ protein-dependent ssHTN, we investigated the involvement of microglia and astrocytes. We elected to examine these as potential mediators of the observed increase in PICs because both microglia (innate immune cells in brain that are tightly linked to the production of PICs; (Galic et al., 2012; P. Shi et al., 2010)) and astrocytes (regulators of CNS inflammation;(Colombo & Farina, 2016; Pekny et al., 2014)) become activated in response to pathological stimuli (e.g. HTN). Our immunohistochemical analysis revealed

no impact of central Gαi2 protein downregulation on PVN astrocytic density or immunoreactivity irrespective of dietary salt intake or HTN. These data suggest that Gαi2 protein-dependent ssHTN occurs independently of astrocyte activation. This finding supports earlier studies conducted in the angiotensin II-dependent model of HTN that reported an absence of astrocyte recruitment despite the presence of HTN and PVN inflammation (Pekny et al., 2014; X. Z. Shen et al., 2015; Verkhratsky & Nedergaard, 2018; Zubcevic et al., 2017). When examining PVN microglia, we saw increased microglial infiltration (assessed as the number of microglia present within the PVN) and activation of microglia, as indicated by reduction in cell size and decreased branching complexity on Sholl analysis, suggesting that microglia play a role in the inflammation observed in Gαi2 protein-dependent ssHTN. Additionally, microglial infiltration, activation and PIC production were not observed in the SFO, a chemosensitive region important in blood pressure regulation. Given that activated microglia are primary producers of CNS PICs, this observation might suggest that the inflammatory mechanism in our model of HTN is PVN specific. Further studies, beyond the scope of the present study, might be undertaken to investigate the potential role of inflammation in other neural control regions, such as the rostral ventrolateral medulla. To test the role of microglia in the observed PVN inflammatory response, we infused minocycline (inactivator of microglia; (Yoon, Patel, & Dougherty, 2012)). In rats in which central Gαi2 proteins were downregulated, minocycline co-infusion abolished PVN microglial infiltration and activation, abolished PIC upregulation at the mRNA level, prevented elevations in plasma NE and significantly attenuated the magnitude of dietary sodium-evoked HTN. Therefore,

we hypothesize that PVN microglia evoke central inflammation that contributes significantly, possibly via modulation of sympathetic outflow, to the pathophysiology of $G\alpha i_2$ protein-dependent ssHTN. To elucidate the potential causal relationship between microglial activation, PIC production and $G\alpha i_2$ protein-dependent ssHTN, future studies, beyond the scope of the present investigations, will assess the time course of microglial activation, PIC production and development of HTN. Additionally, we have not characterized the impact of minocycline on PVN neuron excitability electrophysiologically. It is possible that minocycline, which has been demonstrated in subpopulations of neurons to modulate excitability (Liu, Zhang, Zhu, Luo, & Liu, 2015)), operates independently of microglia to decrease the intrinsic excitability of PVN presympathetic neurons.

Collectively, these data indicate that $G\alpha i_2$ protein signal transduction is a novel CNS mechanism that influences PVN inflammation in response to a chronic HS challenge to counter the development and magnitude of sympathetically mediated ssHTN. Our present findings also suggest a potential role of $G\alpha i_2$ protein signaling in countering PVN inflammatory processes during HS intake to prevent the development of ssHTN. Given that we observed attenuated plasma NE and reductions in PIC and MAP after minocycline infusion, we speculate that microgliosis contributes significantly to $G\alpha i_2$ protein-dependent ssHTN. Our data add to our understanding of the CNS inflammatory pathways influencing blood pressure regulation and contribute to the growing body of evidence that PVN PIC pathways have a direct influence on sympathetic outflow (Z. Shi et al., 2011). Increased understanding of the PVN inflammatory responses to elevations in dietary salt intake has

implications for the development of ssHTN. We speculate that PVN neuro-inflammation, mediated by microglial activation, plays a significant role in the pathophysiology of disease states in which sympathoexcitation is evident (e.g., several forms of HTN, heart failure) and represents a potential therapeutic target. After our report of a positive association between the single nucleotide polymorphism rs10510755 in the human *GNAI2* gene and the salt sensitivity of blood pressure, independently of sex or age, in the Genetic Epidemiology of Salt Sensitivity data set (X. Zhang, Frame, Williams, & Wainford, 2018), our data have translational implications for the development of personalized anti-hypertensive therapeutics designed to target $G\alpha i_2$ protein-gated pathways.

CHAPTER FOUR: High Salt Diet-Induced PVN Inflammation and Sympathoexcitation Occurs in Male but not Female Rats Lacking Central Gαi2 Proteins

Introduction

Hypertension (HTN) is a critical public health issue that is estimated to impact one in two adults in the United States (Reboussin et al., 2018). Additionally, HTN is the leading risk factor for chronic kidney disease, myocardial infarction, and stroke (Lloyd-Jones et al., 2010; D. Mozaffarian et al., 2014). The salt sensitivity of blood pressure, an exaggerated pressor reflex to elevated dietary sodium intake, is a significant contributor to HTN. The impact of the salt sensitivity of blood pressure on HTN risk is compounded by the fact that the average American consumes an excess of three times the American Heart Association's recommended daily intake of sodium (Lloyd-Jones et al., 2010).

Our laboratory has previously demonstrated that site-specific upregulation of Guanine Nucleotide–Binding Protein Alpha Inhibiting Activity Polypeptide 2 subunit ($G\alpha i_2$) proteins in the paraventricular nucleus (PVN) of the hypothalamus is critical to the maintenance of salt resistance in male Sprague-Dawley (SD) and Dahl Salt-Resistant rats (Kapusta et al., 2013; Wainford et al., 2015). Additionally, a failure to upregulate these proteins in response to elevated sodium intake results in salt-sensitive HTN (ssHTN) in male rats (Kapusta et al., 2013; Moreira et al., 2019). Research in multiple models of HTN, including angiotensin-II dependent HTN, has demonstrated a role for PVN inflammation in the development of HTN. We recently demonstrated that in the absence of central $G\alpha i_2$

proteins elevated dietary sodium intake evokes significant microglial-mediated PVN inflammation and sympathoexcitation, as well as ssHTN in male SD rats (Moreira et al., 2019). Moreover, our work demonstrated that inhibition of microglial activation abolished dietary sodium-evoked pro-inflammatory cytokine (PIC) production and increased sympathetic outflow and attenuated the magnitude of HTN. These data suggest a correlation between PVN inflammation and the development of ssHTN.

It remains unknown if PVN inflammation is a result of HTN and elevated sympathetic outflow or if inflammation precedes and possibly drives these phenomena. Additionally, the role of central $G\alpha i_2$ proteins in mediating salt resistance in female rats is unknown. We hypothesized that PVN inflammation precedes sympathoexcitation, and likely drives the development of sympathetically-mediated ssHTN in the absence of central $G\alpha i_2$ proteins in both male and female SD rats. To test this hypothesis, we infused male and female SD rats with either scrambled control (SCR) or targeted $G\alpha i_2$ oligodeoxynucleotides (ODN) and challenged them with a normal or high salt diet over a 7-day time course. We assessed PVN inflammation, plasma and renal norepinephrine (NE) content, and dietary sodium balance over a 7-day time course.

Methods

Animals

Three-month old male and female SD rats weighing 275–300g and 200–225g, respectively, were purchased from Envigo (Indianapolis, IN). Animals were pair-housed before surgical intervention and individually-housed post-operatively. All animals were

housed in the Boston University School of Medicine Laboratory Animal Science Center, a temperature (range 20–26°C) and humidity (range 30–70%) controlled facility, on a 12:12 hour light:dark cycle, and were allowed tap water and standard irradiated rodent diet, which we will refer to as normal salt diet, (NS, 0.6% NaCl, Envigo Teklad, Teklad Global Diet No. 2918, 18% protein, 5% crude fat, 5% fiber, total potassium (K+) content 0.6%, total NaCl content 0.6% [174 mEq Na+/kg]) ad libitum. Rats were randomly assigned to experimental groups. All animal protocols were approved by the Boston University Institutional Animal Care and Use Committee (IACUC) under protocol number AN15241 and in accordance with the National Institutes of Health *Guide for the Care and Use of Laboratory Animals (8th edition)*. Euthanasia was conducted in accordance with approved IACUC protocols.

Surgical Procedures:

Intracerebroventricular Oligodeoxynucleotide Infusions:

Intracerebroventricular (ICV) oligodeoxynucleotide (ODN) infusions were performed as previously described (Moreira et al., 2019; Wainford et al., 2015). In brief, animals were anesthetized [ketamine 30 mg/kg IP + xylazine 3 mg/kg IP] and stereotaxically implanted with a stainless-steel cannula (PlasticsOne) in the right lateral cerebral ventricle. The cannula was connected via silastic tubing (PlasticsOne) to a subcutaneous Alzet Osmotic Minipump (Durect Corporation, Model 2004) filled with either scrambled (SCR) control (sequence: 5′-GGGCGAAGTAGGTCTTGG-3′) or $G\alpha i_2$ targeted (sequence: 5′-CTTGTCGATCATCTTAGA-3′)(Carmichael et al., 2020; Moreira et al., 2019; Wainford & Kapusta, 2012) ODN (Midland Certified Reagents, Midland, TX).

ODNs were infused at a rate of 25µg/ 6µl/ day. In our prior work, we utilized the National Center for Biotechnology Information Basic Local Alignment Search Tool (BLAST) to validate a lack of similarity between our SCR ODN sequence and known Rattus norvegicus gene sequences, and the specificity of our targeted $G\alpha i_2$ ODN for the $G\alpha i_2$ subunit protein sequence (Wainford & Kapusta, 2012). Due to the nature of fixation for immunohistochemical staining, it was not possible to immunoblot for $G\alpha i_2$ proteins in animals in which microglial reactivity was assessed, and so day 7 mean arterial pressure (MAP), sodium balance, and levels of circulating and renal norepinephrine (NE), as known components of $G\alpha i_2$ protein dependent ssHTN (Moreira et al., 2019; Wainford et al., 2013) were used to validate the phenotype in male animals. As we have not previously reported the efficacy of our targeted $G\alpha i_2$ ODN in female rats, brains from female rats in which sodium balance studies and plasma and renal NE content analysis were conducted were used for immunoblotting, and alternative groups were run to assess immunohistochemical markers of neuroinflammation.

Acute Femoral Artery and Femoral Vein Cannulation:

On day 7 of high salt (4% NaCl, HS) diet, subsets of male and female animals infused with either a $G\alpha i_2$ or SCR ODN on a NS or HS diet were anesthetized [sodium brevital 20 mg/kg IP supplemented 10 mg/kg IV as necessary] and the left femoral triangle was dissected out. The left femoral vein was cannulated using a PE50 catheter for the infusion of IV anesthetics and IV isotonic saline, and the left femoral artery cannulated in the same manner for the measurement of MAP. Rats were placed in a plexiglass rat holder and an isotonic infusion of saline (20 µL/ min IV) was given over a 2-hour recovery period

allowing rats to return to full consciousness and stable renal and cardiovascular function. MAP and heart rate (HR) were recorded continuously via the femoral artery cannula using computer driven BIOPAC data acquisition software (MP150 and AcqKnowledge 3.8.2; BIOPAC Systems In., Goleta, CA, USA) connected to an external pressure transducer (P23XL; Viggo Spectramed Inc., Oxnard, CA, USA) (Carmichael et al., 2020).

Transcardial Perfusion:

Subsets of male and female animals used for immunohistochemical analysis of the paraventricular nucleus (PVN) were sacrificed via transcardial perfusion as previously described . In brief, animals were deeply anesthetized [ketamine 30 mg/kg IP + xylazine 3 mg/kg IP] and perfused with ice-cold 0.1M phosphate buffered saline until the liver and kidneys cleared, and then with 4% paraformaldehyde in 0.1M PBS. Brains were extracted and post-fixed in 4% paraformaldehyde for 24 hours, and switched to 30% sucrose in 0.1M PBS for 72 hours, and stored at 4°C until processing.

Experimental Approaches:

Experimental Diet:

After a 5-day recovery following ICV implantation, to allow potential inflammation from surgery to subside, animals were placed on a NS or experimental HS (Envigo Teklad Diets, TD.03095, 19% protein, 5% crude fat, 3% fiber, total K+ content 0.8%, total NaCl content 4% [678 mEq Na+ /kg]) diet for a 1–7-day period and were then euthanized in accordance with IACUC approved protocols.

Metabolic balance studies:

Metabolic balance studies were conducted in male and female SD rats. In brief, rats were continuously housed individually in metabolic cages with ad libitum access to food and water. Following 48 h acclimatization, all rats underwent a 2-day baseline period on a NS diet prior to assignment to a 7-day experimental dietary period of HS intake. Food and water consumption and urine output were measured every 24 hours. Twenty four hour sodium balance was calculated as the difference between dietary sodium intake and urinary sodium excretion, as previously described (Kapusta et al., 2013; Kapusta et al., 2012; Moreira et al., 2019; Wainford et al., 2015).

Plasma and Renal Norepinephrine and Plasma Estrogen Analysis:

On days 1, 3 and 7 of the dietary sodium challenge subgroups of male rats (n=5/group/day) and on day 7 of the dietary sodium challenge subgroups of female rats were sacrificed via conscious decapitation and blood and kidneys were collected. Plasma was isolated from whole blood and was stored with kidneys at -80°C until use. Plasma and Renal NE content was analyzed via ELISA (IB89552, IB89537 respectively; Immuno-Biological Laboratories, Inc., Minneapolis, MN, USA) according to manufacturer's instructions and as previously described (Carmichael et al., 2016; Frame, Carmichael, et al., 2019; Moreira et al., 2019; Wainford et al., 2015). From the same blood samples analyzed for plasma NE in female rats, plasma estrogen levels were determined to identify any potential differences across groups that may impact other study parameters. In brief, plasma extracted from rats was analyzed via ELISA (IB79329 Immuno-Biological Laboratories, Inc., Minneapolis, MN, USA) according to manufacturer's instructions.

Immunohistochemistry:

Brains were sectioned on a cryostat and 40 micrometer thick sections were placed into a storage cryoprotectant solution containing 1M saline, 30% sucrose, 0.1% polyvinylpyrrolidone, and 30% ethylene glycol and stored at 4°C until staining.

Immunohistochemistry for microglial reactivity and astrocyte reactivity were performed in 6-well plates as previously described. Briefly, sections were washed in 0.1M PBS, blocked in 1% hydrogen peroxide and in 3% horse serum, and permeabilized in 0.25% Triton-X, and primary antibodies directed against rat CD 11 b/c (clone OX-42, BD Biosciences Cat# 550299, RRID:AB_393594, 1:100)(Moreira et al., 2019) or rat GFAP (Abcam catalogue no. ab53554, RRID:AB_880202, 1:500, Cambridge, MA, USA) were used in conjunction with secondary biotinylated antibodies (Vector Laboratories Cat# BA-9200 RRID:AB_2336171, 1:100 and BA-9500 RRID: AB_2336123, 1:1000)(Moreira et al., 2019). Vector Laboratories VECTASTAIN Elite ABC HRP kits (Vector Laboratories, Fisher Sci, Cat# NC9313719) and Nickel-DAB substrate was used for staining of biotinylated secondary antibodies (Moreira et al., 2019). Sections were wet mounted on gelatin-subbed slides (Southern Biotechnology), dehydrated in a sequential series of water, ethanol, and xylenes and cover slipped using Toluene permount solution UN1294 (Toluene Solution, Fisher Chemical) (Moreira et al., 2019).

Immunofluorescence:

Brains were sectioned on a cryostat at 40 micrometer thick sections throughout the brain and slices were placed into a storage cryoprotectant solution until staining. Immunofluorescence for cytokine production was performed in 6-well plates. Sections

were washed in 0.1M PBS, blocked in 3% horse serum, permeabilized in 0.25% Triton-X, and primary antibodies directed against pro-inflammatory cytokines (PICs) rat interleukin (IL)-6 (Santa Cruz Biotechnology catalogue no. sc-28343, RRID:AB_627805, 1:100, Santa Cruz, CA, USA; (Moreira et al., 2019)), IL-1β (Santa Cruz Biotechnology catalogue no. sc-32294, RRID:AB_627790, 1:100, Santa Cruz, CA, USA; (Moreira et al., 2019)), tumor necrosis factor (TNF)α (Santa Cruz Biotechnology catalogue no. sc-133192, RRID:AB_1567355, 1:100, Santa Cruz, CA, USA; (Moreira et al., 2019)), were used. Secondary antibodies conjugated to Alexa Fluor 488 and directed against mouse IgG were used (Invitrogen catalogue no. A11001, RRID: AB_2534069, 1:200, Waltham, MA, USA) to detect IL-6, IL-1β, and TNFα.

Microscopy and Image Analysis:

Microscopy was performed on a Keyence BZ-9000 Fluorescence Microscope set to bright field for IHC or fluorescence for IF. Images were captured at 20X and 40X magnification. Brain structures were identified using Paxinos & Watson The Rat Brain Atlas as previously described (Moreira et al., 2019). The PVN was identified between ~ Bregma -1.8 and Bregma -2.0, representing the caudal segment of level 1, all of level 2, and the rostral segment of level 3 of the PVN. A majority of slices contained level 2 as previously reported (Moreira et al., 2019), as the major pre-sympathetic subnuclei (the dorsal parvocellular or dorsal cap and ventrolateral parvocellular) are all present in the same slice at this level and thus local inflammation to these neurons may be the most relevant, if present.

To analyze microglial morphology, on blinded images in each animal, a 200 micron

by 200 micron box was drawn and the microglia within the box were counted for total number. Then, a reactivity assessment was performed as previously described (Moreira et al., 2019). Briefly, each cell was assessed and scored as either ramified or reactive, with the criteria being that a cell must be darkly immunoreactive as well as possess cellular projections that are of no greater length than the approximate soma size (~5 microns). Microglial reactivity was then compared to SCR ODN infused controls as total number, number reactive, and percent of microglia within the scored area that were reactive.

Astrocytes were analyzed as previously described (Moreira et al., 2019). In brief, on ImageJ software, images were converted to 16-bit and set to 'Image → Type → RGB' and then analysis was performed to quantify the percent area of the PVN that the astrocytes composed. Astrocytes were quantified (in pixels) and divided by the total number of pixels in the PVN to obtain a percentage tissue density.

Cytokine analysis was performed using Image J/FIJI (ImageJ 1.52p, Java 1.8.0_172; US National Institutes of Health). Blinded images of fluorescent cytokine stains in the PVN were opened, and the threshold of brightness was adjusted to remove background signal for the analysis. Only brightly stained puncta were counted. Once background was reduced, the image was converted to 16 bit and a threshold selection function was used to select just the fluorescent punctae, and then a percent area of the PVN area was calculated and compared across groups and timepoints.

Sholl analysis of microglia:

Sholl analysis was conducted as previously described (Moreira et al., 2019). In brief, images were blinded and shuffled, and each image was opened in Adobe CC Photoshop

(Adobe, 20.0.4 20190227.r.76), and images were overlaid with a 5 × 2 grid. Ten microglia were randomly sampled from individual grid squares and cropped so that the new image contained only the single microglial cell and its processes. Each new cropped image was opened in ImageJ/FIJI (ImageJ 1.52p, Java 1.8.0_172; US National Institutes of Health), converted to 8-bit, and the 'measure → threshold' function was used to identify the microglia from the background. The selected microglial cell was then subjected to Sholl analysis via the 'Analysis' function of FIJI, where concentric rings were placed equally distant (1 μm) from one another, radiating outwards from the center of the soma. The number of ring intersections at each ring, for a distance of 25 rings, was saved and analyzed using GraphPad Prism software (v.8; GraphPad Software, La Jolla, CA, USA) and plotted as group means at each given ring with standard deviations. Student t-test was used to compare groups with one another at given radii form the soma to determine significant differences at those intersections in branch complexity(Moreira et al., 2019).

Immunoblotting for PVN Gαi₂ Protein in Female Rats

Following a SCR or Gαi₂ ODN infusion, a 5-day recovery period, and a 7-day NS or HS diet, fresh brains were extracted from female rats sacrificed via conscious decapitation and immediately frozen at -80°C. These brains were then mounted on a cryostat and PVN punches were taken using a brain punching tool (Stoelting Co., Wood Dale, IL, USA) as previously described (Kapusta et al., 2012; Wainford et al., 2015). Tissue lysates were prepared and measured via BCA as per manufacturer's instructions (Thermo Scientific, Waltham, MA, USA). Lysates were resolved on a 7.5% SDS–PAGE gel and transferred to a nitrocellulose membrane (catalogue no. 456-1033; BioRad, Hercules, CA, USA). Gαi₂

protein levels were determined as previously published by our laboratory (Kapusta et al., 2012; Moreira et al., 2019; Wainford et al., 2015) using primary antibodies purchased from Santa Cruz Biotechnologies (Santa Cruz, CA, USA), directed against $G\alpha i_2$ (Santa Cruz Biotechnology catalogue no. sc-13534, 1:200, RRID:AB_627644) and horseradish peroxidase-conjugated secondary antibodies from Abcam (Cambridge, MA, USA) against mouse IgG (Abcam catalogue no. Ab6789, 1:2000, RRID: AB_955439); protein levels were normalized to total protein via Coomassie Blue-stained gels. Immunoreactive bands were detected via a horseradish peroxidase-conjugated secondary antibody and data were imaged and semi-quantified using Bio-Rad Quantity One image analysis software.

Statistical Analysis:

Data are expressed as mean ± SD. Differences occurring between treatment groups (e.g., SCR vs. $G\alpha i_2$ ODN in conjunction with dietary intake) were assessed by a two-way ANOVA with treatment group being one fixed effect and dietary intake the other, with the interaction included. Post hoc analysis was performed using Bonferroni's test. Differences occurring between subgroups within ODN treatment group were assessed by an unpaired student t-test. Statistical analysis was carried out using a software program (GraphPad Prism v.8; GraphPad Software, CA). Statistical significance was defined as probability $P<0.05$.

Results

Targeted $G\alpha i_2$ ODN infusion and a 7-day HS diet evokes sodium retention, sympathoexcitation and ssHTN in male rats: In 3-month-old male SD rats, a control central SCR ODN infusion, in conjunction with a 7-day HS diet evoked rapid and robust global

sympathoinhibition by day 1 (SCR ODN NS plasma NE [nmol/L] 66±11 vs. HS Day 1 42±10; $p<0.05$) and reduced sympathetic outflow to the kidney by day 3 (SCR ODN NS renal NE [pg/mg] 516±17 vs. SCR ODN HS D3 448±63; $p<0.05$). Both global and renal specific sympathoinhibition were maintained for the full duration of the 7-day HS intake time course. In these same animals there was a transient increase in 24-h sodium balance on day 1 of HS intake and the maintenance of normotension (Figure 4.1). In contrast, an experimental $G\alpha i_2$ ODN infusion in conjunction with a 7-day HS diet evoked ssHTN by day 7 (mean arterial pressure (MAP) [mmHg] D7: $G\alpha i_2$ ODN NS 124±3 vs. $G\alpha i_2$ ODN HS 149±4; $p<0.05$). It also prevented the observed rapid sympathoinhibitory response observed in SCR ODN treated rats and elicited significant increases in global and renal specific sympathetic outflow by day 3 ($G\alpha i_2$ ODN NS Plasma NE [nmol/L] 72±6 vs. $G\alpha i_2$ ODN HS D3 95±11; $p<0.05$) ($G\alpha i_2$ ODN NS Renal NE [pg/mg] 522±78 vs. $G\alpha i_2$ ODN HS D3 968±109; $p<0.05$). In $G\alpha i_2$ ODN infused rats, we observed significant increases in 24-h sodium retention for days 1-5 of HS intake with a peak sodium of 5 mEq on day 2 of HS (Figure 4.1).

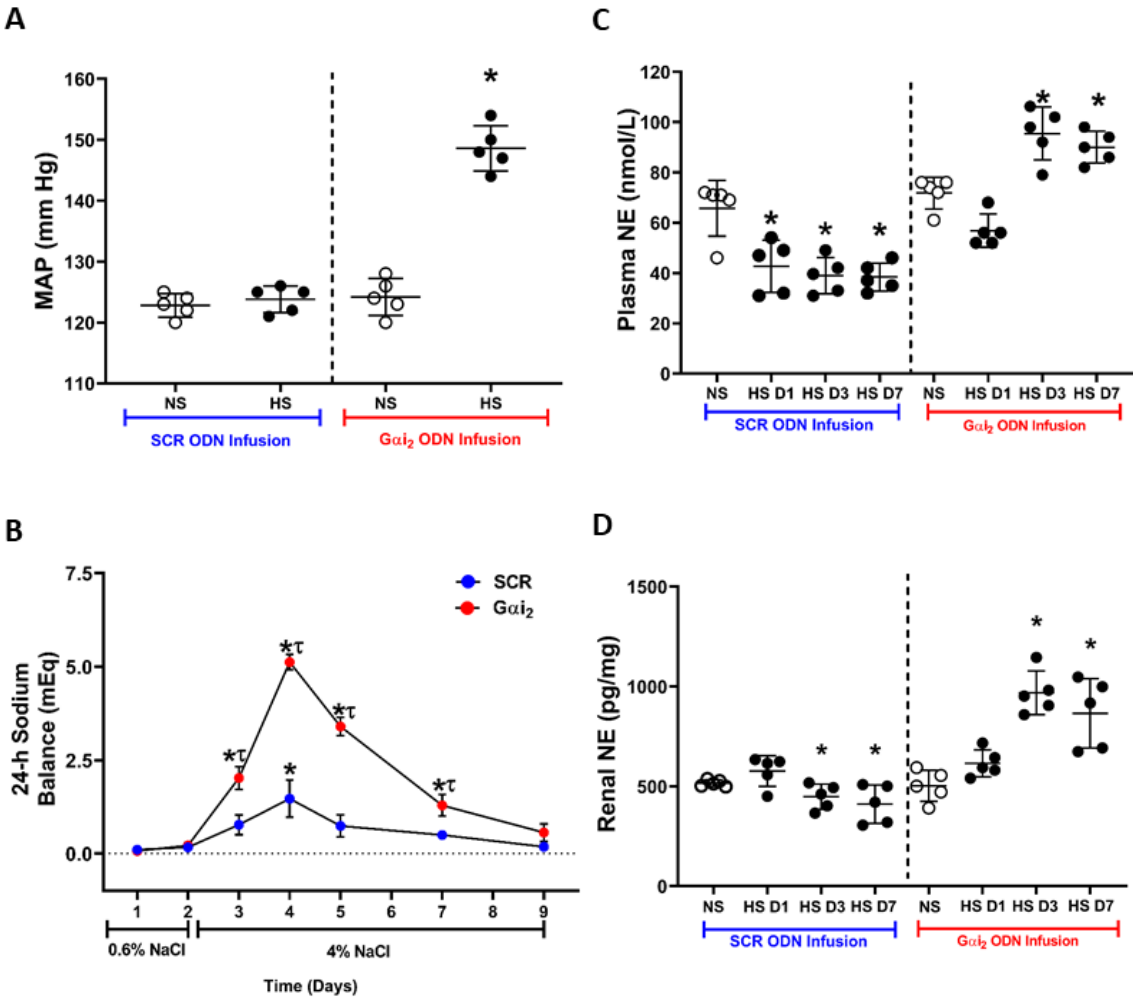

Figure 4.1: Day 7 Mean Arterial Pressure and Temporal Dynamics of Sodium Balance and Sympathetic Tone in Male SD Rats With and Without Central Gαi$_2$ Proteins.

Impact of intracerebroventricular (ICV) control scrambled (SCR) or targeted Gαi$_2$ oligodeoxynucleotide (ODN) infusion (25 µg/ 6µL/ day) and 7-day (A-B) or 1-7-day (C-D) normal (NS, 0.6% NaCl) or high (HS, 4% NaCl) salt diet in 3 month old male Sprague-Dawley rats on A) mean arterial pressure (MAP, mmHg) B) sodium balance (mEq/day), C) plasma norepinephrine (NE, nmol/L) and D) renal NE content (pg/mg) (*p<0.05 compared to NS control within ODN infusion group, τp<0.05 compared to SCR ODN infusion at same time point; n=5/group, 2-way analysis of variance (ANOVA)).

Targeted Gαi$_2$ ODN infusion and a 7-day HS diet evokes PVN neuroinflammation in male rats: In contrast to control SCR ODN infused 3-month-old male SD rats on a HS diet, which display comparable levels of PVN microglial reactivity to SCR ODN infused

animals on NS diet, an experimental Gαi$_2$ ODN infusion and HS diet evoked significant increases in PVN microglial activation by 24 hours (Gαi$_2$ ODN NS percent microglia active per 40,000 μm^2 sample area 12±4% vs. Gαi$_2$ ODN HS D1 25±3%; $p<0.05$) that were maintained over the duration of the study (Figure 4.2). In these animals, the total number of microglia present in the sample area of the PVN was not significantly upregulated in Gαi$_2$ ODN infused male rats until 72 hours post-placement on HS intake (Gαi$_2$ ODN NS total number microglia per 40,000 μm^2 sample area 17±3 vs Gαi$_2$ ODN HS D3 29±3; $p<0.05$) and was maintained until day 7. Sholl analysis in these same animals revealed that the microglial branching complexity, evident as number of intersections in concentric rings radiating from the soma, was significantly decreased at proximal ring intersections beginning on day 1, supporting our morphological analyses (Figure 4.3).

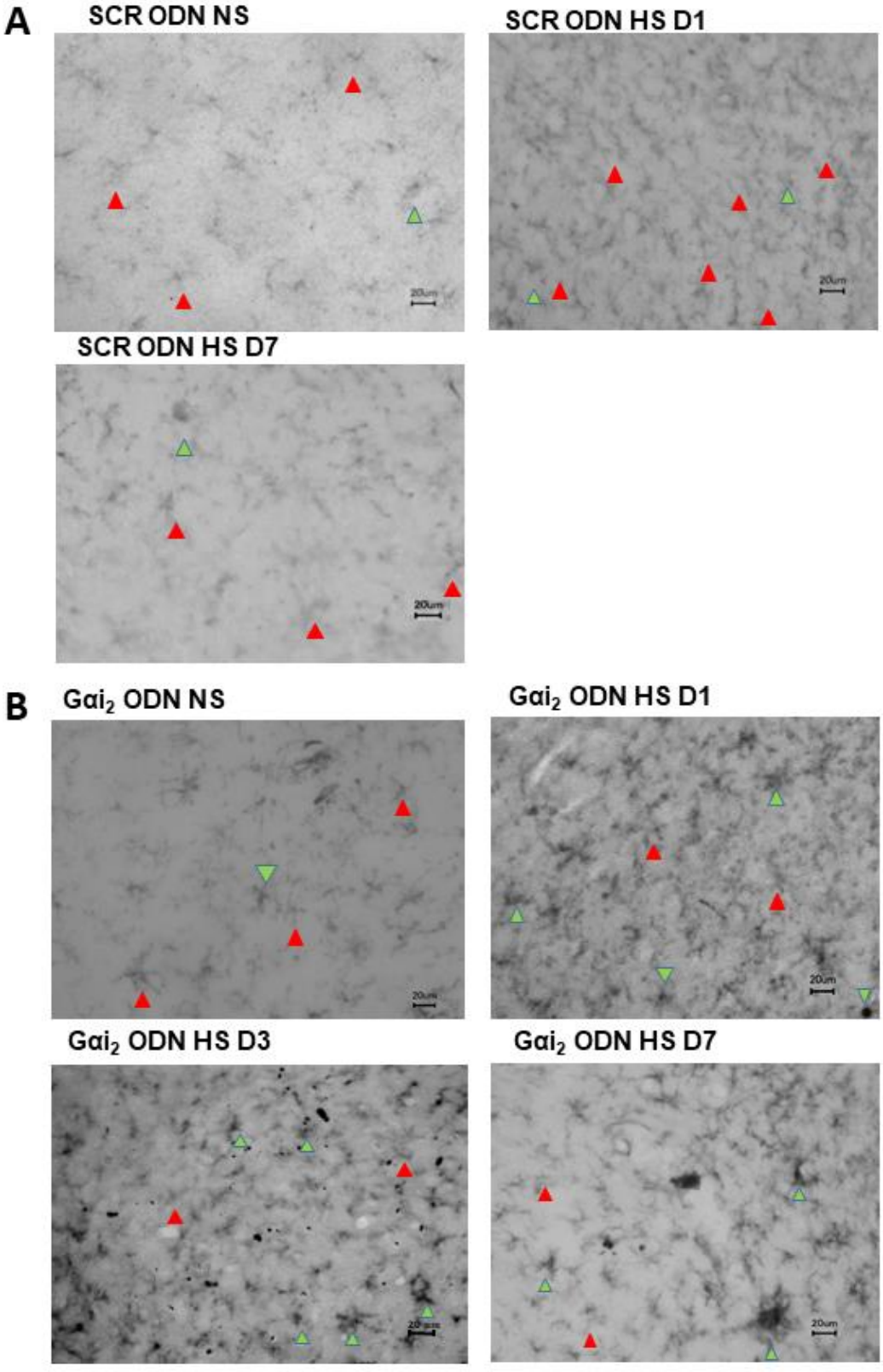
A
SCR ODN NS
SCR ODN HS D1
SCR ODN HS D7
B
Gαi2 ODN NS
Gαi2 ODN HS D1
Gαi2 ODN HS D3
Gαi2 ODN HS D7

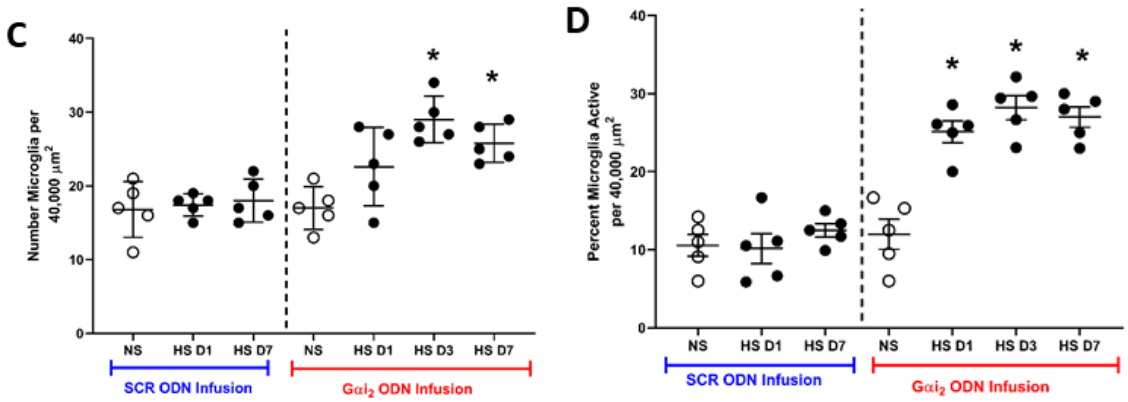

Figure 4.2: Temporal Dynamics of High-Salt-Induced Microglial Activation in Male SD Rats With and Without Central Gαi_2 Proteins.

(A-B) Representative photomicrographs of microglia (OX-42 immunohistochemistry) in the hypothalamic paraventricular nucleus (PVN) of intracerebroventricular (ICV) control scrambled (SCR, A) or targeted Gαi2 (B) oligodeoxynucleotide (ODN) infused (25 µg/ 6µL/ day) male rats subjected to a 1-7-day normal (NS, 0.6% NaCl) or high (HS, 4% NaCl) salt diet. (C-D) Quantification of photomicrographs of PVN microglial activation expressed as (C) total number of all microglia and (D) percent of microglia active per 40,000 µm2 (scale bar = 20 µm, images captured at 40X, red arrows indicate examples of ramified microglia, green arrows indicate examples of active microglia, *p<0.05 compared to NS within ODN infusion group, n=5/group, 2-way analysis of variance (ANOVA)).

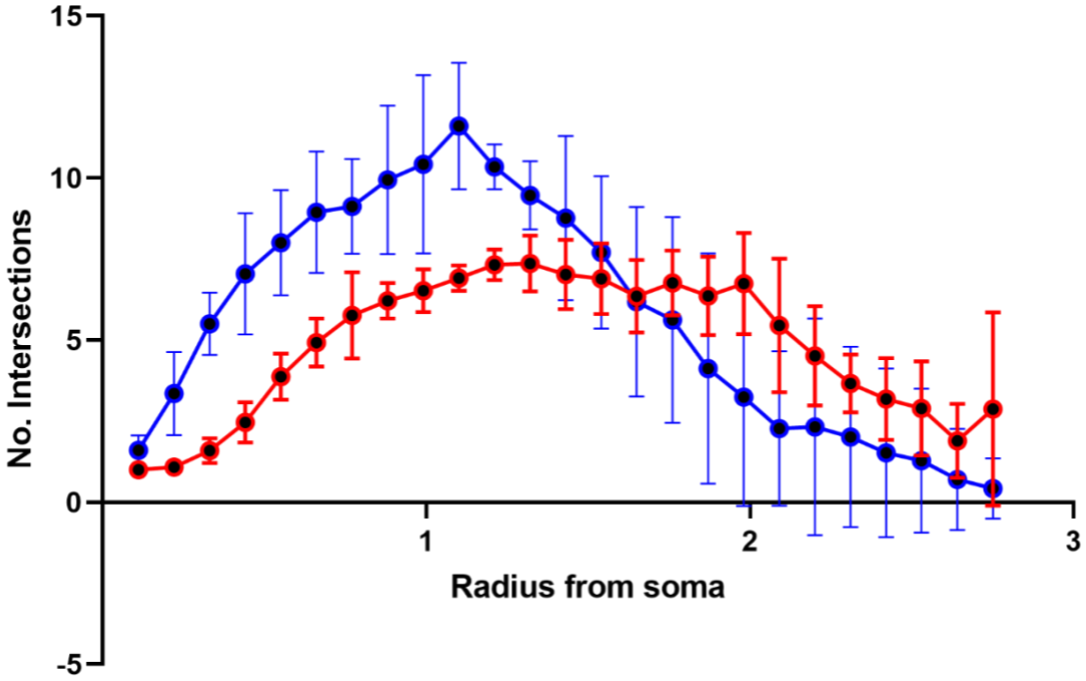

Figure 4.3: Sholl Analysis of Microglial Branching Complexity on Day 1 of HS in Male SD Rats With and Without Central Gαi$_2$ Proteins.

Impact of intracerebroventricular (ICV) infusion of control scrambled (SCR) or targeted Gαi$_2$ oligodeoxynucleotide (ODN) infusion in conjunction with 7-day high (HS; 4% NaCl) salt diet on hypothalamic paraventricular nucleus (PVN) microglial morphology as assessed via Sholl analysis in 3-month-old male Sprague Dawley rats (*$p<0.05$ vs SCR ODN infusion at respective radius from soma, n=5/group at sampling rate of 10 microglia per animal for 50 microglia per group, unpaired student t-test).

In 3-month-old male SD rats, Gαi2 ODN infusion and HS diet evoked significant increases in the immunofluorescence of the PIC IL-1β by day 3 and IL-6 by day 7 with no observable change in the expression of TNFα, in the PVN by day 7 of HS diet compared to SCR ODN and HS (Figures 4.4 and 4.5). Negative controls demonstrating selectivity of the antibodies used in these studies are presented in Figure 4.6.

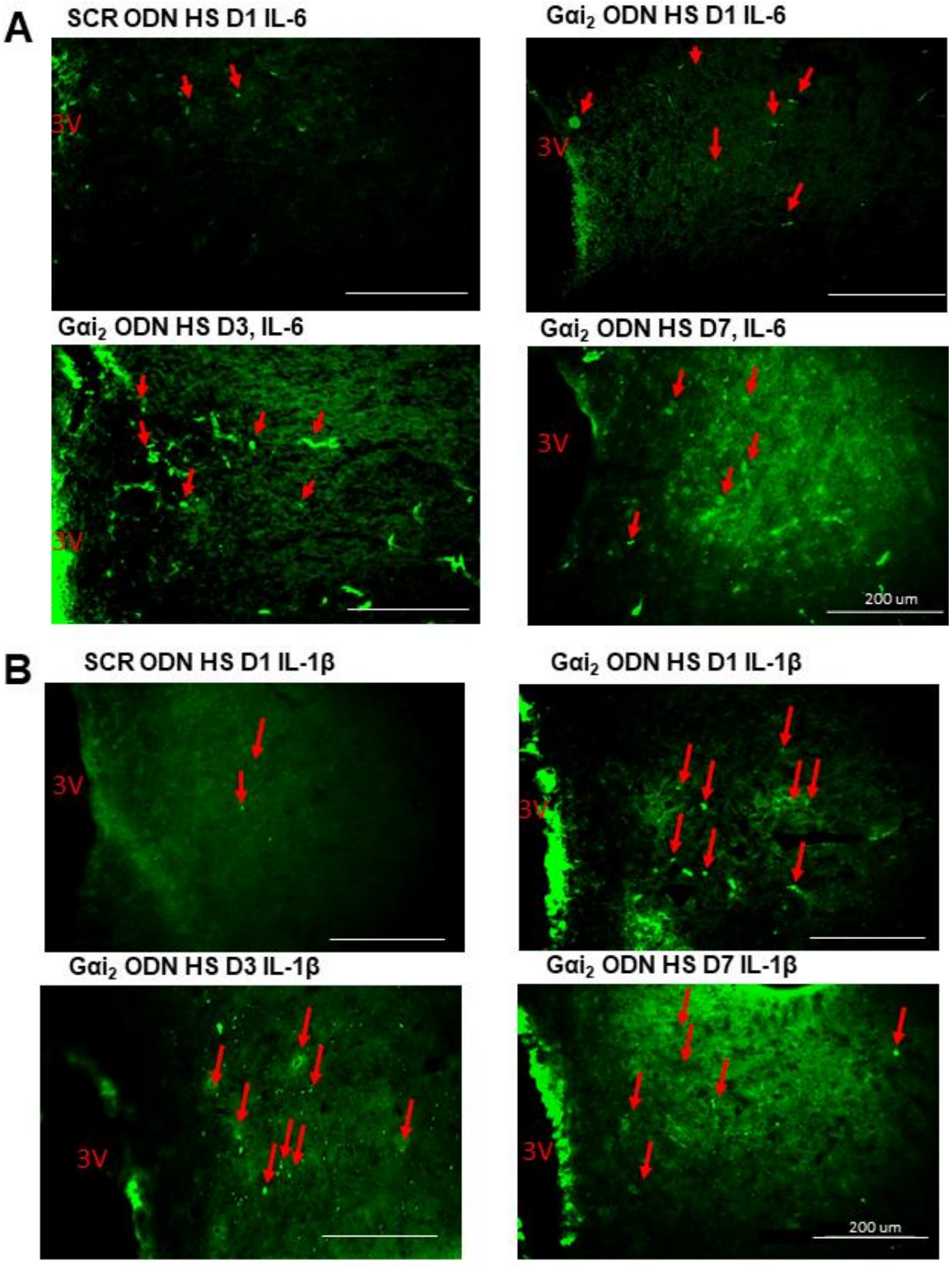
A
SCR ODN HS D1 IL-6
Gαi2 ODN HS D1 IL-6
Gαi2 ODN HS D3, IL-6
Gαi2 ODN HS D7, IL-6
3V
200 um
B
SCR ODN HS D1 IL-1β
Gαi2 ODN HS D1 IL-1β
Gαi2 ODN HS D3 IL-1β
Gαi2 ODN HS D7 IL-1β
3V
200 um

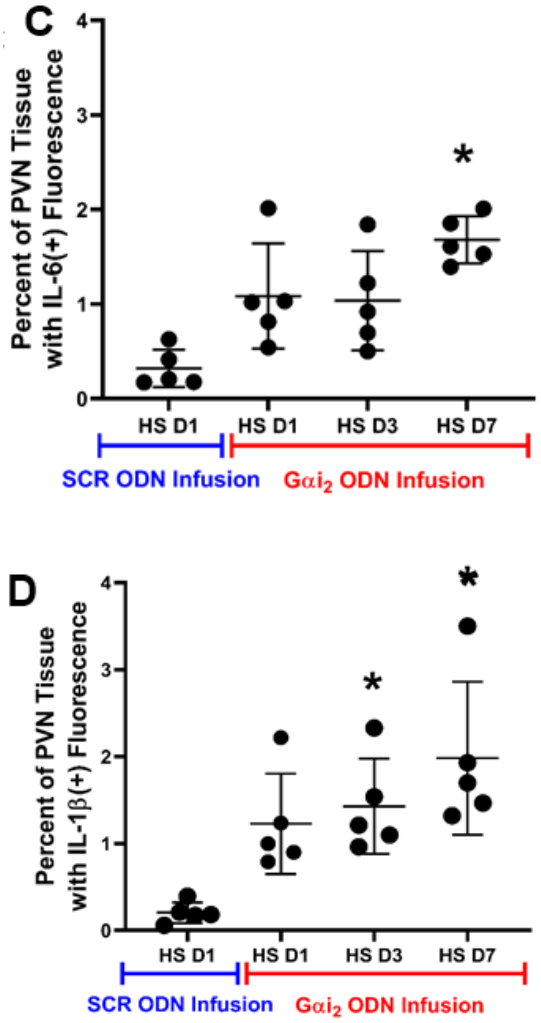

Figure 4.4: Immunofluorescent Stains of PVN Pro-Inflammatory Cytokines IL-1β and IL-6 in Male SD Rats With and Without Central $G\alpha i_2$ Proteins.

(A-B) Representative photomicrographs of cytokine immunofluorescent staining (A, interleukin-6 (IL-6)) and (B, interleukin-1β (IL-1β) in the hypothalamic paraventricular nucleus (PVN) of intracerebroventricular (ICV) control scrambled or targeted $G\alpha i_2$ oligodeoxynucleotide (ODN) infused (25 µg/ 6µL/ day) male rats subjected to a 1-7-day high (4% NaCl) salt diet. (C-D) Quantification of positive immunofluorescent puncta in (A-B) as a percent pixel composition of total PVN area (scale bar = 200 µm, images captured at 20X, red arrows indicate positive puncta, *$p<0.05$ compared to SCR ODN infusion control, n=5/group, 2-way analysis of variance (ANOVA)).

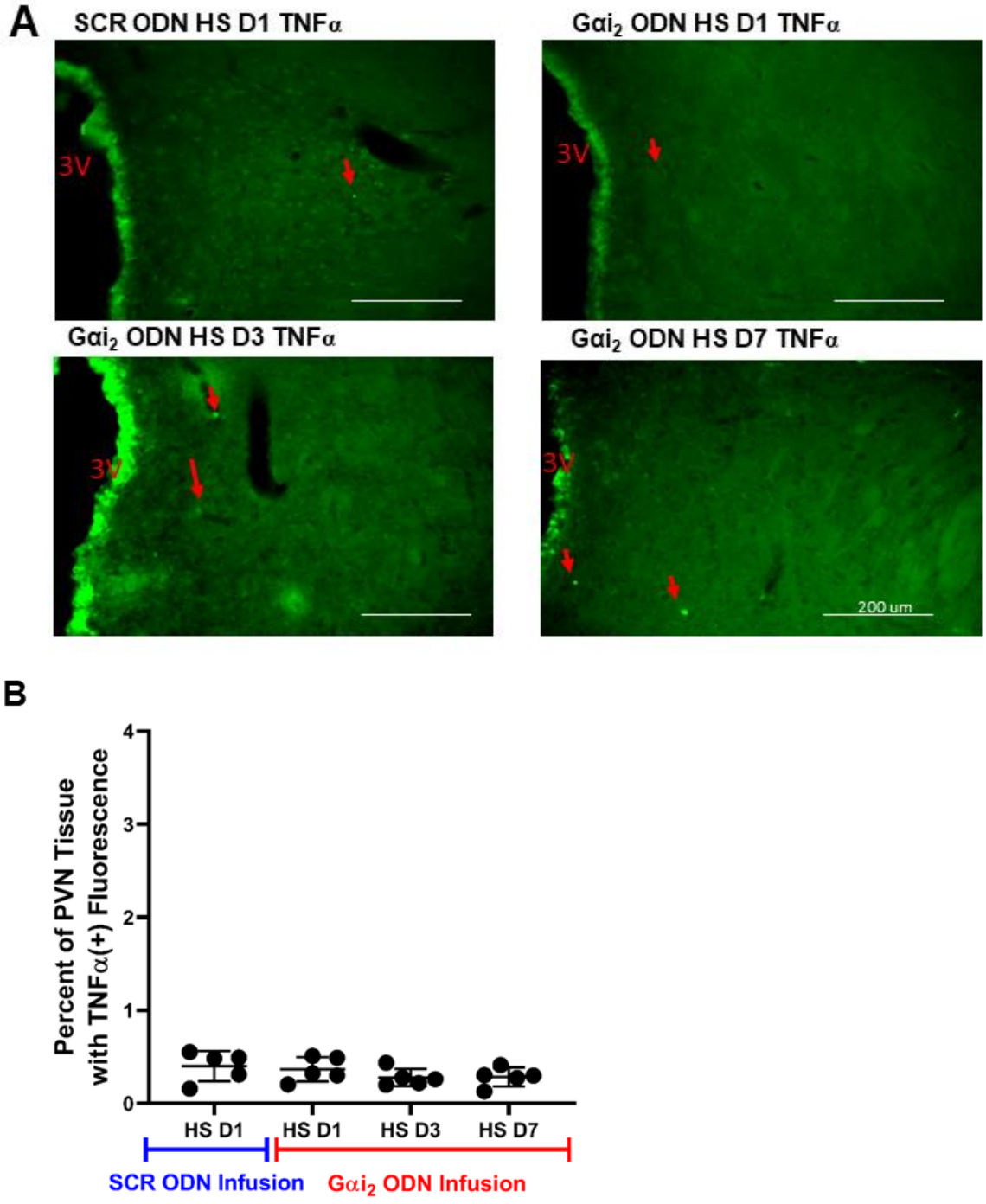

Figure 4.5: Immunofluorescent Stain of PVN Pro-Inflammatory Cytokine TNFα in Male SD Rats With and Without Central Gαi$_2$ Proteins.

(A) Representative photomicrographs of cytokine immunofluorescent staining (A, tumor necrosis factor α (TNFα)) in the hypothalamic paraventricular nucleus (PVN) of intracerebroventricular (ICV) control scrambled or targeted Gαi$_2$ oligodeoxynucleotide (ODN) infused (25 µg/ 6µL/ day)

male rats subjected to a 1–7-day high (4% NaCl) salt diet. (B) Quantification of positive immunofluorescent puncta in (A) as a percent pixel composition of total PVN area (scale bar = 200 μm, images captured at 20X, red arrows indicate positive puncta, *p<0.05 compared to SCR ODN infusion control, n=5/group, 2-way analysis of variance (ANOVA)).

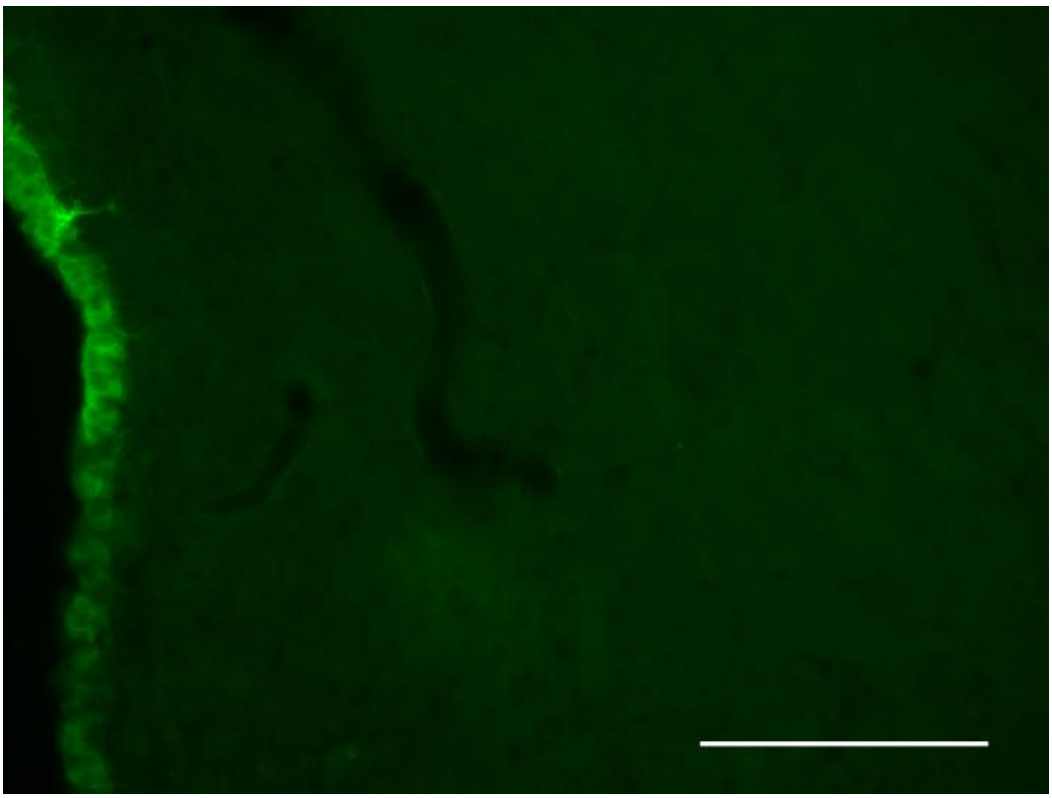

Figure 4.6: Immunofluorescent Control Stain Omitting Primary Antibodies in the PVN of Male SD Rat Lacking Central Gαi_2 Proteins on High-Salt Diet.

Representative photomicrograph of negative control immunofluorescent staining performed of hypothalamic paraventricular nucleus (PVN) cytokines utilizing Alexa-Fluor 488-conjugated goat anti-mouse secondary antibodies but no primary antibodies in 3-month old male Sprague Dawley rats receiving an intracerebroventricular (ICV) infusion (25 μg/ 6 μL/ day) of targeted Gαi_2 oligodeoxynucleotides (ODN) in conjunction with 7-day high (HS; 4% NaCl) salt diet (scale bar = 200 μm, images captured at 20X, n=5/group).

Targeted Gαi_2 ODN infusion and a 7-day HS diet do not induce sympathoexcitation or PVN neuroinflammation in female rats: In 3-month-old female SD rats, as observed in male SD rats, a control SCR ODN infusion in conjunction with a 7-day HS diet resulted in

global sympathoinhibition (SCR ODN NS Plasma NE [nmol/L] 55±8 vs. HS 35±12; $p<0.05$) and renal sympathoinhibition (SCR ODN NS Renal NE [pg/mg] 517±29 vs. HS 417±90; $p<0.05$) accompanied by sodium homeostasis and normotension (Figure 4.7). In contrast to our findings in male SD rats, a $G\alpha i_2$ ODN infusion in conjunction with a 7-day HS diet elicited a significantly lower increase in MAP in female vs. male SD rats compared to rats maintained on a NS intake (ΔMAP [mmHg] Male SD $G\alpha i_2$ ODN NS vs. HS +24±2 vs. Female $G\alpha i_2$ ODN NS vs. HS +7±1; $p<0.05$) and an increase in renal sodium retention on only day 1 of HS intake (Figure 4.7). In opposition to our results obtained in male rats, $G\alpha i_2$ ODN infusion and HS intake failed to elicit sympathoexcitation or increases in total number of PVN microglia or percent of active microglia present (Figures 4.7 and 4.8). In female rats we also observed no $G\alpha i_2$ ODN-induced changes in PVN astrocyte levels. As documented (Figure 4.9), we observed no impact of dietary sodium intake or ODN infusion on plasma estrogen levels. Replicating our prior findings in male SD and DSR rats, we observed a significant approximate 2-fold increase in PVN $G\alpha i_2$ protein expression (Figure 4.10). Validating the efficacy of a targeted $G\alpha i_2$ ODN, but not control SCR ODN, infusion to downregulate $G\alpha i_2$ protein levels we observed significant (greater than 85%) downregulation of PVN $G\alpha i_2$ protein expression (Figure 4.11).

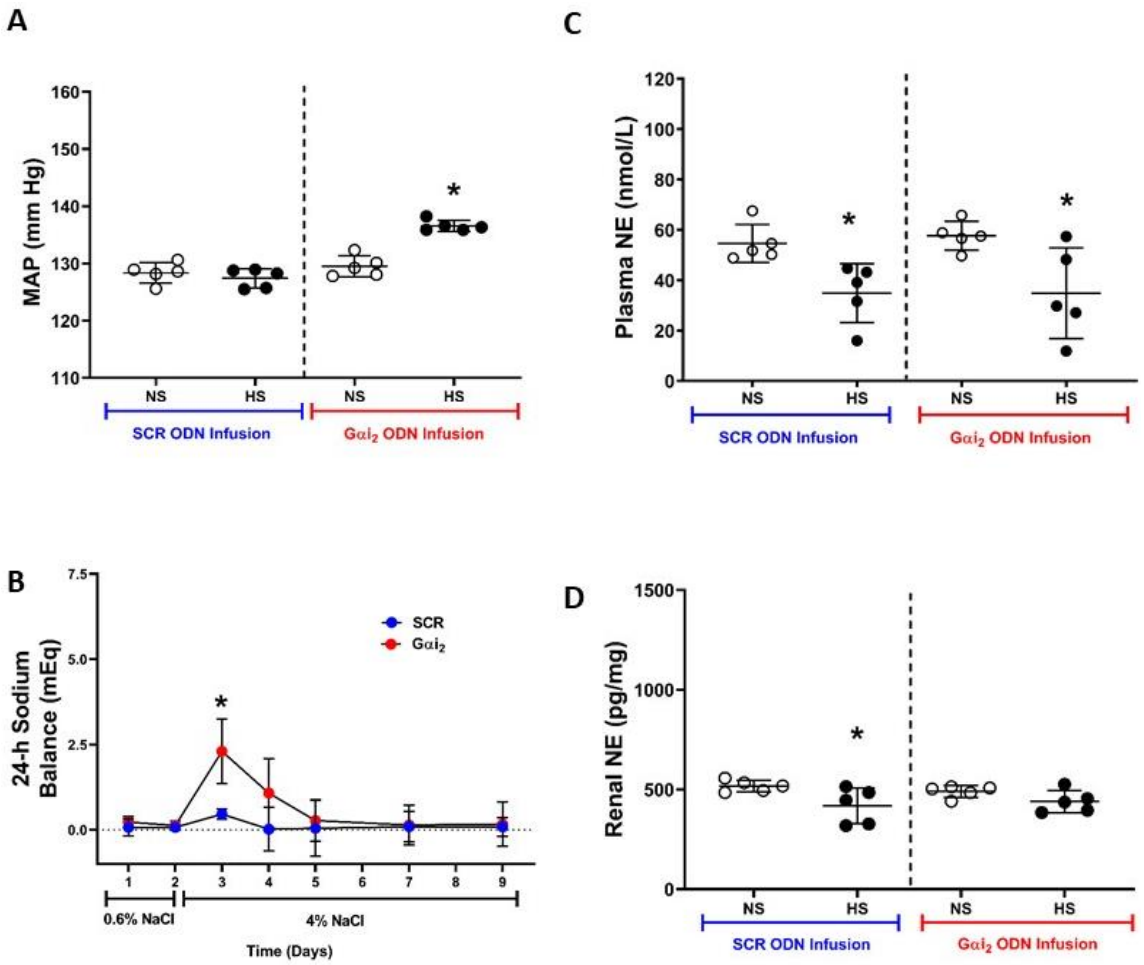

Figure 4.7 Day 7 Mean Arterial Pressure, Sodium Balance and Sympathetic Tone in Female SD Rats With and Without Central $G\alpha i_2$ Proteins.

Impact of intracerebroventricular (ICV) control scrambled (SCR) or targeted $G\alpha i_2$ oligodeoxynucleotide (ODN) infusion (25 µg/ 6µL/ day) and 7-day normal (NS, 0.6% NaCl) or high (HS, 4% NaCl) salt diet in 3 month old female Sprague-Dawley rats on A) mean arterial pressure (MAP, mmHg) B) sodium balance (mEq/day), C) plasma norepinephrine (NE, nmol/L) and D) renal NE content (pg/mg) (*$p<0.05$ compared to NS within ODN infusion group, n=5/group, 2-way analysis of variance (ANOVA)).

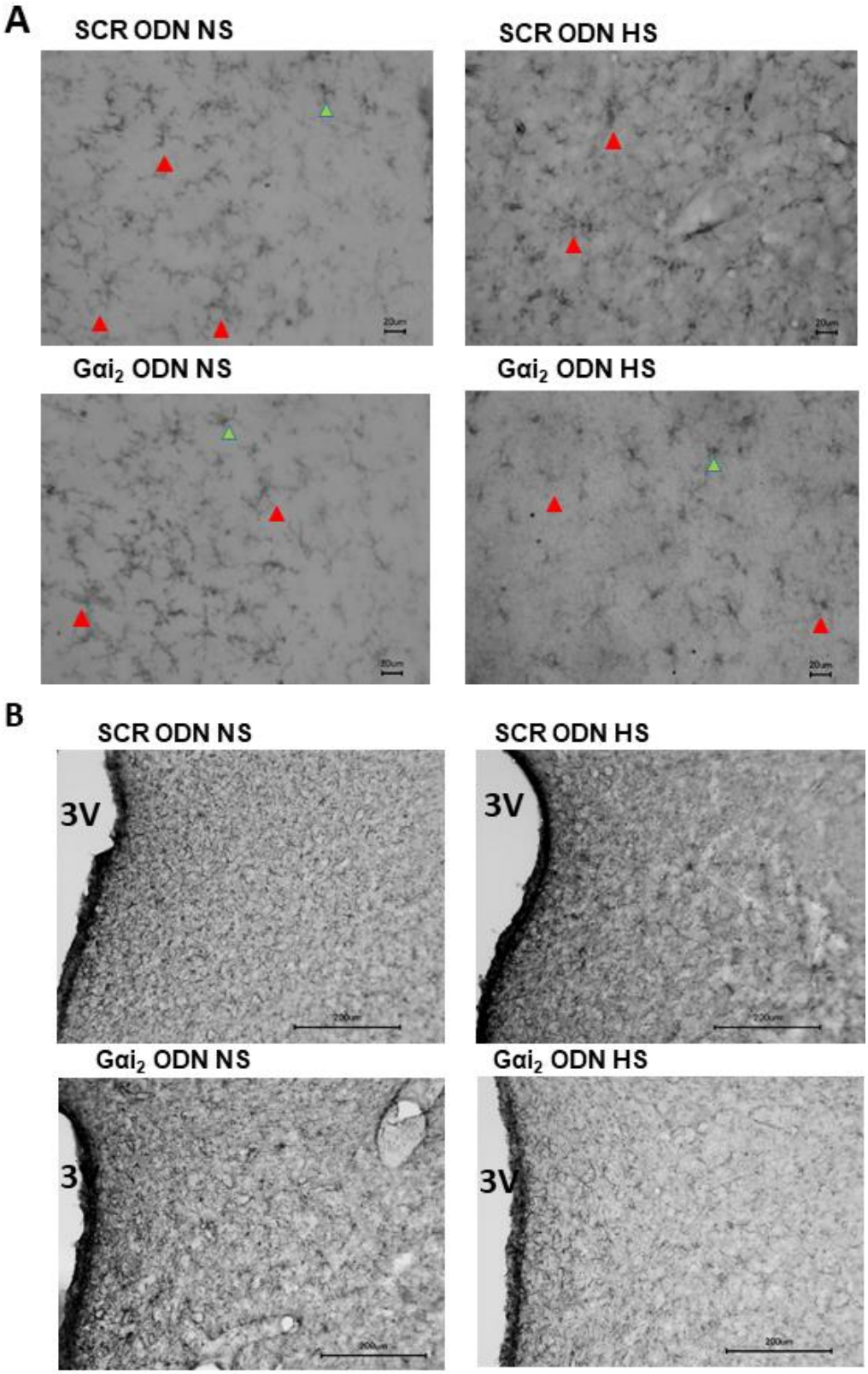
A
SCR ODN NS
SCR ODN HS
Gαi2 ODN NS
Gαi2 ODN HS
B
SCR ODN NS
SCR ODN HS
3V
3V
Gαi2 ODN NS
Gαi2 ODN HS
3
3V

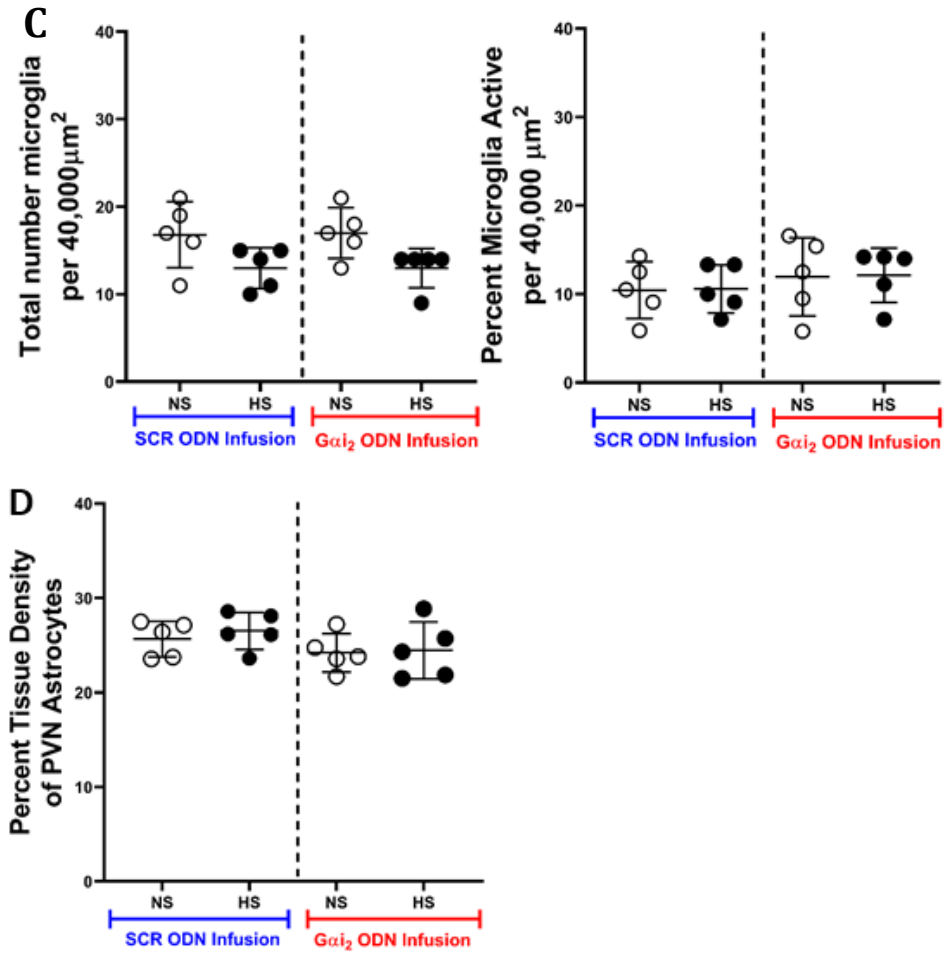

Figure 4.8 Analysis of Microglia and Astrocytes in the PVN of Female SD Rats With and Without Central $G\alpha i_2$ Proteins.

Representative photomicrographs of (A) microglia (OX-42 immunohistochemistry) and (B) astrocytes (GFAP immunohistochemistry) in the hypothalamic paraventricular nucleus (PVN) of intracerebroventricular (ICV) control scrambled (SCR, A) or targeted $G\alpha i_2$ (B) oligodeoxynucleotide (ODN) infused (25 µg/ 6µL/ day) female rats subjected to a 7-day normal (NS, 0.6% NaCl) or high (HS, 4% NaCl) salt diet. (C-D) Quantification of photomicrographs of (A) PVN microglial activation expressed as total number of microglia and percent of microglia active per 40,000 μm^2 and D) astrocyte percent tissue composition of the PVN (scale bar = 20 µm in A, 200 µm in B, images captured at 40X in A and 20X in B, red arrows indicate examples of ramified microglia, green arrows indicate examples of active microglia, n=5/group, 2-way analysis of variance (ANOVA)).

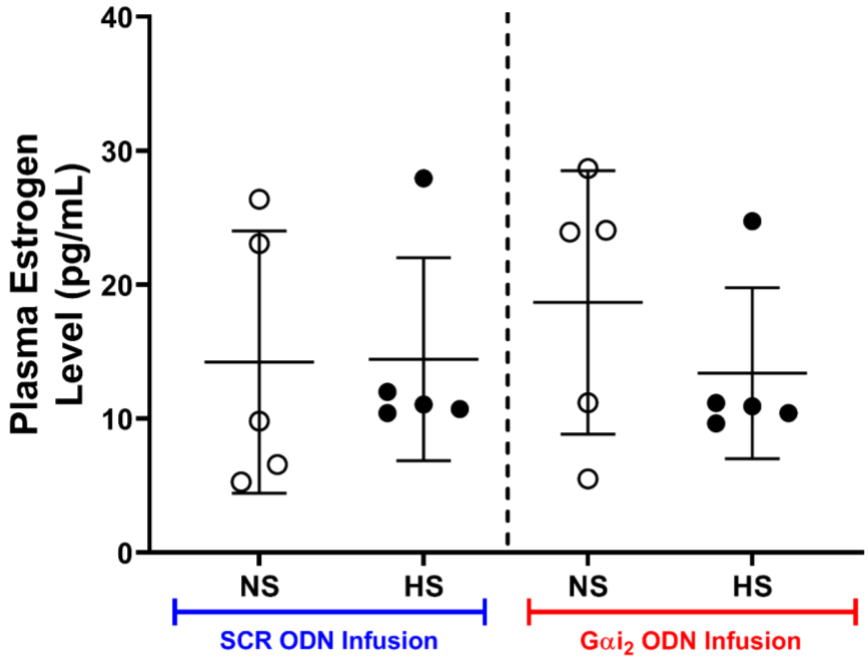

Figure 4.9 Plasma 17β-Estradiol Levels in Female SD Rats With and Without Central Gαi$_2$ Proteins.

Impact of intracerebroventricular (ICV) infusion of control scrambled (SCR) or targeted Gαi$_2$ oligodeoxynucleotide (ODN) infusion (25 µg/ 6 µL/ day) in conjunction with either 7-day normal (NS; 0.6% NaCl) or high (HS; 4% NaCl) salt diet on plasma estrogen levels in 3-month-old female Sprague Dawley rats (n=5/group, 2-way analysis of variance (ANOVA)).

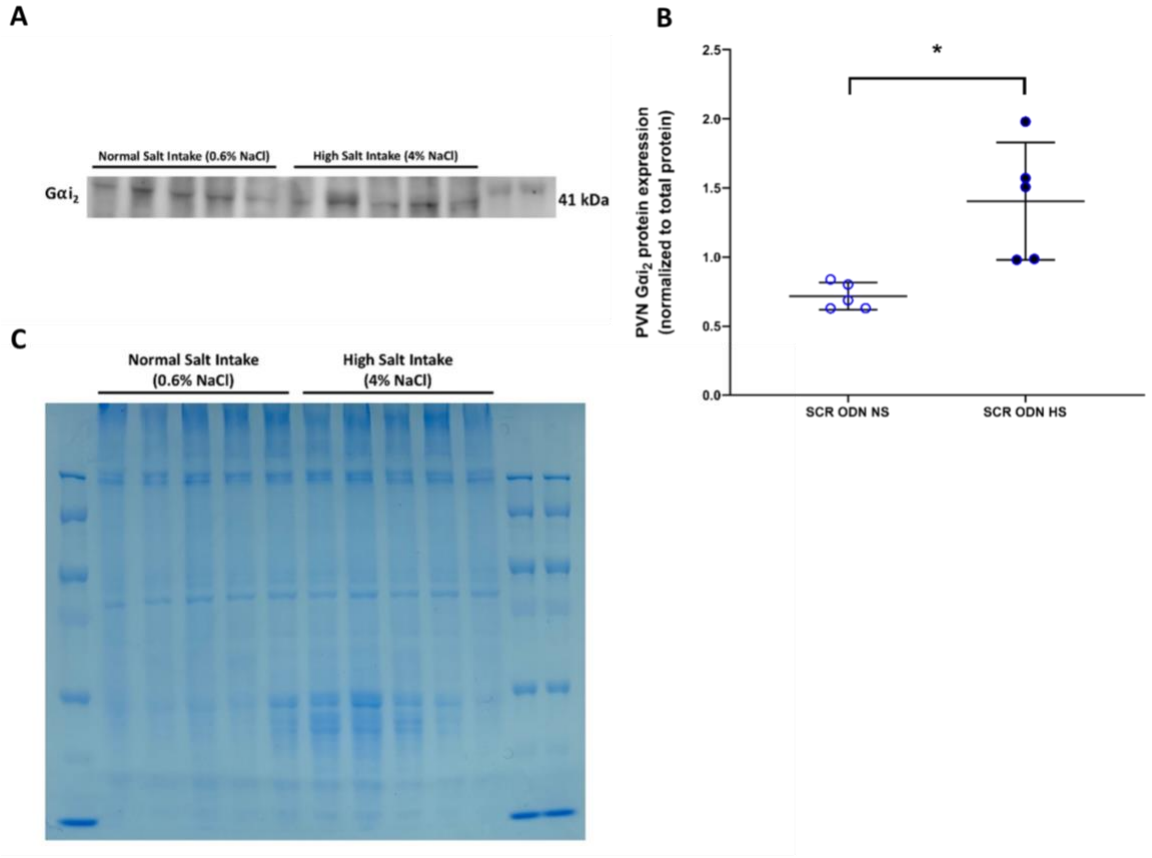

Figure 4.10: Impact of Elevated Dietary Sodium Intake on PVN Gαi_2 Protein Levels in Control Scrambled ODN-Infused Female SD Rats.

(A) Immunoblot demonstrating impact of high (HS; 4% NaCl) salt diet on hypothalamic paraventricular nucleus (PVN) Gαi_2 protein levels in 3-month-old female Sprague-Dawley rats receiving intracerebroventricular (ICV) infusion (25 µg/ 6 µL/ day) of control scrambled (SCR) oligodeoxynucleotides (ODN), (B-C) representative (B) quantification and (C) Coommassie blue-stained gel used for normalization of A. (*$p<0.05$ vs respective control, n=5/group, unpaired student t-test).

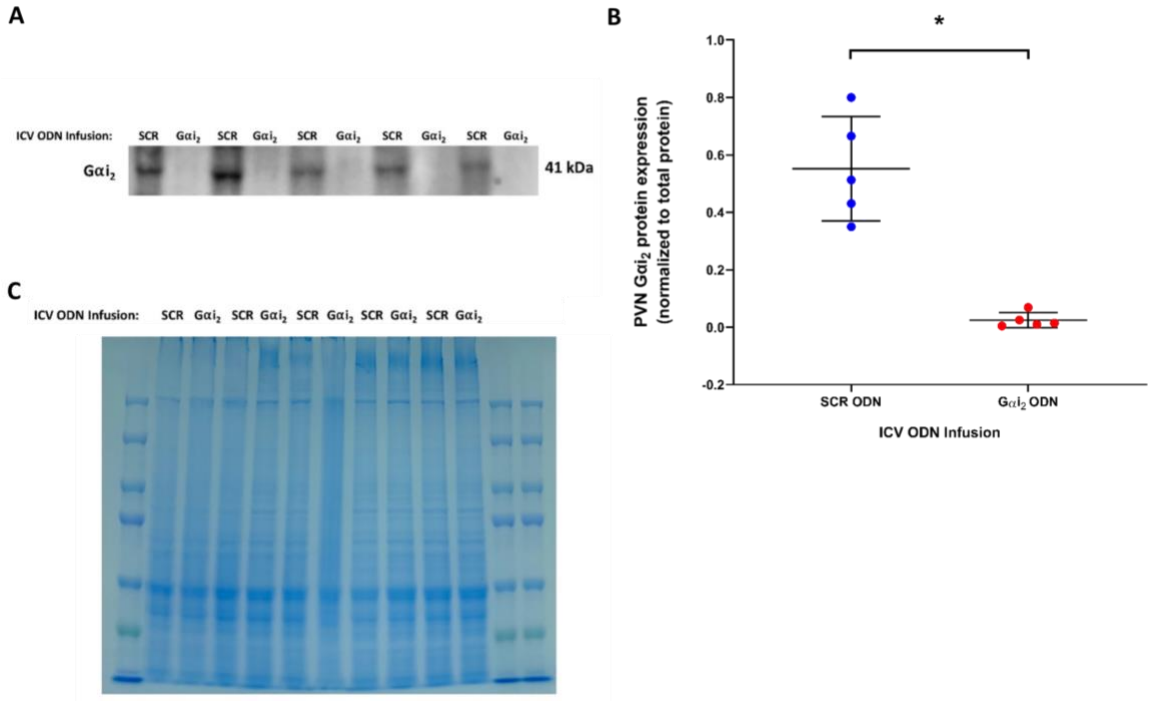

Figure 4.11: Impact of Targeted Gαi$_2$ ODN Infusion on PVN Gαi$_2$ Protein Levels in Female SD Rats.

(A) Immunoblot of impact of ICV infusion of control scrambled (SCR) or targeted Gαi$_2$ oligodeoxynucleotide (ODN) infusion (25 µg/ 6 µL/ day) in 3-month-old female rats in conjunction with 7-day normal (NS; 0.6% NaCl) salt diet on hypothalamic paraventricular nucleus (PVN) Gαi$_2$ protein levels, (B) quantification of PVN Gαi$_2$ protein levels in A and (C) Coommassie blue-stained gel for normalization of protein in A. (*$p<0.05$ vs respective control, n=5/group, unpaired student t-test).

Discussion

These studies were designed to test the hypotheses that 1) microglial-mediated PVN inflammation precedes the development of sympathoexcitation in rats in Gαi$_2$ protein-dependent ssHTN and 2) sex differences would be present in the development of Gαi$_2$ protein-dependent ssHTN. The major finding of this study is that PVN microglial-mediated neuroinflammation following HS administration in Gαi$_2$ ODN infused male rats precedes the development of sympathoexcitation, but develops concurrently with ssHTN. This suggests that the development of Gαi$_2$ dependent ssHTN occurs in a multiphasic manner.

Critically, we identified a sex-difference in the magnitude and contributing components of ssHTN elicited by central downregulation of $G\alpha i_2$ proteins in female SD rats.

Sodium retention and PVN microglial-mediated neuroinflammation precedes sympathoexcitation in the development of $G\alpha i_2$ protein-dependent ssHTN in male SD rats.

We have previously demonstrated, via radiotelemetry, that MAP rises sharply in $G\alpha i_2$ ODN infused male SD and Dahl Salt-resistant rats in the 24-hour period immediately following HS administration. MAP then continues to rise gradually over a 72-h period to reach a new higher set point that is maintained at this new level for a 21-day period (Moreira et al., 2019). In these studies, we verified the development of ssHTN on day 7 of dietary HS, which we have previously reported is well established by day 7 of HS intake in male SD rats (Carmichael et al., 2020; Moreira et al., 2019) via the acute measurement of MAP (Carmichael et al., 2016; Frame, Carmichael, et al., 2019; Kapusta et al., 2013; Kapusta et al., 2012; Wainford et al., 2015; Wainford & Kapusta, 2012).

Recapitulating our prior work in male SD rats, which maintain salt-resistance when challenged with a HS intake, (Carmichael et al., 2020; Kapusta et al., 2013; Kapusta et al., 2012; Moreira et al., 2019; Wainford et al., 2015) we observed that during a control SCR ODN infusion and a 7-day HS intake male SD rats maintain normotension that is accompanied by sympathoinhibition, sodium homeostasis and the absence of PVN inflammation. The current studies provide new insight into the timing of these physiological responses to HS intake. In control SCR ODN infused male SD rats on HS

diet, we observed the rapid suppression of global sympathetic outflow within 24 hours of HS intake that was followed by a significant and persistent reduction in sympathetic outflow to the kidney by 72 hours. Additionally, we observed a transient increase in 24-h sodium balance, observed only on day 2 of the HS intake period. Extending our prior data, in control animals, we observed no PVN microgliosis on day 1 or day 7 of HS intake and very low expression of the PICs IL-1β, IL-6, and TNFα on day 1 of HS intake. These data, in combination with our prior publication (Moreira et al., 2019) in which we saw no change in PVN IL-1β, IL-6, or TNFα levels 7-days post HS intake, strongly suggest in control salt-resistant SD rats receiving an ICV SCR ODN infusion animals there is no activation of PVN inflammatory mechanisms in response to HS intake.

Validating our prior published findings, male SD rats receiving a central targeted $G\alpha i_2$ ODN infusion and a HS intake developed ssHTN, sodium retention, sympathoexcitation and PVN inflammation (Carmichael et al., 2020; Moreira et al., 2019). In contrast to the sympathoinhibitory responses observed in control SCR ODN treated rats, animals receiving a $G\alpha i_2$ ODN failed to exhibit global or renal specific sympathoinhibition at any time point during HS intake. Further in these animals, we observed significant increases in sympathetic outflow systemically and to the kidneys from 72-hours post HS intake. As previously reported in Dahl salt-resistant rats in which the influence of central $G\alpha i_2$ proteins is removed, we observed significant and prolonged sodium retention on days 1-5 of HS intake in male SD rats. Collectively, these data suggest that rapid activation of the pressure-natriuresis mechanism coupled with an absence of sympathoinhibition drives the initial rapid development of ssHTN in animals in which the influence of central $G\alpha i_2$

are removed.

We have previously identified a critical role of PVN microglial-mediated neuroinflammation in mediating enhanced sympathetic outflow in Gαi2 protein-dependent ssHTN (Moreira et al., 2019). The current study extends our previous finding by identifying early and robust PVN microgliosis that occurs within 24 hours of HS intake and is maintained at a consistent elevated level for the duration of the study in Gαi2 ODN infused male rats. This early inflammatory response, which precedes the development of both sympathoexcitation and peak sodium retention suggests that PVN microglial activation plays a prominent role in the development and maintenance of Gαi2 protein-dependent ssHTN. Additionally, we performed immunofluorescent staining in the PVN for the PICs IL-1β, IL-6, and TNFα. In this study, further strengthening the hypothesis that PVN inflammation contributes to the development of Gαi2 protein-dependent ssHTN of we detected significant robust increases in PVN PIC levels of IL-1β and IL-6, but not TNFα, in Gαi2 ODN infused male rats on HS compared to values obtained in SCR ODN pre-treated rats on a HS intake. The absence of an apparent role of PVN TNFα levels in our studies is consistent with our prior study and studies conducted in an Angiotensin-II Salt HTN model which also exhibited no role of PVN TNFα (Bardgett et al., 2014). Our prior work (Moreira et al., 2019) reported that PVN IL-1β, IL-6 and TNFα expression levels are not altered by HS intake in SCR ODN pretreated animals and that baseline expression of these PICs is not different in SCR vs. Gαi2 ODN infused male rats on a NS intake. As such, for the purposes of this study, we compared PIC levels against those detected in control SCR ODN animals on a HS diet. While this is a limitation in that there

are no NS animals for comparison, we believe that the earlier detected absence of a difference between SCR ODN and NS diet and SCR ODN and HS diet facilitates this comparison. Additionally, we acknowledge our inability to determine the cellular localization of a given cytokine via this technique, and as such cannot conclude the source of the cytokines or the definitive target, although we believe they may originate in microglia as immune cells displaying pro-inflammatory cytokine production when active.

Our data suggest that there are temporal changes in PVN PIC expression with IL-1β levels rising more rapidly than those of IL-6. These findings, in conjunction with existing literature demonstrating a role of IL-1β and IL-6 in modulating neuronal excitability (Galic et al., 2012; Vezzani & Viviani, 2015) and neural sympathoexcitatory processes in HTN, (P. Shi et al., 2010; H. Yang et al., 2020) provide strong evidence for the possibility that early PVN microglial activation and microglial-mediated neuroinflammation contribute to the elevations observed in sympathetic outflow in the setting of $G\alpha i_2$ protein-dependent ssHTN. This hypothesis is further supported by the growing body of literature, including from our laboratory, that demonstrates that inactivation of microglia in hypertensive rats via minocycline normalizes sympathetic activity and blood pressure (Du et al., 2017; Moreira et al., 2019; Sharma et al., 2019).

The development of $G\alpha i_2$ protein-dependent ssHTN in male rats is multi-phasic

As proposed by Van Vliet, et al. in the Dahl salt-sensitive rat model of HTN, (V. McLoone, Ringwood, & Van Vliet, 2011; V. I. McLoone, Ringwood, & Van Vliet, 2009; Van Vliet, Chafe, Halfyard, & Leonard, 2006) our studies suggest that the development

and maintenance of central Gαi2 protein-dependent ssHTN occurs in a multiphasic manner. Initially MAP increases rapidly over the first 24-h period (Moreira et al., 2019) of HS intake, during which time, there is a failure to evoke sympathoinhibition to increase the renal excretion of sodium, resulting in activation of the pressure-natriuresis mechanism to aid in the restoration of sodium homeostasis. Our new data demonstrate that PVN microgliosis precedes sympathoexcitation that develops in animals in which central Gαi2 proteins are down-regulated. In conjunction with our previous finding that inhibition of PVN microglial activation abolishes sympathoexcitation, (Moreira et al., 2019) we hypothesize that a component of the long term rise in MAP is driven by PVN microglial-mediated elevations in sympathetic outflow. Our data also suggest that temporal changes in PVN neuroinflammation following microglial activation and increased IL-1β production likely contribute to the development of sympathoexcitation and that persistent microgliosis and elevations in IL-1β and IL-6 are implicated in maintaining prolonged elevations in sympathetic outflow. Collectively, our data support a multiphasic model of Gαi2 protein-dependent ssHTN featuring temporally independent yet additive mechanisms in which pressure-natriuresis rapidly elevates MAP to a new higher set point that is maintained in part by PVN neuroinflammatory mechanisms that drive and maintain sympathoexcitation.

Females rats lacking central Gαi2 proteins maintain sympathoinhibition and an anti-inflammatory neural environment on HS diet

As we have previously demonstrated in male rats (Carmichael et al., 2020; Kapusta et al., 2013; Moreira et al., 2019), salt-resistant female SD rats receiving a control SCR

ODN infusion, which does not impact Gαi2 proteins levels, maintained normotension and exhibited sympathoexcitation and sodium balance during a 7-day HS intake. Extending our prior findings in male SD rats in which we report high dietary salt-evoked up-regulation of PVN Gαi2 proteins (Carmichael et al., 2020; Kapusta et al., 2013; Kapusta et al., 2012) we observed HS evoked up regulation of PVN Gαi2 proteins in female rats. The magnitude of the increase in PVN Gαi2 protein expression was lower than that reported in our prior studies in male rats (Carmichael et al., 2020; Kapusta et al., 2013; Kapusta et al., 2012) however this likely reflects the lower dietary salt intake used in the present study of 4% NaCl and further supports our data that the PVN Gαi2 protein response is strongly regulated by the amount of dietary salt intake (Kapusta et al., 2012).

Despite observing dietary sodium evoked upregulation of PVN Gαi2 proteins, as seen in male SD rats, ODN mediated down regulation of central Gαi2 proteins resulted in different responses in female SD rats compared to those observed in male rats. While female SD rats developed an increase in MAP following 7-days HS intake the magnitude of elevation was greater than 3-fold less than that observed in male SD rats and in contrast to the robust prolonged renal sodium retention observed in male rats there was only a transient increase in sodium balance in female SD rats. These data demonstrate that there is a significant sex difference in the degree to which PVN Gαi2 proteins influence blood pressure and renal sodium retention during high salt intake in male versus female rats. Further, following HS intake unlike, in Gαi2 ODN infused male rats, which display robust sympathoexcitation, we observed the maintenance of global sympathoinhibition and the absence of renal sympathoexcitation following HS administration in female rats. We

speculate that the observed lack of sympathoexcitation, which is a significant contributor to ssHTN in male Gαi2 ODN infused rats, partially accounts for the sex difference observed in the magnitude of Gαi2 protein-dependent ssHTN. Given our finding of an absence of PVN neuroinflammation assessed as the lack of PVN microglial activation or astrocytic reactivity in female Gαi2 ODN infused rats, we hypothesize this contributes to the failure of a HS intake to evoke sympathoexcitation and profound ssHTN as observed in male rats. This is supported by our previous finding in male Gαi2 ODN infused SD rats on a HS diet that inhibition of PVN microglial activation resulted in abolishment of pro-inflammatory cytokine production and sympathoexcitation (Moreira et al., 2019), and a markedly attenuated increase in blood pressure.

Our finding of a sex-difference in the role of central Gαi2 proteins supports the growing body of evidence supporting sex-differences in the mechanisms regulating blood pressure. It is well established that the risk of developing HTN is lower in females prior to menopause (Das Gupta et al., 2020; Everett & Zajacova, 2015). Of interest to our current studies are the known anti-inflammatory and cardioprotective roles of estrogens (Crofton & Share, 1997; Hoeg, Willis, & Weinberger, 1977; Packer, Pelaez, & Kramer, 2001; Villa, Vegeto, Poletti, & Maggi, 2016). Our animal model of 3-month-old female SD rats represents premenopausal women, and as validated in this study, down-regulation of central Gαi2 proteins did not affect the level of plasma estrogen. As such, we speculate that following down regulation of central Gαi2 proteins, estrogens, and potentially other female sex steroid hormones, drive the observed mechanistic differences in male versus female rats during HS intake. There is a robust body of literature demonstrating the anti-

inflammatory and anti-hypertensive effects of estrogens (Hoeg et al., 1977; Packer et al., 2001; Villa et al., 2016), therefore, we speculate that female Gαi2 ODN infused SD rats on HS exhibit blunted HTN due to the anti-inflammatory effects that estrogens exert on PVN microglia and the protective effects they exert on PVN neurons via the highly locally expressed estrogen receptor-β in the PVN (Xue et al., 2013).While we provide strong evidence for a sex difference in the response of male versus female rats to HS intake following central Gαi2 protein downregulation, this study does not directly investigate the role(s) of the sex steroid in these responses. Future studies, beyond the scope of the current work, are needed to fully delineate the mechanisms accounting for observed differences in the inflammatory response and magnitude of HTN seen in female SD rats (e.g. ovariectomy, PVN specific estrogen receptor-β antagonism).

Perspectives

Collectively, our findings suggest that there is a multi-phasic mechanism whereby central downregulation of the Gαi2 protein, in conjunction with a HS intake, evokes the development of ssHTN in male SD rats. In both male and female rats following Gαi2 protein downregulation and administration of HS diet there is initial activation of the pressure-natriuresis mechanism to restore and maintain sodium homeostasis. In male rats only, which develop significantly higher levels of ssHTN than female rats, activation of the pressure-natriuresis mechanism occurs concurrently with PVN microglial-mediated neuroinflammation and subsequent sustained elevations in sympathetic outflow. These data highlight novel sex-specific inflammatory and sympathetic mechanisms contributing to the development of male but not female Gαi2 protein dependent ssHTN. Prior studies

have shown that single nucleotide polymorphisms in the human GNAI2 gene associate with essential HTN in the UK BioBank (Carmichael et al., 2020) and the salt-sensitivity of blood pressure in the GenSalt study (X. Zhang et al., 2018). We speculate that the sex-specific mechanisms observed in our animal studies potentially represent future sex-specific therapeutic targets and approaches for the treatment of human HTN featuring GNAI2 polymorphisms.

CHAPTER FIVE: Altered Balance of Excitatory-Inhibitory Neurotransmission in Gαi2 Protein-Dependent Salt-Sensitive Hypertension

Introduction

Hypertension (HTN) is the leading global cause of mortality, estimated to account for 10.4 million deaths per year (Unger et al., 2020). Additionally, the salt sensitivity of blood pressure, an exaggerated pressor response to elevated dietary salt intake, is estimated to impact 50% of hypertensive and 25% of normotensive individuals (Kotchen, Cowley, & Frohlich, 2013). With the average American consuming three times the daily sodium intake recommended by the American Heart Association (Writing Group et al., 2016), it is becoming increasingly important to identify the mechanisms responsible for propagating hypertensive responses to excess dietary sodium intake.

Our laboratory has previously characterized the role of Hypothalamic Paraventricular Nucleus (PVN) G-Protein Coupled Receptor (GPCR)-coupled α-i_2 ($G\alpha i_2$) subunit proteins in mediating normotensive responses to elevated dietary sodium intake in salt resistant rats (Carmichael et al., 2020; Kapusta et al., 2013; Moreira et al., 2019; Wainford et al., 2015). We have demonstrated that a chronic high sodium diet results in site-specific upregulation of $G\alpha i_2$ proteins and resultant decreases in measures of global and renal sympathetic tone, ultimately facilitating normotension (Carmichael et al., 2020; Kapusta et al., 2013; Wainford et al., 2015). Additionally, when the $G\alpha i_2$ protein is present there is notable dietary sodium-evoked induction of Fos in the parvocellular PVN, a marker of neuronal activation. In contrast, in salt-sensitive animals such as the Dahl Salt-Sensitive (DSS) rat which fails to upregulate these proteins, and in salt-resistant animals in which

these $G\alpha i_2$ proteins are experimentally downregulated, a high salt diet evokes sympathoexcitation, sodium retention, and ultimately the development of salt-sensitive HTN (ssHTN).

Previous studies from our laboratory have demonstrated a robust induction of PVN Fos staining in response to both acute (Carmichael et al., 2016) and chronic (Carmichael et al., 2020) challenges to fluid and electrolyte homeostasis in salt-resistant rats. Moreover, a recent study from our laboratory has demonstrated significant co-expression of *Gnai2* mRNA with *Gad1* mRNA in the parvocellular PVN of naïve male and female SD rats (Chaudhary & Wainford, 2021), suggesting a potential impact of PVN $G\alpha i_2$ proteins on GABAergic signaling. Additionally, there is evidence that the neural pathways mediating normal control of blood pressure involve coordinated signaling through Gamma-amino butyric acid (GABA) B receptors (Li & Pan, 2010; Takenaka et al., 1996) and that GABA(B) receptors facilitate signal transduction via the $G_{i/o}$ inhibitory class of Gα-subunit proteins (Cheng et al., 2014; Yudin & Rohacs, 2018).

As it has been shown that the delicate balance between inhibitory GABAergic signaling and excitatory glutamatergic signaling in the central nervous system is disrupted in models of HTN, favoring excitation (Ferreira-Junior et al., 2019; Korpal et al., 2017; Z. Shen, Weng, Zhang, Wang, & Yang, 2018), we elected to investigate the balance of GABAergic and glutamatergic signaling in rats with and without PVN $G\alpha i_2$ proteins. We performed in-vivo GABAergic and glutamatergic receptor antagonist studies as well as in-situ hybridization studies in male Sprague-Dawley rats infused with either scrambled control (SCR) or targeted $G\alpha i_2$ oligodeoxynucleotides and challenged with a 7-day normal

or high salt dietary sodium intake.

Methods

Animals

Male SD rats weighing 275-299 g (approximately 3 months of age) were purchased from Envigo (Indianapolis, IN, USA). All rats were pair-housed prior to intervention and single-housed post-intervention. Rats were continuously housed in a temperature-controlled (20–26°C) and humidity-controlled (30-70%) facility under a 12-hour light-dark cycle. Tap water and standard normal salt rodent diet (NS, Teklad Global Diet No. 2918, 18% protein, 5% crude fat, 5% fiber, total potassium (K+) content 0.6%, total NaCl content 0.6% [174 mEq Na+/kg], Envigo, Indianapolis, IN, USA) or experimental high sodium diet (HS, Teklad Global Diet No. TD.03095, 19% protein, 5% crude fat, 3% fiber, total K+ content 0.8%, total NaCl content 4% [678 mEq Na+ /kg], Envigo, Indianapolis, IN, USA) were allotted *ad libitum*. All rats were randomly assigned to experimental groups. All animal protocols were approved by the Institutional Animal Care and Use Committee in accordance with the guidelines of the Boston University School of Medicine and the National Institutes of Health *Guide for the Care and Use of Laboratory Animals* (8^{th} edition).

Surgical Procedures

PVN Bilateral Cannula and Subcutaneous Osmotic Minipump Implantation

To achieve PVN $G\alpha i_2$ protein downregulation and the ability to perform subsequent PVN microinjections, animals were anesthetized with intraperitoneal (IP) Ketamine/Xylazine (Ketamine 30 mg/kg IP + Xylazine 3 mg/kg IP). Animals were then

stereotaxically instrumented with a bilateral stainless steel cannula (P1 Technologies, Roanoke, VA, USA) into the PVN utilizing coordinates from Paxinos and Watson *The Rat Brain* atlas (AP -1.8 mm from bregma, ML ±0.5 mm from bregma, DV -8.0 mm from the skull surface) (Paxinos & Watson, 2007). The cannulas were then each connected via silastic tubing to one of two subcutaneous osmotic minipumps, each with an infusion rate of 3.6 μL/day and a max fill volume of approximately 150 μL (Model 2006; Alzet, Cupertino, CA, USA) to infuse rats at a rate of 300 ng/ side/ day with either control scrambled (SCR) (sequence: 5′-GGGCGAAGTAGGTCTTGG-3′) or targeted $G\alpha i_2$ (sequence: : 5′-CTTGTCGATCATCTTAGA-3') oligodeoxynucleotides (ODN) as previously described (Carmichael et al., 2020). Cannulation site was confirmed at the end of the study when microinjections of L-glutamate (15 nmol/side) were made into the PVN to elicit a pressor response. Animals lacking the pressor response were considered mis-cannulations (Carmichael et al., 2020) and not used.

ICV Cannula and Subcutaneous Osmotic Minipump Implantation

To achieve CNS $G\alpha i_2$ protein downregulation in PVN in-situ hybridization studies in which a PVN-specific cannula would have led to destruction of PVN microarchitecture needed for histological studies of neuronal phenotypes, animals were anesthetized with intraperitoneal (IP) Ketamine/Xylazine (Ketamine 30 mg/kg IP + Xylazine 3 mg/kg IP). Animals were then stereotaxically instrumented with a stainless steel cannula (P1 Technologies, Roanoke, VA, USA) into the right lateral cerebral ventricle according to Paxinos and Watson *The Rat Brain* atlas (AP -0.3 mm from bregma, ML +1.3 mm from bregma, DV -4.5 mm from the skull surface) (Moreira et al., 2019; Wainford et al., 2015).

The cannula was connected via silastic tubing to a single subcutaneous osmotic minipump (Model 2004; Alzet, Cupertino, CA, USA) to infuse rats at a rate of 25μg/ 6 μL/ day with either control SCR or targeted $G\alpha i_2$ ODNs with the same sequences as described above.

Acute Femoral Artery and Vein Cannulation

On day 7 of the normal or high salt dietary challenge, subgroups of animals were anesthetized with IP Sodium Brevital (Sodium Brevital 20 mg/kg IP + 10 mg/kg IV as needed). The left femoral vein was cannulated using a PE50 cannula for the delivery of IV drugs and normal saline, and the left femoral artery was cannulated using a PE50 cannula connected to a BIOPAC transducer to record blood pressure as previously described (Carmichael et al., 2016; Carmichael et al., 2020; Frame, Carmichael, et al., 2019). Following cannulation, rats were placed in a plexiglass rat holder and an isotonic infusion of saline (20 μL/min IV) was given over a 2-hour recovery period allowing rats to return to full consciousness and stable renal and cardiovascular function. Mean arterial pressure (MAP) was recorded continuously via the femoral artery cannula using computer driven BIOPAC data acquisition software (MP150 and AcqKnowledge 3.8.2; BIOPAC Systems In., Goleta, CA, USA) connected to an external pressure transducer (P23XL; Viggo Spectramed Inc., Oxnard, CA, USA).

Transcardial Perfusion

Subgroups of rats used for in-situ hybridization studies in the brain were deeply anesthetized using IP ketamine/xylazine (Ketamine 30 mg/g IP + Xylazine 3 mg/kg IP) and perfused through the heart with ice cold 0.1M phosphate buffered saline PBS until the liver and kidneys cleared, and then with ice cold 4% paraformaldehyde in 0.1M PBS until

fully fixed. Brains were then extracted and post-fixed in 4% paraformaldehyde for 48 hours and sealed in 30% sucrose in 0.1M PBS for 72 hours before tissue processing.

In-vivo Procedures

PVN Microinjection Studies

Following femoral artery and vein cannulation and 2-hour recovery, animals underwent a PVN microinjection study utilizing GABA(B) antagonist CGP52432 (3nmol/ side) and glutamatergic antagonist kynurenate (1.4μg/side) to determine basal activity of both glutamatergic (NMDA, AMPA, Kainate) and GABA(B) receptors. First, MAP was recorded for a 20-minute baseline. After that, injections were performed, and MAP responses were recorded for 60 minutes following injections.

Experimental Protocols

In-situ Hybridization

For the co-localization of the *Gnai2* mRNA with *vGlut2* and *Gad1* in the PVN to determine the percent distribution of neuronal phenotypes expressing the Gαi$_2$ protein and to determine the comparative abundance of GABAergic neurons and glutamatergic neurons, in-situ hybridization was performed as described by our laboratory (Chaudhary & Wainford, 2021). Coronal sections of fixed brains were cut on a cryostat at 20 μm and stored in cryoprotectant until tissue processing. In situ hybridization was performed using the RNAscope Assay Fluorescent multiplex kit (ACD 32850, Hayward, CA, USA). Controls for each probe were previously validated by our laboratory and are available in a repository open access at https://doi.org/10.6084/m9.figshare.c.5136317.v1. First, sections were rinsed with 1X PBS and mounted on superfrost plus slides (Fisher 1255015, Fisher

Scientific, Waltham, MA, USA). Slides were then washed in RNase free water (Fisher 10-977-015, Fisher Scientific, Waltham, MA, USA) for 5 minutes and dehydrated through serial ascending concentrations of ethanol, air dried, washed in hydrogen peroxide (ACD 322335, Hayward, CA, USA) to block endogenous peroxidase activity and permeabilized in protease III (ACD 322337, Hayward, CA, USA). Slices were then hybridized using specific target probes for 2 hours at 40°C. Readily available C2 probes *Gad1* (ACD 316401-C2, Hayward, CA, USA) and *Slc17a6*(vGLUT2, ACD 317011-C2, Hayward, CA, USA) were used along with a custom-designed targeted C1 *Gnai2* probe (NPR-0001497; ACD 805201) detecting specific Gai_2 target RNA. The custom probe was designed using the National Center for Biotechnology Information Gene ID 81664 for *Rattus norvegicus Gnai2,* and matches our targeted ODN sequence which has been previously validated to be specific to the *Gnai2* mRNA. For hybridization, the C2 probes (provided at 50X) were diluted at 1:50 in the C1 probe (provided at 1X).

Following probe hybridization, tissue section slides were rinsed twice with 1X wash buffer (ACD 310091; 50X diluted in RNase free water, Hayward, CA, USA) at room temperature for 2 minutes each time. The signal amplification was performed using an RNA scope set of amplifiers (ACD 320851, Hayward, CA, USA) (Amp 1, 30 minutes at 40°C; Amp 2, 15 minutes at 40°C; Amp 3, 30 minutes at 40°C; and Amp 4A, 15 min at 40°C). Washing steps with 1X wash buffer (2 minutes at room temperature x2) were included between Amplification steps. Slides were then coverslipped using Prolong Diamond anti-fade mounting media (Fisher-P36961) to preserve fluorescent signals and stored in the dark in slide cases.

Imaging and Analysis of Neuronal Phenotypic Markers via RNAScope In-situ Hybridization

For in-situ hybridization studies on brain slices, slides were imaged utilizing the GFP filter for green stains and Texas Red filter for red stains at 10X and 20X under similar exposures. To determine positive RNA puncta staining compared to background, the brightness setting was enhanced linearly to an equal degree with respect to the background in all images to allow small puncta to become visible. Contrast was also enhanced equally and linearly in all images to enable signal detection and discrimination from background. To ensure background was identifiable, negative control probes and positive control probes commercially available from Advanced Cell Technology/BioTechne were employed. After image capture, colocalization of *Gad1* and *Gnai2* or *vGlut2* and *Gnai2* was determined using ImageJ/FIJI software from the NIH. On blinded images, a 300 μm x 300 μm box was drawn over the medial parvocellular region of the PVN. This region in specific was chosen for neuronal phenotyping as the large majority (~80%) of *Gnai2*-positive cells were localized here, in addition to the medial parvocellular region being the site of cannula implantation in PVN-cannulated rats, and the site where we previously identified the largest $G\alpha i_2$ ODN-induced deficit in Fos-positive cells following IV hypertonic saline bolus (Carmichael et al., 2016) and 7-day HS diet (Carmichael et al., 2020). Cells were then counted using the cell counter plugin available on ImageJ/FIJI. A cell was determined to be positive for the respective mRNA if it contained >5 punctate dots in that foci, and colocalization was determined to be those foci with a distinct yellow/orange signal, as well as those foci which are not yellow but which possess both red and green foci together in

non-overlapping close proximity. Quantifications of each slice were then used to determine percent of *Gnai2*-expressing neurons that were GABAergic or Glutamatergic, as well as percent of GABAergic neurons containing *Gnai2* and percent of glutamatergic neurons containing *Gnai2*.

Statistical Analyses

All data are expressed as mean ± SD. The magnitude of change in MAP at different time points in response to microinjections was compared with the mean group control value obtained over the first 20 minutes of recording by a one-way repeated-measures analysis of variance (ANOVA) with subsequent Dunnett's test. Group differences in neuronal phenotype abundance and colocalization were assessed via two-way ANOVA with one fixed effect being ODN infusion and the other fixed effect being dietary sodium intake, with the interactions included. Post-hoc multiple comparison analysis was performed using Bonferroni's test.

Results

PVN-specific Gαi$_2$ ODN infusion in male SD rats on HS diet results in the development of ssHTN

As we have previously demonstrated (Carmichael et al., 2020), administration of a 7-day HS diet in PVN SCR ODN infused male rats fails to elicit increases in MAP (SCR ODN NS baseline MAP, mmHg, 126 ± 4 vs SCR ODN HS baseline MAP 126 ± 6, $p>0.05$) (Figure 1). In contrast, a 7-day HS diet in PVN Gαi$_2$ ODN-infused male rats elicits the development of ssHTN (Gαi$_2$ ODN NS baseline MAP, mmHg, 125 ± 4 vs Gαi$_2$ ODN HS baseline MAP 146 ± 6) (Figure 1).

PVN GABA(B) receptor antagonism produces a pressor effect in SCR ODN-infused male SD rats on a high salt diet

While microinjection of GABA(B) antagonist CGP52432 (3nmol/ side) into the PVN induced no change in MAP in both SCR and Gαi$_2$ ODN-infused male rats on NS diet, there was a significant pressor effect of GABA(B) antagonism on SCR ODN-infused rats on HS diet compared to baseline (SCR ODN HS peak ΔMAP to CGP52432 +17 mmHg at 20 minutes post-injection, $p<0.05$) (Figure 1). This effect was absent in Gαi$_2$ ODN-infused male rats on HS diet, as this group displayed sustained HTN throughout the study.

PVN Glutamatergic receptor antagonism produces a depressor effect in Gαi$_2$ ODN-infused male SD rats on a high salt diet

In SCR ODN-infused male SD rats, there was no impact of microinjecting the glutamatergic antagonist Kynurenate (1.4μg/side) on MAP regardless of 7-day dietary sodium intake. Additionally, glutamate antagonism does not impact MAP in Gαi$_2$ ODN-

infused male rats on NS diet, but significantly reduces MAP in Gαi$_2$ ODN-infused male rats on HS diet (Gαi$_2$ ODN HS peak ΔMAP to Kynurenate -12 mmHg at 20 minutes post-injection, $p<0.05$) (Figure 5.1).

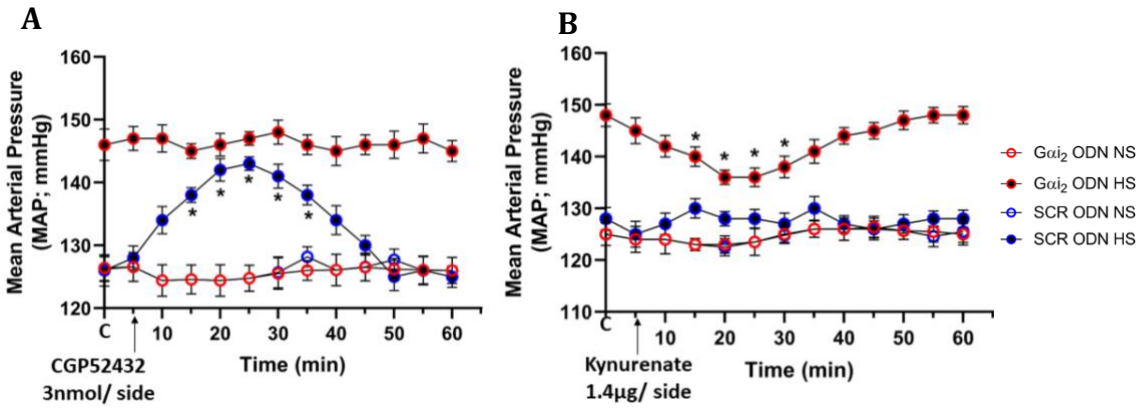

Figure 5.1: Impact of GABA(B) Receptor and Glutamate Receptor Antagonism on MAP in PVN SCR or Gαi$_2$ ODN-Infused Male SD Rats.

Impact of microinjection of (A) CGP52432 (GABA(B) receptor antagonist, 3nmol/side) or (B) Kynurenate (glutamatergic antagonist, 1.4 µg/side) on Mean Arterial Pressure (MAP) in Paraventricular Nucleus (PVN) control scrambled (SCR) or targeted Gαi$_2$ oligodeoxynucleotide (ODN) infused (300 ng/ side/ day) male Sprague-Dawley rats in conjunction with 7-day normal (NS; 0.6% NaCl) or high (4% NaCl) salt diet (*$p<0.05$ vs respective group baseline value, n=6/group, one-way repeated measures analysis of variance (ANOVA)).

Gαi$_2$ ODN infusion and HS diet evoke PVN neuronal plasticity with enhanced glutamatergic and suppressed GABAergic neuronal transcripts

In both SCR and Gαi$_2$ ODN-infused male SD rats, an HS diet did not evoke changes in the proportion of neurons in level 2 of the PVN that expressed the *Gnai2* gene nor the subregion of the PVN that the majority of expression was localized to, counted as neurons positively fluoresced with targeted *Gnai2* RNAScope probes (Figure 2). Moreover, there were no dietary sodium-evoked changes in the total number of GABAergic neurons (Figure 3) or glutamatergic neurons (Figure 4) in the medial parvocellular region of the PVN in

SCR ODN-infused male SD rats, nor the percent of either type of neuron that colocalized to *Gnai2*-positive cells. In contrast, an HS diet in conjunction with Gαi$_2$ ODN infusion evoked a significant decrease in the abundance of *Gad1*-positive neurons (average number positive neurons per sample area Gαi$_2$ ODN NS 89 ± 8 vs Gαi$_2$ ODN HS 77 ± 5, $p<0.05$) (Figure 3) and a significant increase in the abundance of *vGlut2*-positive neurons (average number positive neurons per sample area Gαi$_2$ ODN NS 77 ± 8 vs Gαi$_2$ ODN HS 95 ± 8 $p<0.05$) (Figure 4) in the medial parvocellular region of the PVN. Additionally, HS diet and Gαi$_2$ ODN infusion evoked a significant decrease in the colocalization of *Gad1* to *Gnai2*-positive cells (percent cells positive for *Gnai2* also positive for *Gad1* in sample area Gαi$_2$ ODN NS 89% ± 7% vs Gαi$_2$ ODN HS 76% ± 3%, $p<0.05$) (Figure 3) and a significant increase in the colocalization of *vGlut2* to *Gnai2*-positive cells (percent cells positive for *Gnai2* also positive for *vGlut2* in sample area Gαi$_2$ ODN NS 78% ± 5% vs Gαi$_2$ ODN HS 86% ± 3%, $p<0.05$) (Figure 4) in the medial parvocellular PVN.

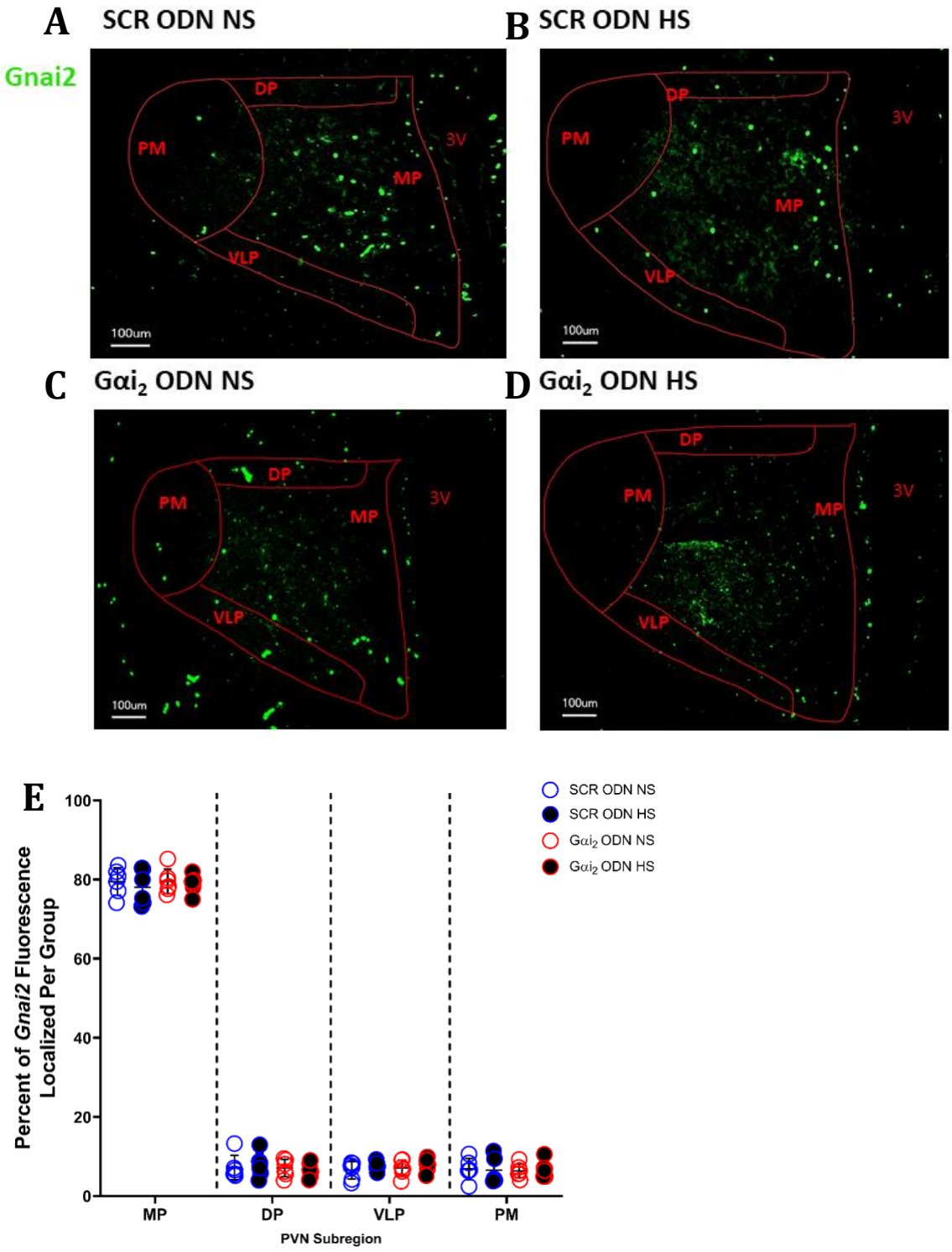

Figure 5.2: Distribution of *Gnai2* positive cells across PVN subnuclei at level 2 in SCR or Gαi$_2$ ODN-Infused Male SD Rats.

Representative photomicrographs of impact of control scrambled (SCR, A-B) or targeted $G\alpha i_2$ (C-D) intracerebroventricular oligodeoxynucleotide (ODN) infusion (25 µg / 6 µL/ day) in conjunction with normal (0.6% NaCl NS) or high (4% NaCl) salt diet on *Gnai2* fluorescent staining in level 2 of the Paraventricular Nucleus (PVN) and (E) group quantifications by PVN subnuclear region (Photos captured at 10X, scale bar = 100 µm, n=6/group).

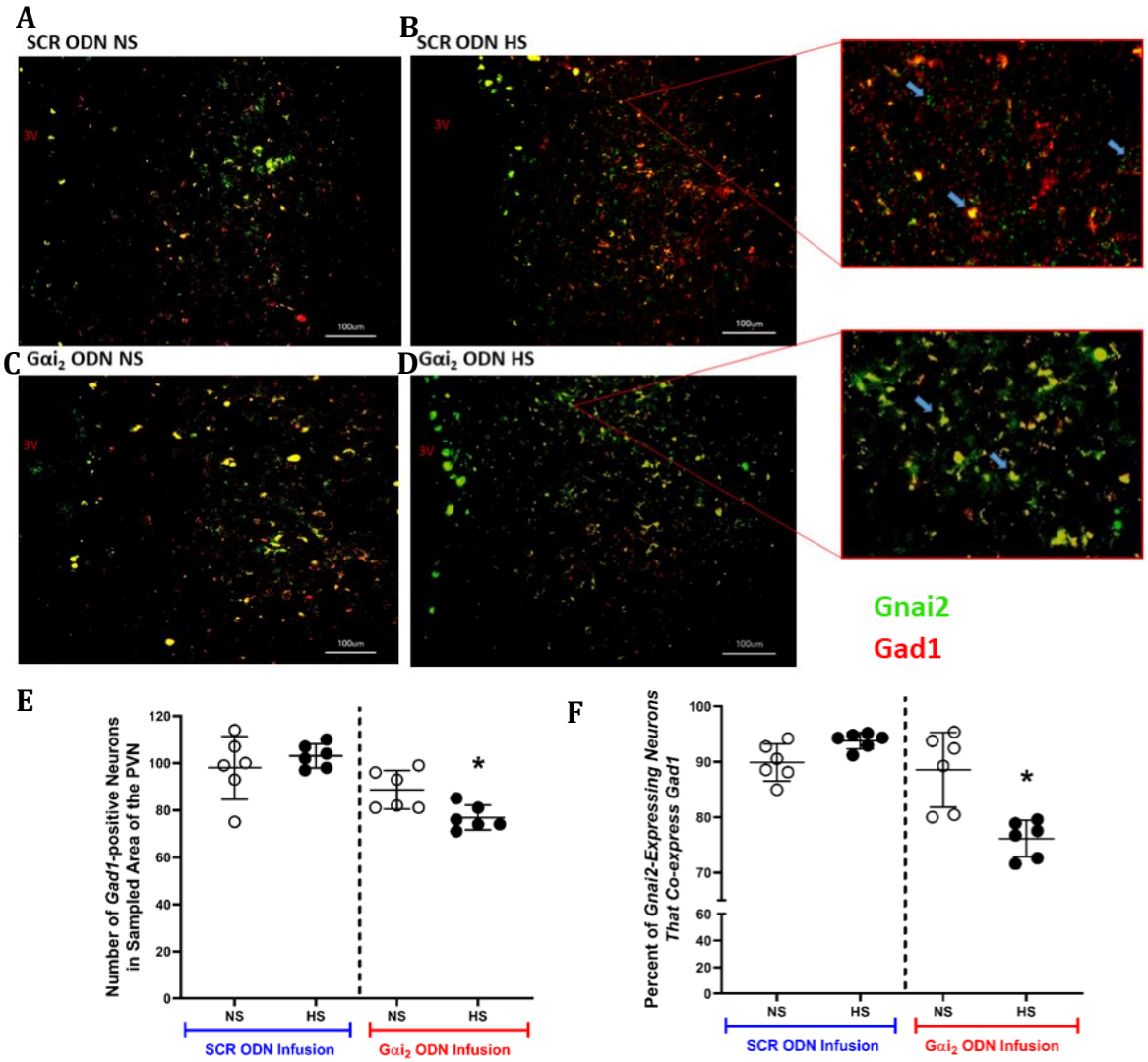

Figure 5.3: Expression of PVN *Gad1* and Colocalization of *Gad1-Gnai2* positive cells at level 2 in SCR or $G\alpha i_2$ ODN-Infused Male SD Rats.

Representative photomicrographs of impact of control scrambled (SCR, A-B) or targeted $G\alpha i_2$ (C-D) intracerebroventricular oligodeoxynucleotide (ODN) infusion (25 µg / 6 µL/ day) in conjunction with normal (0.6% NaCl NS) or high (4% NaCl) salt diet on *Gad1 and Gnai2* fluorescent staining and colocalization in level 2 of the Paraventricular Nucleus (PVN) and (E-F) quantifications of (E) *Gad1* abundance and (F) coexpression of *Gad-1* by *Gnai2*-positive cells (*$p<0.05$ vs. respective NS control value, photos captured at 20X, scale bar = 100 µm, green is *Gnai2*, red is *Gad1*, n=6/group, two-way analysis of variance (ANOVA)).

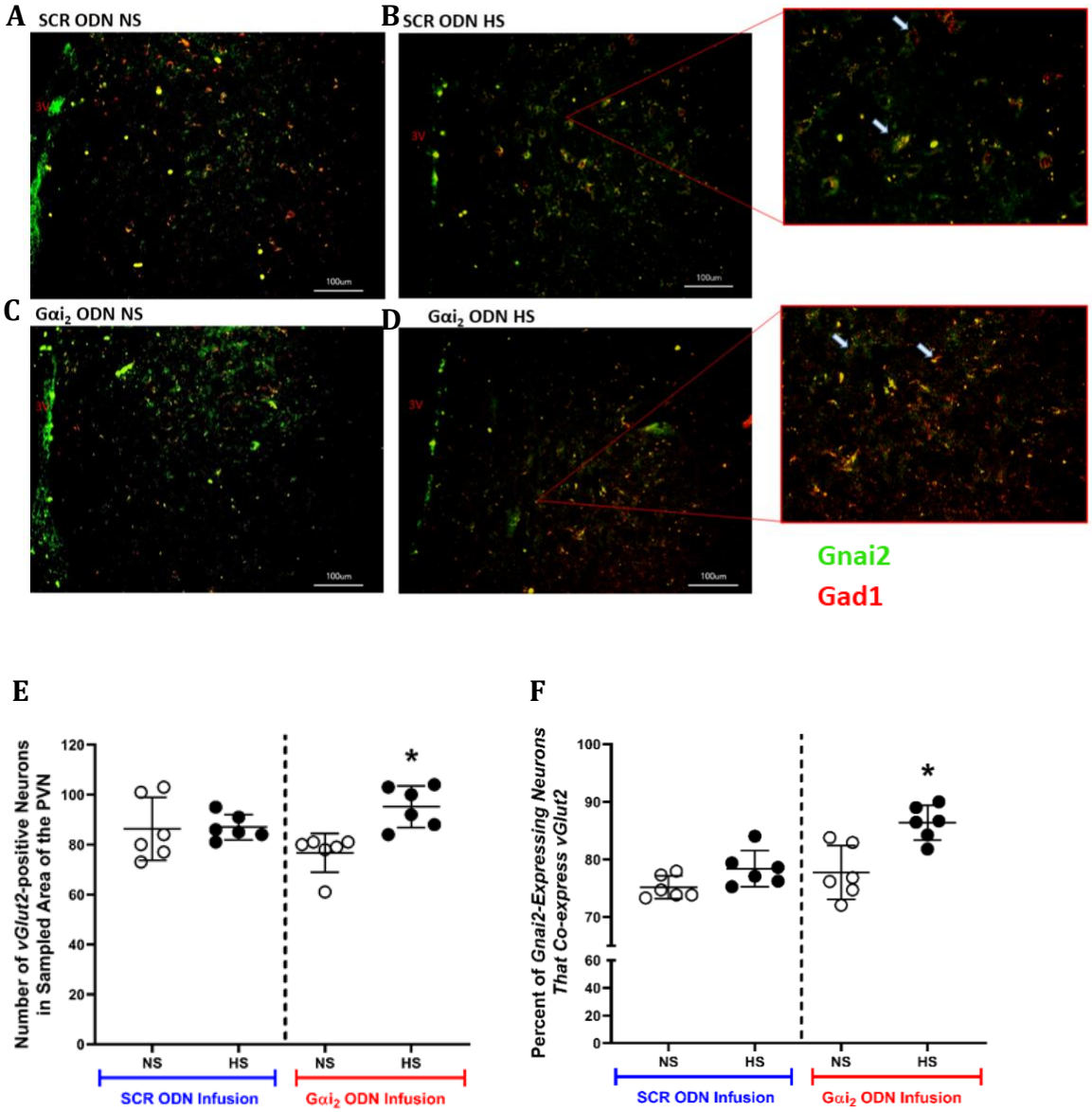

Figure 5.4: Expression of PVN *vGlut2* and Colocalization of *vGlut2-Gnai2* positive cells at level 2 in SCR or Gαi$_2$ ODN-Infused Male SD Rats.

Representative photomicrographs of impact of control scrambled (SCR, A-B) or targeted Gαi$_2$ (C-D) intracerebroventricular oligodeoxynucleotide (ODN) infusion (25 µg / 6 µL/ day) in conjunction with normal (0.6% NaCl NS) or high (4% NaCl) salt diet on *vGlut2 and Gnai2* fluorescent staining and colocalization in level 2 of the Paraventricular Nucleus (PVN) and (E-F) quantifications of (E) *vGlut21* abundance and (F) coexpression of *vGlut2* by *Gnai2*-positive cells (*p<0.05 vs. respective NS control value, photos captured at 20X, scale bar = 100 µm, green is *Gnai2*, red is *vGlut2*, n=6/group, two-way analysis of variance (ANOVA)).

Discussion

These studies were designed to test the hypothesis that downregulation of PVN Gαi2 proteins results in altered neuronal receptor activity and phenotypic abundance, which contributes to the sustained sodium-dependent increase in MAP in Gαi2 protein-dependent ssHTN in male SD rats. Significantly, we found that downregulation of PVN Gαi2 proteins results in loss of HS diet-induced tonic GABA(B) receptor signaling and gain of HS diet-induced glutamatergic signaling. Additionally, we found that central downregulation of Gαi2 proteins results in alterations to PVN parvocellular neuronal phenotypes, with medial parvocellular neurons displaying plasticity towards an enhanced abundance of glutamatergic neurons and reduced abundance of GABAergic neurons.

Tonic PVN GABA(B) receptor signaling is involved in the maintenance of normotension in male SD rats on HS diet

Previous work from our laboratory has identified a critical role of PVN neurons in the sympathoinhibitory, normotensive responses to acute challenges to fluid and electrolyte homeostasis (Carmichael et al., 2016) as well as chronic elevations in dietary sodium intake (Carmichael et al., 2020). In these prior studies, we have found that SCR ODN infused male SD rats display a robust PVN Fos protein induction in response to these acute and chronic challenges, suggestive of neuronal activation, and that these challenges repeatedly result in sympathoinhibition as well as the elimination of excess sodium and water, ultimately facilitating normotension. In contrast, our prior studies have demonstrated that in male SD rats, Gαi2 ODN infusion attenuates both acute and chronic

PVN Fos protein induction, sympathoinhibition, natriuretic responses, and elicits a prolongation of elevated MAP in the acute setting and the development of sustained ssHTN with chronic high sodium intake, suggesting the critical role of PVN $G\alpha i_2$ proteins in the neural signal transduction pathways regulating sodium and water balance.

This work extends our prior findings suggesting PVN neuronal activation as an effector of the normotensive responses to elevated sodium intake by delineating some of the receptor signaling pathways that are activated in response to elevated sodium intake in salt-resistance, and describing how those pathways appear to change in salt-sensitive HTN. Our current finding that PVN GABA(B) receptor antagonism in male SCR ODN-infused SD rats on HS diet elicits a significant hypertensive response signifies that tonic PVN GABA(B) receptor activity may be playing a critical role in the maintenance of the previously identified sympathoinhibitory, normotensive signaling elicited by chronic HS intake (Carmichael et al., 2020; Kapusta et al., 2013; Moreira et al., 2019). Moreover, this finding corroborates previous findings in the spontaneously hypertensive rat that HTN is attenuated by enhanced GABA(B) receptor activity (Li & Pan, 2006, 2007). In addition, we believe that there is a significant role of the $G\alpha i_2$ protein in facilitating tonic PVN GABA(B) receptor signaling as in $G\alpha i_2$ ODN-infused male rats on HS diet, which display robust HTN, there is an absence of a PVN GABA(B) receptor antagonism-induced hypertensive response. We believe that in the absence of the $G\alpha i_2$ protein, through which GABA(B) receptors have been demonstrated to potentially signal (Straiker, Borden, & Sullivan, 2002), there is a loss of HS-induced tonic GABA(B) receptor signaling, thus contributing to the failure to remain normotensive. While the synaptic localization of the

GABA(B) receptor remains unclear, it is possible that this receptor contributes to both presynaptic inhibition of excitatory neurotransmitter release, and slow-wave postsynaptic hyperpolarization to ultimately facilitate PVN sympathoinhibitory responses to HS.

Tonic PVN glutamatergic receptor signaling is enhanced in Gαi$_2$ ODN-infused male SD rats on HS diet

Our previous studies characterizing Gαi$_2$ protein-dependent ssHTN have not only identified a failure to suppress sympathetic outflow in response to HS in these hypertensive rats, but also a significant exacerbation of sympathetic outflow, known as sympathoexcitation (Carmichael et al., 2020; Kapusta et al., 2013; Moreira et al., 2019). Extending these findings that not only is sympathoinhibition lost but sympathoexcitation gained, our current study demonstrates that while tonic normotensive PVN GABA(B) receptor activity is attenuated, there is an enhancement of tonic hypertensive PVN glutamatergic signaling. In Gαi$_2$ ODN-infused male rats on HS diet, but not in any other group, PVN glutamatergic receptor antagonism elicited a significant depressor response. These data also corroborate previous findings by other groups that enhancement of PVN glutamatergic signaling promotes HTN and is common in multiple models of HTN (Gabor & Leenen, 2012a; Glass et al., 2015; Li & Pan, 2017; Qiao, Zhou, Li, & Pan, 2017), and that excessive excitatory PVN signaling correlates with elevations in blood pressure.

Male SD rats lacking central Gαi$_2$ proteins display robust sodium-dependent PVN neuronal plasticity

To further understand the context of our pharmacologic data, we used RNAScope technology for fluorescent in-situ hybridization to determine the relative abundance of

Gnai2-expressing neurons in the various subnuclei of the PVN, and the proportions of *Gad1*- and *vGlut2*-*Gnai2* colocalized neurons in the medial parvocellular PVN where *Gnai2* is the most abundant, per our previous finding (Chaudhary & Wainford, 2021). We show here that in the medial parvocellular subnucleus of the PVN at level 2, there is the highest abundance of *Gnai2* transcripts, and this relative proportionality remains unchanged regardless of OND infusion or HS intake. Moreover, we see that with respect to parvocellular neurons, there is a significant $G\alpha i_2$ ODN and HS-induced reduction in *Gad1* total expression and *Gad1*-*Gnai2* colocalization, and an increase in *vGlut2* total expression and *vGlut2*-*Gnai2* colocalization. These data provide new evidence of transcriptional-level neuronal phenotypic plasticity in ssHTN, and provide evidence that not only do functional changes occur in receptor signaling, but possibly reorganization of the abundance of neuronal phenotypes occurs in ssHTN.

As mentioned above, it has been demonstrated in several models of HTN that there is prohypertensive glutamatergic tone (Dampney et al., 2018; Glass et al., 2015; Li & Pan, 2017; Qiao et al., 2017) and antihypertensive GABAergic tone (Badr, Rao, & Manee, 2021; Li & Pan, 2006, 2007). What is not clear, however, is the mechanism whereby actual synaptic reorganization occurs facilitating enhanced glutamatergic PVN input and reduced GABAergic input. Of the few reports detailing this phenomenon, Biancardi et al (Biancardi, Campos, & Stern, 2010) describe significant reorganization of PVN-rostral ventrolateral medulla-projecting neurons in renovascular HTN, favoring glutamatergic inputs over GABAergic inputs at the immunohistochemical level. Their data, in conjunction with our novel data demonstrating mRNA-level alterations in the markers of

neuronal phenotypes, suggest a broad phenomenon whereby alterations in neuronal signaling are correlated with, and possibly exacerbated by, an overall reduction in antihypertensive GABAergic neurons and enhancement of prohypertensive glutamatergic neurons through which to signal.

With respect to the multiple pathways that may potentially impact neuronal transcription of neurotransmitter-related genes, significant consideration may be given to PVN inflammation and the impact of microglial-derived cytokines on neuronal signaling. Studies, including from our laboratory, have shown that multiple models of HTN feature robust neuroinflammation (Moreira et al., 2019; Sharma et al., 2019; P. Shi et al., 2010; Worker et al., 2020). Additionally, it has been demonstrated that cytokines can have a direct impact on neuronal firing and signaling (Clarkson et al., 2017; Galic et al., 2012; Hadjilambreva, Mix, Rolfs, Muller, & Strauss, 2005; Riazi, Galic, & Pittman, 2010). These findings together suggest a possible mechanism whereby HS intake-induced PVN inflammation may exacerbate the enhancement seen in prohypertensive glutamatergic signaling in $G\alpha i_2$ protein-dependent ssHTN. Future studies may utilize a minocycline-ODN co-infusion strategy as previously described (Moreira et al., 2019) to delineate a potential role of microglial-mediated PNV inflammation in the aforementioned neuronal plasticity.

Conclusions

We have demonstrated here that following PVN $G\alpha i_2$ ODN infusion, an elevated dietary sodium intake evokes the development of ssHTN featuring enhanced glutamatergic tone and abundance of parvocellular glutamatergic neurons, loss of tonic GABA(B)

receptor signaling and reductions in the abundance of PVN parvocellular GABAergic neurons. These data provide additional mechanistic insight into the role of the $G\alpha i_2$ protein in the maintenance of normotension and salt-resistance in male SD rats, and may lead to the discovery of potential therapeutic targets in the management of HTN.

CHAPTER SIX: Overall Discussion

The importance of understanding the integrated central neural mechanisms involved in the regulation of sodium homeostasis and blood pressure in health and disease is underscored by the multitude of human diseases that feature sodium and fluid dysregulation, such as salt-sensitive hypertension (ssHTN) (Bayorh et al., 1998; Kammerlander, 2019). The work contained in this dissertation sought to provide an enhanced understanding of the central neural and inflammatory mechanisms which regulate sodium balance and blood pressure, and the pathophysiological processes which contribute to the development of ssHTN. Our novel data demonstrate a critical role for central $G\alpha i_2$ proteins in the regulation of central sympathetic outflow in response to a chronic challenge to sodium homeostasis in the form of elevated dietary sodium intake.

First, we have demonstrated that in the absence of central $G\alpha i_2$ proteins, male but not female SD rats develop robust PVN-specific microglial-mediated neuroinflammation, which correlates with increased sympathetic outflow and an elevated magnitude of ssHTN. These data suggest that central $G\alpha i_2$ proteins plays both an anti-inflammatory and sympathoinhibitory central role in the response to a high salt diet. Moreover, we have shown that this male-specific PVN inflammation develops rapidly following high sodium intake and precedes the development of sympathoexcitation in the absence of $G\alpha i_2$ proteins, but develops concurrently with pressure-natriuresis induced elevations in blood pressure, suggesting altogether a sex-dependent multi-phasic mechanism whereby high salt diet induces the development of $G\alpha i_2$ protein-dependent ssHTN. Lastly, we have shown that significant PVN neuronal plasticity following $G\alpha i_2$ protein downregulation contributes

to the sodium-dependent enhancement in blood pressure, featuring reductions in tonic GABA(B) receptor signaling and enhancement of glutamatergic signaling, disrupting proper excitation-inhibition coupling in the PVN intended to regulate blood pressure.

The Potential Integration of a High Salt Diet, Neuronal Signaling Alterations, and PVN Inflammation

As described above, this work highlights both an anti-inflammatory and GABA(B) receptor-mediated inhibitory role of PVN $G\alpha i_2$ proteins in the maintenance of salt-resistance. What remains unclear, however, is the potential link that exists between these phenomena directly and between these phenomena and an elevated dietary sodium intake. With respect to PVN inflammation, as described in Chapter 4, it appears that as soon as 24 hours following HS dietary intake and $G\alpha i_2$ ODN infusion, male SD rats develop robust PVN neuroinflammation. This occurrence suggests the possibility that elevated dietary sodium intake directly evokes microglial reactivity and is congruent with other literature suggesting a role for salt in inducing pro-inflammatory microglial activity (T. Zhang et al., 2020). Due to the fact that the PVN is close in proximity to the 3rd ventricle, it is quite possible that acute elevations in cerebrospinal fluid sodium concentrations due to HS intake, as described in by several laboratories (Gomes et al., 2017; Zera, Nowinski, Segiet, & Smykiewicz, 2019), act locally to enhance microglial reactivity.

Moreover, it is likely that uncoupling of excitation and inhibition contributes to the development of PVN inflammation as well. As reported by our laboratory, signaling via the afferent renal nerves in SD rats is necessary to facilitate sympathoinhibitory and normotensive responses to a HS diet (Frame, Carmichael, et al., 2019). This afferent renal

nerve signaling, which was shown to evoke PVN cFos activation via immunohistochemistry, may represent the mechanism whereby PVN GABAergic pathways, shown to be important for maintaining normotension in this thesis, are activated in response to a HS diet. With respect to the downregulation of PVN $G\alpha i_2$ proteins, it may be that the afferent renal nerves send a signal which is unable to be synaptically received, thus uncoupling inhibition from excitatory signaling. This failure to inhibit via a loss of the $G\alpha i_2$ protein, and resultant excitation-inhibition uncoupling with excessive excitatory signaling, may then go on to result in excitotoxicity to some PVN neurons, ultimately leading to neuronal stress signaling and the induction of additional pro-inflammatory microglial reactivity.

This multifaceted mechanism possibly inducing the microglial reactivity seen following $G\alpha i_2$ ODN infusion and HS diet, may additionally help explain the apparent PVN site-specificity of microglial activation, as it appears that only in the PVN are multiple insults occurring that combine to create a pro-inflammatory environment, which our minocycline infusion data in Chapter 3 demonstrate is directly related to the magnitude of ssHTN. It thus appears that there may be a plethora of mechanisms, some even undiscovered yet, contributing to the development of ssHTN, including a bidirectional relationship between HS diet and neuronal excitotoxicity-evoked induction of microglial activation and the influence of microglial-mediated cytokine production on sympathetic outflow likely via actions on local presympathetic neuronal circuits which are already disrupted via loss of HS-diet induced tonic GABA(B) receptor signaling.

Together, our work supports a PVN-specific $G\alpha i_2$ protein-gated signal transduction

pathway that regulates inflammatory signaling, as well as facilitates enhanced GABA(B) receptor signaling in response to chronic elevations in sodium intake to maintain a salt-resistant phenotype. The identification of these neural mechanisms promoted by PVN $G\alpha i_2$ protein upregulation in salt-resistance may enhance mechanistic understanding of the development of ssHTN.

Future Directions

First, future studies in the laboratory will be aimed at understanding the electrophysiological impacts of $G\alpha i_2$ proteins on PVN neuronal firing. While the studies described in this dissertation provide insight into the phenotypes of neurons possibly participating in the altered sympathetic outflow observed in HTN, as well as the receptor types through which signaling may be altered, future studies may utilize whole-cell patch clamp techniques, in addition to microelectrode array technology to identify the impact of $G\alpha i_2$ proteins downregulation on individual neuronal firing rates as well as intra-nuclear synaptic signaling between local inhibitory and excitatory neurons. Moreover, tracer studies may be utilized to help identify the populations of neurons which project to sympathetic nuclei in the brain stem and spinal cord as described by other groups (Biancardi et al., 2010).

In addition to electrophysiology studies, our laboratory may investigate the impact of the loss of GPCR-coupled $G\alpha i_2$ protein signal transduction on the spatial transcriptomics of PVN neurons. As described here, the loss of $G\alpha i_2$ protein signal transduction appears to be correlated with an alteration on the abundance of both vGlut2 and Gad1 transcripts, suggesting an impact of $G\alpha i_2$ protein signal transduction on transcriptional regulation of

PVN neuronal phenotypes. Additionally, it is possible that inflammation-related cytokine receptor signaling, as seen described in animals lacking $G\alpha i_2$ proteins on HS diet, may result in changes to neuronal activity as well as altered transcripts as cytokine receptors have been well-characterized to influence neuronal excitability (Vezzani & Viviani, 2015) and to activate a host of transcription factors, including those related to the JAK-STAT (Villarino, Kanno, Ferdinand, & O'Shea, 2015) and ERK (E. K. Kim & Choi, 2010) pathway.

Finally, owing to our recent identification of correlations in distinct single nucleotide polymorphisms (SNPs) in the human GNAI2 gene and the salt sensitivity of blood pressure in the GenSalt study (X. Zhang et al., 2018) and essential HTN in subjects from the UK BioBank (Carmichael et al., 2020), future studies from our laboratory may further attempt to identify the utility of GNAI2 SNPs as a biomarker used to predict HTN risk, investigating possible correlations between SNPs in GNAI2 and physiological factors such as blood pressure, circulating catecholamines, and estimates of renal function. With respect to these SNPs and the work contained in this thesis, it is quite possible that impairments in human GNAI2 transcriptional regulation, as described in Menzaghi et al. (Menzaghi et al., 2006), contribute to the inability to effectively signal through brain $G\alpha i_2$ proteins, resulting in elevations in sympathetic outflow that promote the previously described salt-sensitivity and essential HTN in humans via the mechanistic changes described in Chapters 3-5. Namely, it is possible that the impairment in human $G\alpha i_2$ protein signaling dysregulates excitation-inhibition coupling and promotes a sex-dependent inflammatory environment, as it is likely that $G\alpha i_2$ protein function is evolutionarily

conserved.

Strengths and Limitations

With respect to the studies described in this dissertation, there are several advantages to our approach. First, utilizing an ODN-mediated downregulation technique in a salt-resistant rat model (the SD rat) enhances our ability to isolate the impact of central $G\alpha i_2$ proteins on the response to elevated dietary sodium intake in salt-resistance and how $G\alpha i_2$ protein absence facilitates the development of ssHTN. Second, our use of the young SD rat prevents the confounding that occurs when animals develop age-related HTN. Last, these studies are strengthened by our ability to target the $G\alpha i_2$ protein in just the PVN utilizing PVN-specific ODN infusions as performed in subsets of animals in Chapter 5, isolating the impact of PVN-specific $G\alpha i_2$ protein expression on blood pressure regulation.

Limitations do exist, however. While these studies provide insight into the ways in which a failure to upregulate $G\alpha i_2$ proteins results in ssHTN, they do not identify the mechanisms whereby salt-resistant SD rats facilitate PVN-specific upregulation of $G\alpha i_2$ proteins in response to HS diet. Additionally, we are unsure why exactly GNAI2 SNPs correlate with the salt-sensitivity of blood pressure or HTN. We speculate that, at least in a subset of individuals with GNAI2 SNPs, as described by Menzaghi et al., correlations in GNAI2 polymorphisms and HTN exist due to an impact on the transcriptional regulation of the GNAI2 gene owing to the polymorphism existing at a transcription factor binding site (Menzaghi et al., 2006). This impairment in GNAI2 transcription may underlie the inability of salt-sensitive humans to regulate sodium appropriately, and the potential lack of $G\alpha i_2$ protein expression in these individuals may contribute to the development of HTN

in a manner similar to our studies described herein, with a loss of control over neuronal circuitry normally responsible for sympathoinhibition.

Moreover, while our studies identified sex differences in the magnitude of ssHTN following HS diet, our approach did not investigate the impacts of female sex steroid hormones on HTN. Human and animal studies have suggested that premenopausal females receive cardio-protection from estrogens such as 17β-estradiol. Our studies in the future may utilize ovariectomy-based approaches to determine if the robust sex differences observed in this dissertation were the result of estrogens or some other unidentified factor(s). Lastly, our studies are not able to currently identify whether the implicated GABA(B) receptor which appears to be tonically active in salt-resistant SD rats on HS diet exerts its sympathoinhibitory effects in a presynaptic or postsynaptic manner. This may be clarified using electrophysiologic methods as described in the future directions section, where whole-cell patch clamping may be able to delineate a more specific role of these inhibitory receptors.

Perspectives

The identification of novel mechanisms, and potential therapeutic targets, driving the development and maintenance of ssHTN remains critically important in the 21st century. With antihypertensive drug development having been virtually unmoving for over a decade (Shah & Stafford, 2017), and HTN contributing to an estimated 10.4 million deaths worldwide per year (Unger et al., 2020), we hope that our work to identify novel central signal transduction pathways involved in the regulation of sympathetic outflow will help provide new therapeutic targets for future pharmaceutical research in HTN.

The importance of our basic science work to delineate the neural mechanisms contributing to the development of ssHTN is underscored by 1) The significant correlations our laboratory has identified between those with GNAI2 SNPs and essential HTN (Carmichael et al., 2020) and the salt-sensitivity of blood pressure (X. Zhang et al., 2018), both in fairly large proportions of their respective populations, 2) the excess of dietary sodium consumed worldwide (Appel et al., 2011) and 3) the findings in the recent SPRINT trial (Group et al., 2015), amongst many other blood pressure reduction randomized clinical trials conducted since the mid-20th century which have been reviewed extensively through large-scale meta analyses (Zanchetti, Thomopoulos, & Parati, 2015) noting significant benefits of reducing blood pressure. We believe our work will help achieve the goal of having a population with well-controlled blood pressure through the provision of an enhanced understanding of central mechanisms dysregulating sympathetic outflow, supporting the identification of novel potential therapeutic targets, such that individuals may be treated in a personalized, mechanism and genotype-based way that enhances the success of antihypertensive therapy.

List of Abbreviated Journal

ACS Chem Neurosci … ACS Chemical Neuroscience

Acta Physiol … Acta Physiologica

Adv Pharmacol … Advances in Pharmacology

Am Heart J … American Heart Journal

Am J Coll Nutr … American Journal of the College of Nutrition

Am J Hypertens … American Journal of Hypertension

Am J Physiol … American Journal of Physiology

Am J Physiol Endocrinol Metab … American Journal of Physiology – Endocrinology & Metabolism

Am J Physiol Heart Circ Physiol … American Journal of Physiology – Heart and Circulatory Physiology

Am J Physiol Regul Integr Comp Physiol … American Journal of Physiology Regulatory, Integrative and Comparative Physiology

Am J Physiol Renal Physiol … American Journal of Physiology – Renal Physiology

Ann Intern Med … Annals of Internal Medicine

Ann N Y Acad Sci … Annals of the New York Academy of Sciences

Annu Rev Med … The Annual Review of Medicine

Auton Neurosci … Autonomic Neuroscience

Biochim Biophys Acta … Biochimica et Biophysica Acta

Biochim Biophys Acta Mol Bas Dis … Biomicha et Biophysica Acta. Molecular Basis of Disease

Biodemography Soc Biol … Biodemography and Social Biology

Biol Reprod … Biology of Reproduction

Biol Signals … Biological Signals

Biomed Pharmacother … Biomedicine & Pharmacotherapy

Blood Press Suppl … Blood Pressure Supplement

BMC Physiol … BMC Physiology

Br J Pharmacol … British Journal of Pharmacology

Brain Res … Brain Research

Can J Physiol Pharmacol … Canadian Journal of Physiology & Pharmacology

Cardiovasc Res … Cardiovascular Research

Circ Res … Circulation Research

Clin Exp Hypertens … Clinical and Experimental Hypertension

Clin Exp Pharmacol Physiol … Clinical and Experimental Pharmacology & Physiology

Clin Sci … Clinical Science

Cochrane Database Syst Rev … Cochrane Database of Systematic Reviews

Comput Methods Programs Biomed … Computer Methods and Programs in Biomedicine

Curr Hypertens Rep … Current Hypertension Reports

Curr Pharm Des … Current Pharmaceutical Design

Endocr Rev … Endocrine Reviews

Epilepsy Res … Epilepsy Research

Exp Mol Med … Experimental & Molecular Medicine

Exp Physiol … Experimental Physiology

Expert Opin Ther Targets … Expert Opinion on Therapeutic Targets

FASEB J … FASEB Journal

Front Biosci … Frontiers in Bioscience

Front Cell Neurosci … Frontiers in Cellular Neuroscience

Front Neuroendocrinol … Frontiers in Neuroendocrinology

Front Neurosci … Frontiers in Neuroscience

Front Physiol … Frontiers in Physiology

Int J Cardiol … International Journal of Cardiology

Int J Mol Sci … International Journal of Molecular Science

Int J Neuropsycopharmacol … International Journal of Neuropsychopharmacology

J Am Coll Cardiol … Journal of the American College of Cardiology

J Am Soc Nephrol … Journal of the American Society of Nephrology

J Appl Physiol … Journal of Applied Physiology

J Auton Nerv Syst … Journal of the Autonomic Nervous System

J Biosoc Sci … Journal of Biosocial Science

J Cardiovasc Pharmacol … Journal of Cardiovascular Pharmacology

J Clin Invest … Journal of Clinical Investigation

J Comp Neurol … Journal of Comparative Neurology

J Gend Specif Med … Journal of Gender Specific Medicine

J Hypertens … Journal of Hypertension

J Immunol … Journal of Immunology

J Korean Med Sci … Journal of Korean Medical Science

J Neuroendocrinol … Journal of Neuroendocrinology

J Neuroinflammation … Journal of Neuroinflammation

J Neurophysiol … Journal of Neurophysiology

J Neurosci … Journal of Neuroscience

J Phrmacol Exp Ther … Journal of Pharmacology & Experimental Therapeutics

J Physiol … Journal of Physiology

Mol Med Rep … Molecular Medicine Reports

Mol Pain … Molecular Pain

Mol Pharmacol … Molecular Pharmacology

N Engl J Med … New England Journal of Medicine

Nat Clin Pract Cardiovasc Med … Nature Clinical Practice. Cardiovascular Medicine

Nat Med … Nature Medicine

Neurosci Bull … Neuroscience Bulletin

Neurosci Lett … Neuroscience Letters

Neurosci Res … Neuroscience Research

Physiol Behav … Physiology & Behavior

Physiol Genomics … Physiological Genomics

Physiol Rep … Physiological Reports

Physiol Rev … Physiology Reviews

Qual Life Res … Quality of Life Research

Sci Rep … Scientific Reports

StatPearls … Statistics Pearls

Toxicol Appl Pharmacol … Toxicology and Applied Pharmacology

Trends Immunol … Trends in Immunology

References

Andani, R., & Khan, Y. S. (2020). Anatomy, Head and Neck, Carotid Sinus. In *StatPearls*. Treasure Island (FL).

Appel, L. J., Frohlich, E. D., Hall, J. E., Pearson, T. A., Sacco, R. L., Seals, D. R., . . . Van Horn, L. V. (2011). The importance of population-wide sodium reduction as a means to prevent cardiovascular disease and stroke: a call to action from the American Heart Association. *Circulation, 123*(10), 1138-1143. doi:10.1161/CIR.0b013e31820d0793

Ashraf, M. S., & Vongpatanasin, W. (2006). Estrogen and hypertension. *Curr Hypertens Rep, 8*(5), 368-376. doi:10.1007/s11906-006-0080-1

Badr, H. E., Rao, S., & Manee, F. (2021). Gender differences in quality of life, physical activity, and risk of hypertension among sedentary occupation workers. *Qual Life Res*. doi:10.1007/s11136-020-02741-w

Bardgett, M. E., Holbein, W. W., Herrera-Rosales, M., & Toney, G. M. (2014). Ang II-salt hypertension depends on neuronal activity in the hypothalamic paraventricular nucleus but not on local actions of tumor necrosis factor-alpha. *Hypertension, 63*(3), 527-534. doi:10.1161/HYPERTENSIONAHA.113.02429

Bayorh, M. A., Ogbolu, E. C., Williams, E., Thierry-Palmer, M., Sanford, G., Emmett, N., . . . Chenault, V. M. (1998). Possible mechanisms of salt-induced hypertension in Dahl salt-sensitive rats. *Physiol Behav, 65*(3), 563-568. doi:10.1016/s0031-9384(98)00194-2

Biancardi, V. C., Campos, R. R., & Stern, J. E. (2010). Altered balance of gamma-aminobutyric acidergic and glutamatergic afferent inputs in rostral ventrolateral medulla-projecting neurons in the paraventricular nucleus of the hypothalamus of renovascular hypertensive rats. *J Comp Neurol, 518*(5), 567-585. doi:10.1002/cne.22256

Biancardi, V. C., Stranahan, A. M., Krause, E. G., de Kloet, A. D., & Stern, J. E. (2016). Cross talk between AT1 receptors and Toll-like receptor 4 in microglia contributes to angiotensin II-derived ROS production in the hypothalamic paraventricular nucleus. *Am J Physiol Heart Circ Physiol, 310*(3), H404-415. doi:10.1152/ajpheart.00247.2015

Bristow, M. R., Hershberger, R. E., Port, J. D., Gilbert, E. M., Sandoval, A., Rasmussen, R., . . . Feldman, A. M. (1990). Beta-adrenergic pathways in nonfailing and failing human ventricular myocardium. *Circulation, 82*(2 Suppl), I12-25. Retrieved from https://www.ncbi.nlm.nih.gov/pubmed/2164894

Brodde, O. E. (1990). Physiology and pharmacology of cardiovascular catecholamine receptors: implications for treatment of chronic heart failure. *Am Heart J, 120*(6 Pt 2), 1565-1572. doi:10.1016/0002-8703(90)90060-b

Brooks, V. L., Haywood, J. R., & Johnson, A. K. (2005). Translation of salt retention to central activation of the sympathetic nervous system in hypertension. *Clin Exp Pharmacol Physiol, 32*(5-6), 426-432. doi:10.1111/j.1440-1681.2005.04206.x

Brouwers, S., Smolders, I., Wainford, R. D., & Dupont, A. G. (2015). Hypotensive and sympathoinhibitory responses to selective central AT2 receptor stimulation in spontaneously hypertensive rats. *Clin Sci (Lond), 129*(1), 81-92. doi:10.1042/CS20140776

Carmichael, C. Y., Carmichael, A. C., Kuwabara, J. T., Cunningham, J. T., & Wainford, R. D. (2016). Impaired sodium-evoked paraventricular nucleus neuronal activation and blood pressure regulation in conscious Sprague-Dawley rats lacking central Galphai2 proteins. *Acta Physiol (Oxf), 216*(3), 314-329. doi:10.1111/apha.12610

Carmichael, C. Y., Kuwabara, J. T., Pascale, C. L., Moreira, J. D., Mahne, S. E., Kapusta, D. R., . . . Wainford, R. D. (2020). Hypothalamic Paraventricular Nucleus Galphai2 (Guanine Nucleotide-Binding Protein Alpha Inhibiting Activity Polypeptide 2) Protein-Mediated Neural Control of the Kidney and the Salt Sensitivity of Blood Pressure. *Hypertension, 75*(4), 1002-1011. doi:10.1161/HYPERTENSIONAHA.119.13777

Caverson, M. M., & Ciriello, J. (1988). Renal and cardiovascular afferent inputs to hypothalamic paraventriculo-spinal neurons. *Neurosci Lett, 95*(1-3), 167-172. doi:10.1016/0304-3940(88)90651-9

Chaudhary, P., & Wainford, R. D. (2021). Neuroanatomical characterization of Galphai2-expressing neurons in the hypothalamic paraventricular nucleus of male and female Sprague-Dawley rats. *Physiol Genomics, 53*(1), 12-21. doi:10.1152/physiolgenomics.00097.2020

Chen, W., Sheng, J., Guo, J., Peng, G., Hong, J., Li, B., . . . Wang, S. (2017). Cytokine cascades induced by mechanical trauma injury alter voltage-gated sodium channel activity in intact cortical neurons. *J Neuroinflammation, 14*(1), 73. doi:10.1186/s12974-017-0847-0

Cheng, Z. Y., Wang, X. P., Schmid, K. L., & Han, X. G. (2014). GABAB1 and GABAB2 receptor subunits co-expressed in cultured human RPE cells regulate intracellular Ca2+ via Gi/o-protein and phospholipase C pathways. *Neuroscience, 280*, 254-261. doi:10.1016/j.neuroscience.2014.09.021

Clarkson, B. D. S., Kahoud, R. J., McCarthy, C. B., & Howe, C. L. (2017). Inflammatory cytokine-induced changes in neural network activity measured by waveform analysis of high-content calcium imaging in murine cortical neurons. *Sci Rep, 7*(1), 9037. doi:10.1038/s41598-017-09182-5

College, O. (2020). *Anatomy & Physiology* Rice University, 6100 Main Street MS-375, Houston, TX 77005: Rice University.

Colombo, E., & Farina, C. (2016). Astrocytes: Key Regulators of Neuroinflammation. *Trends Immunol, 37*(9), 608-620. doi:10.1016/j.it.2016.06.006

Coote, J. H. (1995). Cardiovascular function of the paraventricular nucleus of the hypothalamus. *Biol Signals, 4*(3), 142-149. Retrieved from https://www.ncbi.nlm.nih.gov/pubmed/8750940

Cowley, A. W., Jr., Liard, J. F., & Guyton, A. C. (1973). Role of baroreceptor reflex in daily control of arterial blood pressure and other variables in dogs. *Circ Res, 32*(5), 564-576. doi:10.1161/01.res.32.5.564

Crofton, J. T., & Share, L. (1997). Gonadal hormones modulate deoxycorticosterone-salt hypertension in male and female rats. *Hypertension, 29*(1 Pt 2), 494-499. doi:10.1161/01.hyp.29.1.494

da Silva, J. S., Sun, X., Ahmad, S., Wang, H., Sudo, R. T., Varagic, J., . . . Groban, L. (2019). G-Protein-Coupled Estrogen Receptor Agonist G1 Improves Diastolic Function and Attenuates Cardiac Renin-Angiotensin System Activation in Estrogen-Deficient Hypertensive Rats. *J Cardiovasc Pharmacol, 74*(5), 443-452. doi:10.1097/FJC.0000000000000721

Dampney, R. A., Michelini, L. C., Li, D. P., & Pan, H. L. (2018). Regulation of sympathetic vasomotor activity by the hypothalamic paraventricular nucleus in normotensive and hypertensive states. *Am J Physiol Heart Circ Physiol, 315*(5), H1200-H1214. doi:10.1152/ajpheart.00216.2018

Das Gupta, R., Shabab Haider, S., Sutradhar, I., Hasan, M., Joshi, H., Rifat Haider, M., & Sarker, M. (2020). Gender differences in hypertension awareness, antihypertensive use and blood pressure control in Nepalese adults: findings from a nationwide cross-sectional survey. *J Biosoc Sci, 52*(3), 412-438. doi:10.1017/S0021932019000531

DiBona, G. F. (1985). Neural control of renal function: role of renal alpha adrenoceptors. *J Cardiovasc Pharmacol, 7 Suppl 8*, S18-23. Retrieved from https://www.ncbi.nlm.nih.gov/pubmed/2417043

Drews, H. J., Yenkoyan, K., Lourhmati, A., Buadze, M., Kabisch, D., Verleysdonk, S., . . . Danielyan, L. (2019). Intranasal Losartan Decreases Perivascular Beta Amyloid, Inflammation, and the Decline of Neurogenesis in Hypertensive Rats. *Neurotherapeutics*. doi:10.1007/s13311-019-00723-6

Du, D., Hu, L., Wu, J., Wu, Q., Cheng, W., Guo, Y., . . . Xia, C. (2017). Neuroinflammation contributes to autophagy flux blockage in the neurons of rostral ventrolateral medulla in stress-induced hypertension rats. *J Neuroinflammation, 14*(1), 169. doi:10.1186/s12974-017-0942-2

Dubey, R. K., Oparil, S., Imthurn, B., & Jackson, E. K. (2002). Sex hormones and hypertension. *Cardiovasc Res, 53*(3), 688-708. doi:10.1016/s0008-6363(01)00527-2

Elhawary, A. M., & Pang, C. C. (1994). Alpha 1b-adrenoceptors mediate renal tubular sodium and water reabsorption in the rat. *Br J Pharmacol, 111*(3), 819-824. doi:10.1111/j.1476-5381.1994.tb14811.x

Everett, B., & Zajacova, A. (2015). Gender differences in hypertension and hypertension awareness among young adults. *Biodemography Soc Biol, 61*(1), 1-17. doi:10.1080/19485565.2014.929488

Ferguson, A. V., Latchford, K. J., & Samson, W. K. (2008). The paraventricular nucleus of the hypothalamus - a potential target for integrative treatment of autonomic dysfunction. *Expert Opin Ther Targets, 12*(6), 717-727. doi:10.1517/14728222.12.6.717

Ferreira-Junior, N. C., Ruggeri, A., Silva, S. D., Jr., Zampieri, T. T., Ceroni, A., & Michelini, L. C. (2019). Exercise training increases GAD65 expression, restores the depressed GABAA receptor function within the PVN and reduces sympathetic modulation in hypertension. *Physiol Rep, 7*(13), e14107. doi:10.14814/phy2.14107

Flock, T., Hauser, A. S., Lund, N., Gloriam, D. E., Balaji, S., & Babu, M. M. (2017). Selectivity determinants of GPCR-G-protein binding. *Nature, 545*(7654), 317-322. doi:10.1038/nature22070

Foss, J. D., Fink, G. D., & Osborn, J. W. (2013). Reversal of genetic salt-sensitive hypertension by targeted sympathetic ablation. *Hypertension, 61*(4), 806-811. doi:10.1161/HYPERTENSIONAHA.111.00474

Frame, A. A., Carmichael, C. Y., Kuwabara, J. T., Cunningham, J. T., & Wainford, R. D. (2019). Role of the afferent renal nerves in sodium homeostasis and blood pressure regulation in rats. *Exp Physiol, 104*(8), 1306-1323. doi:10.1113/EP087700

Frame, A. A., Puleo, F., Kim, K., Walsh, K. R., Faudoa, E., Hoover, R. S., & Wainford, R. D. (2019). Sympathetic regulation of NCC in norepinephrine-evoked salt-sensitive hypertension in Sprague-Dawley rats. *Am J Physiol Renal Physiol, 317*(6), F1623-F1636. doi:10.1152/ajprenal.00264.2019

Franco, V., & Oparil, S. (2006). Salt sensitivity, a determinant of blood pressure, cardiovascular disease and survival. *J Am Coll Nutr, 25*(3 Suppl), 247S-255S. doi:10.1080/07315724.2006.10719574

Frohlich, E. D., & Varagic, J. (2004). The role of sodium in hypertension is more complex than simply elevating arterial pressure. *Nat Clin Pract Cardiovasc Med, 1*(1), 24-30. doi:10.1038/ncpcardio0025

Fujita, M., & Fujita, T. (2013). The role of CNS in salt-sensitive hypertension. *Curr Hypertens Rep, 15*(4), 390-394. doi:10.1007/s11906-013-0358-z

Fujita, M., & Fujita, T. (2016). The Role of CNS in the Effects of Salt on Blood Pressure. *Curr Hypertens Rep, 18*(2), 10. doi:10.1007/s11906-015-0620-7

Gabor, A., & Leenen, F. H. (2009). Mechanisms in the PVN mediating local and central sodium-induced hypertension in Wistar rats. *Am J Physiol Regul Integr Comp Physiol, 296*(3), R618-630. doi:10.1152/ajpregu.90417.2008

Gabor, A., & Leenen, F. H. (2012a). Cardiovascular effects of angiotensin II and glutamate in the PVN of Dahl salt-sensitive rats. *Brain Res, 1447*, 28-37. doi:10.1016/j.brainres.2012.01.060

Gabor, A., & Leenen, F. H. (2012b). Central neuromodulatory pathways regulating sympathetic activity in hypertension. *J Appl Physiol, 113*(8), 1294-1303. doi:10.1152/japplphysiol.00553.2012

Galic, M. A., Riazi, K., & Pittman, Q. J. (2012). Cytokines and brain excitability. *Front Neuroendocrinol, 33*(1), 116-125. doi:10.1016/j.yfrne.2011.12.002

Gerber, Y. N., Saint-Martin, G. P., Bringuier, C. M., Bartolami, S., Goze-Bac, C., Noristani, H. N., & Perrin, F. E. (2018). CSF1R Inhibition Reduces Microglia Proliferation, Promotes Tissue Preservation and Improves Motor Recovery After Spinal Cord Injury. *Front Cell Neurosci, 12*, 368. doi:10.3389/fncel.2018.00368

Gilman, T. L., Mitchell, N. C., Daws, L. C., & Toney, G. M. (2019). Neuroinflammation Contributes to High Salt Intake-Augmented Neuronal Activation and Active Coping Responses to Acute Stress. *Int J Neuropsychopharmacol, 22*(2), 137-142. doi:10.1093/ijnp/pyy099

Gingerich, S., & Krukoff, T. L. (2006). Estrogen in the paraventricular nucleus attenuates L-glutamate-induced increases in mean arterial pressure through estrogen receptor beta and NO. *Hypertension, 48*(6), 1130-1136. doi:10.1161/01.HYP.0000248754.67128.ff

Glass, M. J., Wang, G., Coleman, C. G., Chan, J., Ogorodnik, E., Van Kempen, T. A., . . . Pickel, V. M. (2015). NMDA Receptor Plasticity in the Hypothalamic Paraventricular Nucleus Contributes to the Elevated Blood Pressure Produced by Angiotensin II. *J Neurosci, 35*(26), 9558-9567. doi:10.1523/JNEUROSCI.2301-14.2015

Gomes, P. M., Sa, R. W. M., Aguiar, G. L., Paes, M. H. S., Alzamora, A. C., Lima, W. G., . . . Cardoso, L. M. (2017). Chronic high-sodium diet intake after weaning lead to neurogenic hypertension in adult Wistar rats. *Sci Rep, 7*(1), 5655. doi:10.1038/s41598-017-05984-9

Group, S. R., Wright, J. T., Jr., Williamson, J. D., Whelton, P. K., Snyder, J. K., Sink, K. M., . . . Ambrosius, W. T. (2015). A Randomized Trial of Intensive versus Standard Blood-Pressure Control. *N Engl J Med, 373*(22), 2103-2116. doi:10.1056/NEJMoa1511939

Guyton, A. C., Coleman, T. G., Young, D. B., Lohmeier, T. E., & DeClue, J. W. (1980). Salt balance and long-term blood pressure control. *Annu Rev Med, 31*, 15-27. doi:10.1146/annurev.me.31.020180.000311

Hadjilambreva, G., Mix, E., Rolfs, A., Muller, J., & Strauss, U. (2005). Neuromodulation by a cytokine: interferon-beta differentially augments neocortical neuronal activity and excitability. *J Neurophysiol, 93*(2), 843-852. doi:10.1152/jn.01224.2003

Hadjimarkou, M. M., Silva, R. M., Rossi, G. C., Pasternak, G. W., & Bodnar, R. J. (2002). Feeding induced by food deprivation is differentially reduced by G-protein alpha-subunit antisense probes in rats. *Brain Res, 955*(1-2), 45-54. Retrieved from https://www.ncbi.nlm.nih.gov/pubmed/12419520

Hardy, S. T., Loehr, L. R., Butler, K. R., Chakladar, S., Chang, P. P., Folsom, A. R., . . . Avery, C. L. (2015). Reducing the Blood Pressure-Related Burden of Cardiovascular Disease: Impact of Achievable Improvements in Blood Pressure Prevention and Control. *Journal of the American Heart Association, 4*(10), e002276. doi:10.1161/JAHA.115.002276

Hart, E. C., & Charkoudian, N. (2011). Sympathetic neural mechanisms in human blood pressure regulation. *Curr Hypertens Rep, 13*(3), 237-243. doi:10.1007/s11906-011-0191-1

Hiyama, T. Y., & Noda, M. (2016). Sodium sensing in the subfornical organ and body-fluid homeostasis. *Neurosci Res, 113*, 1-11. doi:10.1016/j.neures.2016.07.007

Hiyama, T. Y., Watanabe, E., Okado, H., & Noda, M. (2004). The subfornical organ is the primary locus of sodium-level sensing by Na(x) sodium channels for the control of salt-intake behavior. *J Neurosci, 24*(42), 9276-9281. doi:10.1523/JNEUROSCI.2795-04.2004

Hoeg, J. M., Willis, L. R., & Weinberger, M. H. (1977). Estrogen attenuation of the development of hypertension in spontaneously hypertensive rats. *Am J Physiol, 233*(3), H369-373. doi:10.1152/ajpheart.1977.233.3.H369

Jembrek, M. J., & Vlainic, J. (2015). GABA Receptors: Pharmacological Potential and Pitfalls. *Curr Pharm Des, 21*(34), 4943-4959. doi:10.2174/1381612821666150914121624

Jiang, E., Chapp, A. D., Fan, Y., Larson, R. A., Hahka, T., Huber, M. J., . . . Shan, Z. (2018). Expression of Proinflammatory Cytokines Is Upregulated in the Hypothalamic Paraventricular Nucleus of Dahl Salt-Sensitive Hypertensive Rats. *Front Physiol, 9*, 104. doi:10.3389/fphys.2018.00104

Jonklaas, J., & Buggy, J. (1984). Angiotensin-estrogen interaction in female brain reduces drinking and pressor responses. *Am J Physiol, 247*(1 Pt 2), R167-172. doi:10.1152/ajpregu.1984.247.1.R167

Kammerlander, A. A. (2019). With a grain of salt: Sodium levels in heart failure. *Int J Cardiol, 290*, 125-126. doi:10.1016/j.ijcard.2019.05.027

Kanaya, M., Higo, S., & Ozawa, H. (2019). Neurochemical Characterization of Neurons Expressing Estrogen Receptor beta in the Hypothalamic Nuclei of Rats Using in Situ Hybridization and Immunofluorescence. *Int J Mol Sci, 21*(1). doi:10.3390/ijms21010115

Kannan, H., Hayashida, Y., & Yamashita, H. (1989). Increase in sympathetic outflow by paraventricular nucleus stimulation in awake rats. *Am J Physiol, 256*(6 Pt 2), R1325-1330. doi:10.1152/ajpregu.1989.256.6.R1325

Kapusta, D. R., & Kenigs, V. A. (1999). Cardiovascular and renal responses produced by central orphanin FQ/nociceptin occur independent of renal nerves. *Am J Physiol, 277*(4), R987-995. doi:10.1152/ajpregu.1999.277.4.R987

Kapusta, D. R., Pascale, C. L., Kuwabara, J. T., & Wainford, R. D. (2013). Central nervous system Galphai2-subunit proteins maintain salt resistance via a renal nerve-dependent sympathoinhibitory pathway. *Hypertension, 61*(2), 368-375. doi:10.1161/HYPERTENSIONAHA.111.00014

Kapusta, D. R., Pascale, C. L., & Wainford, R. D. (2012). Brain heterotrimeric Galphai(2)-subunit protein-gated pathways mediate central sympathoinhibition to maintain fluid and electrolyte homeostasis during stress. *FASEB J, 26*(7), 2776-2787. doi:10.1096/fj.11-196550

Kato, K., Chu, C. P., Kannan, H., Ishida, Y., Nishimori, T., & Nose, H. (2004). Regional differences in the expression of Fos-like immunoreactivity after central salt loading in conscious rats: modulation by endogenous vasopressin and role of the area postrema. *Brain Res, 1022*(1-2), 182-194. doi:10.1016/j.brainres.2004.02.082

Kaur, D., Sharma, V., & Deshmukh, R. (2019). Activation of microglia and astrocytes: a roadway to neuroinflammation and Alzheimer's disease. *Inflammopharmacology*. doi:10.1007/s10787-019-00580-x

Kim, E. K., & Choi, E. J. (2010). Pathological roles of MAPK signaling pathways in human diseases. *Biochim Biophys Acta, 1802*(4), 396-405. doi:10.1016/j.bbadis.2009.12.009

Kim, J. G., Leem, Y. E., Kwon, I., Kang, J. S., Bae, Y. M., & Cho, H. (2018). Estrogen modulates serotonin effects on vasoconstriction through Src inhibition. *Exp Mol Med, 50*(12), 1-9. doi:10.1038/s12276-018-0193-z

Koba, S., Hanai, E., Kumada, N., Kataoka, N., Nakamura, K., & Watanabe, T. (2018). Sympathoexcitation by hypothalamic paraventricular nucleus neurons projecting to the rostral ventrolateral medulla. *J Physiol, 596*(19), 4581-4595. doi:10.1113/JP276223

Korpal, A. K., Han, S. Y., Schwenke, D. O., & Brown, C. H. (2017). A switch from GABA inhibition to excitation of vasopressin neurons exacerbates the development angiotensin II-dependent hypertension. *J Neuroendocrinol*. doi:10.1111/jne.12564

Kotchen, T. A., Cowley, A. W., Jr., & Frohlich, E. D. (2013). Salt in health and disease--a delicate balance. *N Engl J Med, 368*(26), 2531-2532. doi:10.1056/NEJMc1305326

Kuriyama, K., Hirouchi, M., & Nakayasu, H. (1993). Structure and function of cerebral GABAA and GABAB receptors. *Neurosci Res, 17*(2), 91-99. doi:10.1016/0168-0102(93)90087-7

Lanfranchi, A., Spaziani, D., Seravalle, G., Turri, C., Dell'Oro, R., Grassi, G., & Mancia, G. (1998). Sympathetic control of circulation in hypertension and congestive heart failure. *Blood Press Suppl, 3*, 40-45. Retrieved from https://www.ncbi.nlm.nih.gov/pubmed/10321454

Lee, J. Y., Choi, H. Y., Ju, B. G., & Yune, T. Y. (2018). Estrogen alleviates neuropathic pain induced after spinal cord injury by inhibiting microglia and astrocyte activation. *Biochim Biophys Acta Mol Basis Dis, 1864*(7), 2472-2480. doi:10.1016/j.bbadis.2018.04.006

Li, D. P., & Pan, H. L. (2006). Plasticity of GABAergic control of hypothalamic presympathetic neurons in hypertension. *Am J Physiol Heart Circ Physiol, 290*(3), H1110-1119. doi:10.1152/ajpheart.00788.2005

Li, D. P., & Pan, H. L. (2007). Role of gamma-aminobutyric acid (GABA)A and GABAB receptors in paraventricular nucleus in control of sympathetic vasomotor tone in hypertension. *J Pharmacol Exp Ther, 320*(2), 615-626. doi:10.1124/jpet.106.109538

Li, D. P., & Pan, H. L. (2010). Role of GABAB receptors in autonomic control of systemic blood pressure. *Adv Pharmacol, 58*, 257-286. doi:10.1016/S1054-3589(10)58011-6

Li, D. P., & Pan, H. L. (2017). Glutamatergic Regulation of Hypothalamic Presympathetic Neurons in Hypertension. *Curr Hypertens Rep, 19*(10), 78. doi:10.1007/s11906-017-0776-4

Liu, N., Zhang, D., Zhu, M., Luo, S., & Liu, T. (2015). Minocycline inhibits hyperpolarization-activated currents in rat substantia gelatinosa neurons. *Neuropharmacology, 95*, 110-120. doi:10.1016/j.neuropharm.2015.03.001

Lloyd-Jones, D. M., Hong, Y., Labarthe, D., Mozaffarian, D., Appel, L. J., Van Horn, L., . . . Rosamond, W. D. (2010). Defining and setting national goals for cardiovascular health promotion and disease reduction: the American Heart Association's strategic Impact Goal through 2020 and beyond. *Circulation, 121*(4), 586-613. doi:10.1161/circulationaha.109.192703

Lohmeier, T. E., Hildebrandt, D. A., & Hood, W. A. (1999). Renal nerves promote sodium excretion during long-term increases in salt intake. *Hypertension, 33*(1 Pt 2), 487-492. doi:10.1161/01.hyp.33.1.487

Machado, B. H. (2001). Neurotransmission of the cardiovascular reflexes in the nucleus tractus solitarii of awake rats. *Ann N Y Acad Sci, 940*, 179-196. doi:10.1111/j.1749-6632.2001.tb03676.x

Marques-Lopes, J., Tesfaye, E., Israilov, S., Van Kempen, T. A., Wang, G., Glass, M. J., . . . Milner, T. A. (2017). Redistribution of NMDA Receptors in Estrogen-Receptor-beta-Containing Paraventricular Hypothalamic Neurons following Slow-Pressor Angiotensin II Hypertension in Female Mice with Accelerated Ovarian Failure. *Neuroendocrinology, 104*(3), 239-256. doi:10.1159/000446073

Matrai, M., Hetthessy, J. R., Nadasy, G. L., Szekacs, B., Mericli, M., Acs, N., . . . Varbiro, S. (2016). Estrogen therapy may counterbalance eutrophic remodeling of coronary arteries and increase bradykinin relaxation in a rat model of menopausal hypertension. *Menopause, 23*(7), 778-783. doi:10.1097/GME.0000000000000654

McLoone, V., Ringwood, J., & Van Vliet, B. (2011). A 5-component mathematical model for salt-induced hypertension in Dahl-S and Dahl-R rats. *Comput Methods Programs Biomed, 101*(2), 220-229. doi:10.1016/j.cmpb.2010.04.008

McLoone, V. I., Ringwood, J. V., & Van Vliet, B. N. (2009). A multi-component model of the dynamics of salt-induced hypertension in Dahl-S rats. *BMC Physiol, 9*, 20. doi:10.1186/1472-6793-9-20

Menzaghi, C., Paroni, G., De Bonis, C., Soccio, T., Marucci, A., Bacci, S., & Trischitta, V. (2006). The -318 C>G single-nucleotide polymorphism in GNAI2 gene promoter region impairs transcriptional activity through specific binding of Sp1 transcription factor and is associated with high blood pressure in Caucasians from Italy. *J Am Soc Nephrol, 17*(4 Suppl 2), S115-119. doi:10.1681/ASN.2005121340

Miron, V. E., & Priller, J. (2020). Investigating Microglia in Health and Disease: Challenges and Opportunities. *Trends Immunol, 41*(9), 785-793. doi:10.1016/j.it.2020.07.002

Mishra, J. S., More, A. S., Gopalakrishnan, K., & Kumar, S. (2019). Testosterone plays a permissive role in angiotensin II-induced hypertension and cardiac hypertrophy in male rats. *Biol Reprod, 100*(1), 139-148. doi:10.1093/biolre/ioy179

Mohsin, M., Souza, L. A. C., Aliabadi, S., Worker, C. J., Cooper, S. G., Afrin, S., . . . Feng Earley, Y. (2020). Increased (Pro)renin Receptor Expression in the Hypertensive Human Brain. *Front Physiol, 11*, 606811. doi:10.3389/fphys.2020.606811

Moreira, J. D., Chaudhary, P., Frame, A. A., Puleo, F., Nist, K. M., Abkin, E. A., . . . Wainford, R. D. (2019). Inhibition of microglial activation in rats attenuates paraventricular nucleus inflammation in Galphai2 protein-dependent, salt-sensitive hypertension. *Exp Physiol, 104*(12), 1892-1910. doi:10.1113/EP087924

Mozaffarian, D., Benjamin, E. J., Go, A. S., Arnett, D. K., Blaha, M. J., Cushman, M., . . . Fullerton, H. J. J. C. (2016). Heart disease and stroke statistics-2016 update a report from the American Heart Association. *Circulation, 133*(4), e38-e48.

Mozaffarian, D., Fahimi, S., Singh, G. M., Micha, R., Khatibzadeh, S., Engell, R. E., . . . Chronic Diseases Expert, G. (2014). Global sodium consumption and death from cardiovascular causes. *N Engl J Med, 371*(7), 624-634. doi:10.1056/NEJMoa1304127

Mu, S., Shimosawa, T., Ogura, S., Wang, H., Uetake, Y., Kawakami-Mori, F., . . . Fujita, T. (2011). Epigenetic modulation of the renal beta-adrenergic-WNK4 pathway in salt-sensitive hypertension. *Nat Med, 17*(5), 573-580. doi:10.1038/nm.2337

Nakayasu, H., Kimura, H., & Kuriyama, K. (1995). Cerebral GABAA and GABAB receptors. Structure and function. *Ann N Y Acad Sci, 757*, 516-527. doi:10.1111/j.1749-6632.1995.tb17511.x

Ngo, D. H., & Vo, T. S. (2019). An Updated Review on Pharmaceutical Properties of Gamma-Aminobutyric Acid. *Molecules, 24*(15). doi:10.3390/molecules24152678

Ni, X., Zhang, L., Ma, X., Shan, L. Y., Li, L., Si, J. Q., . . . Ma, K. T. (2019). betaestradiol alleviates hypertension and concanavalin Amediated inflammatory responses via modulation of connexins in peripheral blood lymphocytes. *Mol Med Rep, 19*(5), 3743-3755. doi:10.3892/mmr.2019.10037

Nishihara, M., Takesue, K., & Hirooka, Y. (2017). Renal denervation enhances GABA-ergic input into the PVN leading to blood pressure lowering in chronic kidney disease. *Auton Neurosci, 204*, 88-97. doi:10.1016/j.autneu.2016.09.018

Oparil, S., Zaman, M. A., & Calhoun, D. A. (2003). Pathogenesis of hypertension. *Ann Intern Med, 139*(9), 761-776. doi:10.7326/0003-4819-139-9-200311040-00011

Osborn, J. W., Collister, J. P., & Guzman, P. (2008). Effect of peripheral sympathetic nerve dysfunction on salt sensitivity of arterial pressure. *Clin Exp Pharmacol Physiol, 35*(3), 273-279. doi:10.1111/j.1440-1681.2007.04827.x

Ozdemir Kumral, Z. N., Kolgazi, M., Ustunova, S., Kasimay Cakir, O., Cevik, O. D., Sener, G., & Yegen, B. C. (2016). Estrogen receptor agonists alleviate cardiac and renal oxidative injury in rats with renovascular hypertension. *Clin Exp Hypertens, 38*(6), 500-509. doi:10.3109/10641963.2015.1116550

Packer, C. S., Pelaez, N. J., & Kramer, J. A. (2001). Estrogen protects against hypertension in the spontaneously hypertensive rat, but its protective mechanism is unrelated to impaired arterial muscle relaxation. *J Gend Specif Med, 4*(1), 20-27. Retrieved from https://www.ncbi.nlm.nih.gov/pubmed/11324236

Palmada, M., & Centelles, J. J. (1998). Excitatory amino acid neurotransmission. Pathways for metabolism, storage and reuptake of glutamate in brain. *Front Biosci, 3*, d701-718. doi:10.2741/a314

Patel, K. P. (1991). Central alpha-2 adrenergic mechanisms in the renal nerve mediated natriuresis and diuresis produced by acute volume expansion. *J Auton Nerv Syst, 36*(1), 47-54. doi:10.1016/0165-1838(91)90129-q

Paxinos, G., & Watson, C. (2007). *The rat brain in stereotaxic coordinates* (6th ed.). Amsterdam ; Boston ;: Academic Press/Elsevier.

Pekny, M., Wilhelmsson, U., & Pekna, M. (2014). The dual role of astrocyte activation and reactive gliosis. *Neurosci Lett, 565*, 30-38. doi:10.1016/j.neulet.2013.12.071

Pingili, A. K., Kara, M., Khan, N. S., Estes, A. M., Lin, Z., Li, W., . . . Malik, K. U. (2015). 6beta-hydroxytestosterone, a cytochrome P450 1B1 metabolite of testosterone, contributes to angiotensin II-induced hypertension and its pathogenesis in male mice. *Hypertension, 65*(6), 1279-1287. doi:10.1161/HYPERTENSIONAHA.115.05396

Qi, J., Yu, X. J., Fu, L. Y., Liu, K. L., Gao, T. T., Tu, J. W., . . . Kang, Y. M. (2019). Exercise Training Attenuates Hypertension Through TLR4/MyD88/NF-kappaB Signaling in the Hypothalamic Paraventricular Nucleus. *Front Neurosci, 13*, 1138. doi:10.3389/fnins.2019.01138

Qiao, X., Zhou, J. J., Li, D. P., & Pan, H. L. (2017). Src Kinases Regulate Glutamatergic Input to Hypothalamic Presympathetic Neurons and Sympathetic Outflow in Hypertension. *Hypertension, 69*(1), 154-162. doi:10.1161/HYPERTENSIONAHA.116.07947

Rashid, P., Leonardi-Bee, J., & Bath, P. (2003). Blood pressure reduction and secondary prevention of stroke and other vascular events: a systematic review. *Stroke, 34*(11), 2741-2748. doi:10.1161/01.STR.0000092488.40085.15

Reboussin, D. M., Allen, N. B., Griswold, M. E., Guallar, E., Hong, Y., Lackland, D. T., . . . Vupputuri, S. J. J. o. t. A. C. o. C. (2018). Systematic review for the 2017 ACC/AHA/AAPA/ABC/ACPM/AGS/APhA/ASH/ASPC/NMA/PCNA guideline for the prevention, detection, evaluation, and management of high blood pressure in adults: a report of the American College of Cardiology/American Heart Association Task Force on Clinical Practice Guidelines. *Hypertension, 71*(19), 2176-2198.

Riazi, K., Galic, M. A., & Pittman, Q. J. (2010). Contributions of peripheral inflammation to seizure susceptibility: cytokines and brain excitability. *Epilepsy Res, 89*(1), 34-42. doi:10.1016/j.eplepsyres.2009.09.004

Ribeiro, N., Panizza Hdo, N., Santos, K. M., Ferreira-Neto, H. C., & Antunes, V. R. (2015). Salt-induced sympathoexcitation involves vasopressin V1a receptor activation in the paraventricular nucleus of the hypothalamus. *Am J Physiol Regul Integr Comp Physiol, 309*(11), R1369-1379. doi:10.1152/ajpregu.00312.2015

Riedel, K., Deussen, A. J., Tolkmitt, J., Weber, S., Schlinkert, P., Zatschler, B., . . . Kopaliani, I. (2019). Estrogen determines sex differences in adrenergic vessel

tone by regulation of endothelial beta-adrenoceptor expression. *Am J Physiol Heart Circ Physiol, 317*(2), H243-H254. doi:10.1152/ajpheart.00456.2018

Rodriguez-Gomez, J. A., Kavanagh, E., Engskog-Vlachos, P., Engskog, M. K. R., Herrera, A. J., Espinosa-Oliva, A. M., . . . Burguillos, M. A. (2020). Microglia: Agents of the CNS Pro-Inflammatory Response. *Cells, 9*(7). doi:10.3390/cells9071717

Rosenbaum, D. M., Rasmussen, S. G., & Kobilka, B. K. (2009). The structure and function of G-protein-coupled receptors. *Nature, 459*(7245), 356-363. doi:10.1038/nature08144

Rossi, G. C., Standifer, K. M., & Pasternak, G. W. (1995). Differential blockade of morphine and morphine-6 beta-glucuronide analgesia by antisense oligodeoxynucleotides directed against MOR-1 and G-protein alpha subunits in rats. *Neurosci Lett, 198*(2), 99-102. Retrieved from https://www.ncbi.nlm.nih.gov/pubmed/8592651

Roy, E. R., Wang, B., Wan, Y. W., Chiu, G., Cole, A., Yin, Z., . . . Cao, W. (2020). Type I interferon response drives neuroinflammation and synapse loss in Alzheimer disease. *J Clin Invest, 130*(4), 1912-1930. doi:10.1172/JCI133737

Segiet, A., Smykiewicz, P., Kwiatkowski, P., & Zera, T. (2019). Tumour necrosis factor and interleukin 10 in blood pressure regulation in spontaneously hypertensive and normotensive rats. *Cytokine, 113*, 185-194. doi:10.1016/j.cyto.2018.07.003

Shah, S. J., & Stafford, R. S. (2017). Current Trends of Hypertension Treatment in the United States. *Am J Hypertens, 30*(10), 1008-1014. doi:10.1093/ajh/hpx085

Sharma, R. K., Oliveira, A. C., Kim, S., Rigatto, K., Zubcevic, J., Rathinasabapathy, A., . . . Raizada, M. K. (2018). Involvement of Neuroinflammation in the Pathogenesis of Monocrotaline-Induced Pulmonary Hypertension. *Hypertension, 71*(6), 1156-1163. doi:10.1161/HYPERTENSIONAHA.118.10934

Sharma, R. K., Yang, T., Oliveira, A. C., Lobaton, G. O., Aquino, V., Kim, S., . . . Raizada, M. K. (2019). Microglial Cells Impact Gut Microbiota and Gut Pathology in Angiotensin II-Induced Hypertension. *Circ Res, 124*(5), 727-736. doi:10.1161/CIRCRESAHA.118.313882

Shen, X. Z., Li, Y., Li, L., Shah, K. H., Bernstein, K. E., Lyden, P., & Shi, P. (2015). Microglia participate in neurogenic regulation of hypertension. *Hypertension, 66*(2), 309-316. doi:10.1161/HYPERTENSIONAHA.115.05333

Shen, Z., Weng, C., Zhang, Z., Wang, X., & Yang, K. (2018). Renal sympathetic denervation lowers arterial pressure in canines with obesity-induced hypertension

by regulating GAD65 and AT1R expression in rostral ventrolateral medulla. *Clin Exp Hypertens, 40*(1), 49-57. doi:10.1080/10641963.2017.1306542

Shi, P., Diez-Freire, C., Jun, J. Y., Qi, Y., Katovich, M. J., Li, Q., . . . Raizada, M. K. (2010). Brain microglial cytokines in neurogenic hypertension. *Hypertension, 56*(2), 297-303. doi:10.1161/HYPERTENSIONAHA.110.150409

Shi, Z., Gan, X. B., Fan, Z. D., Zhang, F., Zhou, Y. B., Gao, X. Y., . . . Zhu, G. Q. (2011). Inflammatory cytokines in paraventricular nucleus modulate sympathetic activity and cardiac sympathetic afferent reflex in rats. *Acta Physiol (Oxf), 203*(2), 289-297. doi:10.1111/j.1748-1716.2011.02313.x

Silva, R. M., Rossi, G. C., Mathis, J. P., Standifer, K. M., Pasternak, G. W., & Bodnar, R. J. (2000). Morphine and morphine-6beta-glucuronide-induced feeding are differentially reduced by G-protein alpha-subunit antisense probes in rats. *Brain Res, 876*(1-2), 62-75. Retrieved from https://www.ncbi.nlm.nih.gov/pubmed/10973594

Simon, J. K., & Ciriello, J. (1989). Contribution of afferent renal nerves to the metabolic activity of central structures involved in the control of the circulation. *Can J Physiol Pharmacol, 67*(9), 1130-1139. doi:10.1139/y89-180

Singh, P., Song, C. Y., Dutta, S. R., Gonzalez, F. J., & Malik, K. U. (2020). Central CYP1B1 (Cytochrome P450 1B1)-Estradiol Metabolite 2-Methoxyestradiol Protects From Hypertension and Neuroinflammation in Female Mice. *Hypertension, 75*(4), 1054-1062. doi:10.1161/HYPERTENSIONAHA.119.14548

Somsanith, N., Kim, Y. K., Jang, Y. S., Lee, Y. H., Yi, H. K., Jang, J. H., . . . Lee, M. H. (2018). Enhancing of Osseointegration with Propolis-Loaded TiO(2) Nanotubes in Rat Mandible for Dental Implants. *Materials (Basel), 11*(1). doi:10.3390/ma11010061

Song, X. A., Jia, L. L., Cui, W., Zhang, M., Chen, W., Yuan, Z. Y., . . . Kang, Y. M. (2014). Inhibition of TNF-alpha in hypothalamic paraventricular nucleus attenuates hypertension and cardiac hypertrophy by inhibiting neurohormonal excitation in spontaneously hypertensive rats. *Toxicol Appl Pharmacol, 281*(1), 101-108. doi:10.1016/j.taap.2014.09.004

Souza, L. A. C., Worker, C. J., Li, W., Trebak, F., Watkins, T., Gayban, A. J. B., . . . Feng, Y. (2019). (Pro)renin receptor knockdown in the paraventricular nucleus of the hypothalamus attenuates hypertension development and AT1 receptor-mediated calcium events. *Am J Physiol Heart Circ Physiol, 316*(6), H1389-H1405. doi:10.1152/ajpheart.00780.2018

Standifer, K. M., Rossi, G. C., & Pasternak, G. W. (1996). Differential blockade of opioid analgesia by antisense oligodeoxynucleotides directed against various G protein alpha subunits. *Mol Pharmacol, 50*(2), 293-298. Retrieved from https://www.ncbi.nlm.nih.gov/pubmed/8700136

Stern, J. E., Son, S., Biancardi, V. C., Zheng, H., Sharma, N., & Patel, K. P. (2016). Astrocytes Contribute to Angiotensin II Stimulation of Hypothalamic Neuronal Activity and Sympathetic Outflow. *Hypertension, 68*(6), 1483-1493. doi:10.1161/HYPERTENSIONAHA.116.07747

Stern, J. E., Sonner, P. M., Son, S. J., Silva, F. C., Jackson, K., & Michelini, L. C. (2012). Exercise training normalizes an increased neuronal excitability of NTS-projecting neurons of the hypothalamic paraventricular nucleus in hypertensive rats. *J Neurophysiol, 107*(10), 2912-2921. doi:10.1152/jn.00884.2011

Stern, J. E., & Zhang, W. (2003). Preautonomic neurons in the paraventricular nucleus of the hypothalamus contain estrogen receptor beta. *Brain Res, 975*(1-2), 99-109. doi:10.1016/s0006-8993(03)02594-0

Stocker, S. D., Madden, C. J., & Sved, A. F. (2010). Excess dietary salt intake alters the excitability of central sympathetic networks. *Physiol Behav, 100*(5), 519-524. doi:10.1016/j.physbeh.2010.04.024

Stocker, S. D., Monahan, K. D., & Browning, K. N. (2013). Neurogenic and sympathoexcitatory actions of NaCl in hypertension. *Curr Hypertens Rep, 15*(6), 538-546. doi:10.1007/s11906-013-0385-9

Straiker, A. J., Borden, C. R., & Sullivan, J. M. (2002). G-protein alpha subunit isoforms couple differentially to receptors that mediate presynaptic inhibition at rat hippocampal synapses. *J Neurosci, 22*(7), 2460-2468. doi:20026225

Swanson, L. W., & Kuypers, H. G. (1980). The paraventricular nucleus of the hypothalamus: cytoarchitectonic subdivisions and organization of projections to the pituitary, dorsal vagal complex, and spinal cord as demonstrated by retrograde fluorescence double-labeling methods. *J Comp Neurol, 194*(3), 555-570. doi:10.1002/cne.901940306

Swanson, L. W., & Sawchenko, P. E. (1980). Paraventricular nucleus: a site for the integration of neuroendocrine and autonomic mechanisms. *Neuroendocrinology, 31*(6), 410-417. doi:10.1159/000123111

Takenaka, K., Sasaki, S., Uchida, A., Fujita, H., Nakamura, K., Ichida, T., . . . Nakagawa, M. (1996). GABAB-ergic stimulation in hypothalamic pressor area induces larger sympathetic and cardiovascular depression in spontaneously hypertensive rats. *Am J Hypertens, 9*(10 Pt 1), 964-972. doi:10.1016/0895-7061(96)00171-9

Tanoue, A., Koba, M., Miyawaki, S., Koshimizu, T. A., Hosoda, C., Oshikawa, S., & Tsujimoto, G. (2002). Role of the alpha1D-adrenergic receptor in the development of salt-induced hypertension. *Hypertension, 40*(1), 101-106. doi:10.1161/01.hyp.0000022062.70639.1c

Tapiero, H., Mathe, G., Couvreur, P., & Tew, K. D. (2002). II. Glutamine and glutamate. *Biomed Pharmacother, 56*(9), 446-457. doi:10.1016/s0753-3322(02)00285-8

Unger, T., Borghi, C., Charchar, F., Khan, N. A., Poulter, N. R., Prabhakaran, D., . . . Schutte, A. E. (2020). 2020 International Society of Hypertension Global Hypertension Practice Guidelines. *Hypertension, 75*(6), 1334-1357. doi:10.1161/HYPERTENSIONAHA.120.15026

Van Vliet, B. N., Chafe, L. L., Halfyard, S. J., & Leonard, A. M. (2006). Distinct rapid and slow phases of salt-induced hypertension in Dahl salt-sensitive rats. *J Hypertens, 24*(8), 1599-1606. doi:10.1097/01.hjh.0000239296.25260.e0

Verkhratsky, A., & Nedergaard, M. (2018). Physiology of Astroglia. *Physiol Rev, 98*(1), 239-389. doi:10.1152/physrev.00042.2016

Vezzani, A., & Viviani, B. (2015). Neuromodulatory properties of inflammatory cytokines and their impact on neuronal excitability. *Neuropharmacology, 96*(Pt A), 70-82. doi:10.1016/j.neuropharm.2014.10.027

Villa, A., Vegeto, E., Poletti, A., & Maggi, A. (2016). Estrogens, Neuroinflammation, and Neurodegeneration. *Endocr Rev, 37*(4), 372-402. doi:10.1210/er.2016-1007

Villarino, A. V., Kanno, Y., Ferdinand, J. R., & O'Shea, J. J. (2015). Mechanisms of Jak/STAT signaling in immunity and disease. *J Immunol, 194*(1), 21-27. doi:10.4049/jimmunol.1401867

Wainford, R. D. (2014). Presympathetic neuron dysfunction--time to reconsider increased intrinsic activity as the cause of neurogenic hypertension. *Exp Physiol, 99*(7), 935-936. doi:10.1113/expphysiol.2014.080077

Wainford, R. D., Carmichael, C. Y., Pascale, C. L., & Kuwabara, J. T. (2015). Galphai2-protein-mediated signal transduction: central nervous system molecular mechanism countering the development of sodium-dependent hypertension. *Hypertension, 65*(1), 178-186. doi:10.1161/HYPERTENSIONAHA.114.04463

Wainford, R. D., & Kapusta, D. R. (2012). Functional selectivity of central Galpha-subunit proteins in mediating the cardiovascular and renal excretory responses evoked by central alpha(2) -adrenoceptor activation in vivo. *Br J Pharmacol, 166*(1), 210-220. doi:10.1111/j.1476-5381.2011.01662.x

Wainford, R. D., Pascale, C. L., & Kuwabara, J. T. (2013). Brain Galphai2-subunit protein-gated pathways are required to mediate the centrally evoked sympathoinhibitory mechanisms activated to maintain sodium homeostasis. *J Hypertens, 31*(4), 747-757. doi:10.1097/HJH.0b013e32835ebd54

Wang, Q., Guo, R., Rong, S., Yang, G., Zhu, Q., Jiang, Y., . . . Huang, J. (2013). Noninvasive renal sympathetic denervation by extracorporeal high-intensity focused ultrasound in a pre-clinical canine model. *J Am Coll Cardiol, 61*(21), 2185-2192. doi:10.1016/j.jacc.2013.02.050

Whelton, P. K., Appel, L. J., Sacco, R. L., Anderson, C. A., Antman, E. M., Campbell, N., . . . Van Horn, L. V. (2012). Sodium, blood pressure, and cardiovascular disease: further evidence supporting the American Heart Association sodium reduction recommendations. *Circulation, 126*(24), 2880-2889. doi:10.1161/CIR.0b013e318279acbf

Whelton, P. K., Carey, R. M., Aronow, W. S., Casey, D. E., Jr., Collins, K. J., Dennison Himmelfarb, C., . . . Wright, J. T., Jr. (2018). 2017 ACC/AHA/AAPA/ABC/ACPM/AGS/APhA/ASH/ASPC/NMA/PCNA Guideline for the Prevention, Detection, Evaluation, and Management of High Blood Pressure in Adults: A Report of the American College of Cardiology/American Heart Association Task Force on Clinical Practice Guidelines. *Hypertension, 71*(6), e13-e115. doi:10.1161/HYP.0000000000000065

Williams, G. H., & Hollenberg, N. K. (1989). Sodium-sensitive essential hypertension: emerging insights into an old entity. *J Am Coll Nutr, 8*(6), 490-494. doi:10.1080/07315724.1989.10720318

Wolf, S. A., Boddeke, H. W., & Kettenmann, H. (2017). Microglia in Physiology and Disease. *Annu Rev Physiol, 79*, 619-643. doi:10.1146/annurev-physiol-022516-034406

Worker, C. J., Li, W., Feng, C. Y., Souza, L. A. C., Gayban, A. J. B., Cooper, S. G., . . . Feng Earley, Y. (2020). The neuronal (pro)renin receptor and astrocyte inflammation in the central regulation of blood pressure and blood glucose in mice fed a high-fat diet. *Am J Physiol Endocrinol Metab, 318*(5), E765-E778. doi:10.1152/ajpendo.00406.2019

Wright, J. M., Musini, V. M., & Gill, R. (2018). First-line drugs for hypertension. *Cochrane Database Syst Rev, 4*, CD001841. doi:10.1002/14651858.CD001841.pub3

Writing Group, M., Mozaffarian, D., Benjamin, E. J., Go, A. S., Arnett, D. K., Blaha, M. J., . . . Stroke Statistics, S. (2016). Executive Summary: Heart Disease and Stroke

Statistics--2016 Update: A Report From the American Heart Association. *Circulation, 133*(4), 447-454. doi:10.1161/CIR.0000000000000366

Xue, B., Zhang, Y., & Johnson, A. K. (2020). Interactions of the Brain Renin-Angiotensin-System (RAS) and Inflammation in the Sensitization of Hypertension. *Front Neurosci, 14*, 650. doi:10.3389/fnins.2020.00650

Xue, B., Zhang, Z., Beltz, T. G., Johnson, R. F., Guo, F., Hay, M., & Johnson, A. K. (2013). Estrogen receptor-beta in the paraventricular nucleus and rostroventrolateral medulla plays an essential protective role in aldosterone/salt-induced hypertension in female rats. *Hypertension, 61*(6), 1255-1262. doi:10.1161/HYPERTENSIONAHA.111.00903

Yamamoto, K., Eubank, W., Franzke, M., & Mifflin, S. (2013). Resetting of the sympathetic baroreflex is associated with the onset of hypertension during chronic intermittent hypoxia. *Auton Neurosci, 173*(1-2), 22-27. doi:10.1016/j.autneu.2012.10.015

Yang, H., Song, X., Wei, Z., Xia, C., Wang, J., Shen, L., & Wang, J. (2020). TLR4/MyD88/NF-kappaB signaling in the rostral ventrolateral medulla is involved in the depressor effect of candesartan in stress-induced hypertensive rats. *ACS Chem Neurosci*. doi:10.1021/acschemneuro.0c00029

Yang, J. H., Choi, S. H., & Gwon, H. C. (2013). Percutaneous renal sympathetic denervation for the treatment of resistant hypertension with heart failure: first experience in Korea. *J Korean Med Sci, 28*(6), 951-954. doi:10.3346/jkms.2013.28.6.951

Ye, C., Qiu, Y., Zhang, F., Chen, A. D., Zhou, H., Wang, J. J., . . . Zhu, G. Q. (2020). Chemical Stimulation of Renal Tissue Induces Sympathetic Activation and a Pressor Response via the Paraventricular Nucleus in Rats. *Neurosci Bull, 36*(2), 143-152. doi:10.1007/s12264-019-00417-1

Yoon, S. Y., Patel, D., & Dougherty, P. M. (2012). Minocycline blocks lipopolysaccharide induced hyperalgesia by suppression of microglia but not astrocytes. *Neuroscience, 221*, 214-224. doi:10.1016/j.neuroscience.2012.06.024

Yudin, Y., & Rohacs, T. (2018). Inhibitory Gi/O-coupled receptors in somatosensory neurons: Potential therapeutic targets for novel analgesics. *Mol Pain, 14*, 1744806918763646. doi:10.1177/1744806918763646

Zanchetti, A., Thomopoulos, C., & Parati, G. (2015). Randomized controlled trials of blood pressure lowering in hypertension: a critical reappraisal. *Circ Res, 116*(6), 1058-1073. doi:10.1161/CIRCRESAHA.116.303641

Zera, T., Nowinski, A., Segiet, A., & Smykiewicz, P. (2019). Microglia and brain angiotensin type 1 receptors are involved in desensitising baroreflex by intracerebroventricular hypertonic saline in male Sprague-Dawley rats. *Auton Neurosci, 217*, 49-57. doi:10.1016/j.autneu.2019.01.002

Zhang, T., Wang, D., Li, X., Jiang, Y., Wang, C., Zhang, Y., . . . Wang, G. (2020). Excess salt intake promotes M1 microglia polarization via a p38/MAPK/AR-dependent pathway after cerebral ischemia in mice. *Int Immunopharmacol, 81*, 106176. doi:10.1016/j.intimp.2019.106176

Zhang, X., Frame, A. A., Williams, J. S., & Wainford, R. D. (2018). GNAI2 polymorphic variance associates with salt sensitivity of blood pressure in the Genetic Epidemiology Network of Salt Sensitivity study. *Physiol Genomics, 50*(9), 724-725. doi:10.1152/physiolgenomics.00141.2017

Zubcevic, J., Santisteban, M. M., Perez, P. D., Arocha, R., Hiller, H., Malphurs, W. L., . . . Raizada, M. K. (2017). A Single Angiotensin II Hypertensive Stimulus Is Associated with Prolonged Neuronal and Immune System Activation in Wistar-Kyoto Rats. *Front Physiol, 8*, 592. doi:10.3389/fphys.2017.00592

Zuriaga, M. A., Fuster, J. J., Farb, M. G., MacLauchlan, S., Breton-Romero, R., Karki, S., . . . Walsh, K. (2017). Activation of non-canonical WNT signaling in human visceral adipose tissue contributes to local and systemic inflammation. *Scientific Reports, 7*. doi:10.1038/s41598-017-17509-5

CURRICULUM VITAE